Phase 1

FINAL REPORT

HIGH—SHOCK FM TRANSMITTER

CONTRACT NO. NAS1-5042

7060/FR1

PREPARED BY

G. E. BROWN, B. SC.
J. E. DAWSON, B. SC.
J. R. BECK, B. SC.

22 OCTOBER, 1965

Computing Devices
OF CANADA LIMITED
P. O. BOX 508 • OTTAWA 4 • CANADA

ABSTRACT

This report describes the work performed under Phase I of Contract NAS1-5042 for the Design, Development, Fabrication, and Testing of High Shock FM Transmitters. Phase I of the Contract was concerned with the qualification of electronic components for use in the transmitters and the development of a transmitter meeting the electrical and physical requirements of the specification. Included in the report are the results of the electronic component test program, the evaluation of the electrical and physical properties of candidate epoxy encapsulants, and a description, schematic diagram, and electrical test results for the transmitter developed under this phase of the contract.

Felix Pitts

7061/FR1

22 NOVEMBER 1965

ERRATA
FOR
FINAL REPORT
HIGH–SHOCK FM TRANSMITTER

Computing Devices
OF CANADA LIMITED
P. O. BOX 508 • OTTAWA 4 • CANADA

ERRATA
FOR
FINAL REPORT
HIGH-SHOCK FM TRANSMITTER
7060/FR1

The following corrections are to be incorporated in this publication:

CONTENTS

Page i, Figure 2-7

Change "American Technical Ceramic"
to read "CTS of Berne Inc."

SECTION 1

Page 2, Paragraph 6, Line 4

Change "is being compared"
to read "is long compared"

SECTION 2

Page 5, Paragraph 2

Change "Figure 1-5 shows a typical test package."
to read "Figure 1-6 shows a typical test package."

Page 8, Paragraph 14, Line 3

Add the following sentence after "before/after measurements."
"As an essentially constant current source is used to drive the resistor, the variation in voltage drop is proportional to the resistance change."

Page 8, Paragraph 15, Line 5

Delete sentence
"As an essentially constant current source is used to drive the resistor, the variation in voltage drop is proportional to the resistance change."

Page 9, Paragraph 18, Line 1
Change "American Technical Ceramics"
to read "CTS of Berne Inc."

Page 12, Line 9
Change "$\epsilon_r = \mu\epsilon_2$"
to read "$\epsilon_r = \mu\epsilon_\ell$"

SECTION 4

Page 34, Line 10
Change "$= 1.3 \times 10^{-3}$ seconds"
to read "$= 1.03 \times 10^{-3}$ seconds"

Page 35, Paragraph 8, Line 4
Change "= 0.872 lbs."
to read "= 0.0872 lbs."

SECTION 5

Page 40, Paragraph 3, Line 7
Change "The ratio of C_1 to C_2 determines etc."
to read "The ratio of C_3 to C_4 determines etc."

Page 40, Paragraph 4, Line 5
Change "$n = C_3/C_4$"
to read "$n = C_4/C_3$"

SECTION 6

Page 47, Paragraph 5, Line 4
Change "Figure 6-1) time"
to read "Figure 6-1) warm-up time"

Page 51, Paragraph 3, Line 3
Change "incomplete wiring of the fiberglass"
to read "incomplete wetting of the fiberglass"

REFERENCES

Page 52, Table 7-1 Under "Manufacturer"
Change "American Technical Ceramics"
to read "CTS of Berne Inc."

ILLUSTRATIONS

Page 59, Line 2
Change "Hood strain output"
to read "Load strain output"

Add
"Lower trace, Strain 7,200 microstrain/cm"

Page 65, Figure 2-1
Photograph printed upside down

Page 70, Figure 2-7
Change "Impact Tests on American Technical Ceramics"
to read "Impact Tests on CTS of Berne Inc."

Page 76, Figure 2-13
Change Coordinates "% ERROR" in three places
to read "% COMPONENT CHANGE"

Page 77, Figure 2-14
Change Coordinates "% ERROR" in three places
to read "% COMPONENT CHANGE"

Page 91, Figure 3-1
Change "Stress Level See Figure 5"
to read "Stress Level See Figure 3-3"

Page 99, Figure 3-9
Change "Plastic Modulus $\epsilon = 5.1 \times 10^5$"
to read "Elastic Modulus $\epsilon = 5.1 \times 10^5$"

Page 117, Component List Under "Manufacturer"
Change "ATC"
to read "CTS of Berne Inc."

Page 134, Figure 6-2 Under "Frequency Change (Kc/s)" coordinate
Change scale "100, 80, 60, 40, 30, 20, 10, 0"
to read "100, 80, 60, 40, 20, 0, -20, -40"

Printed and published in Canada by
Computing Devices
OF CANADA LIMITED

CONTENTS

LIST OF ILLUSTRATIONS

LIST OF ILLUSTRATIONS (CONT'D)

LIST OF ILLUSTRATIONS (CONT'D)

LIST OF ILLUSTRATIONS (CONT'D)

LIST OF TABLES

SECTION 1

TEST FACILITIES

INTRODUCTION

1 The high shock transmitter being developed in this Program must operate properly as well as survive during several high level shocks. An important phase of the development program is the qualification of components for this application. In-house test equipment was used for these tests.

2 The qualifying test for the transmitter requires that it operate satisfactorily when encapsulated in a hard epoxy ball impacting concrete at 150 ft/sec. Because the time of impact of the ball is long compared with the transit time of a stress wave to propagate throughout the ball, a quasistatic stress distribution is produced.

3 Under high shock conditions circuit components are subjected to large acceleration forces. Shock accelerations are difficult to duplicate in the laboratory since only complicated procedures approaching the complexity of the actual application can be used. Careful consideration of the acceleration forces acting on the component reveals that these forces can be considered to have two components: the force on the component because of its own weight and the force on the component because of the surrounding medium. The first is the result of the acceleration forces on the component. The second is a stress caused by the loading effects of the plastic encapsulant used and can be produced without accelerating the component package since it is external to the component. The second stress is, in general, much higher then the first and hence a test program simulating this stress can yield valid results concerning component qualification.

PENDULUM IMPACT TESTER

4 Two facilities were made available for component tests during this portion of the program and although they were developed as part of a Computing Devices in-house project, a brief description is included here to provide an understanding of the tests and the problems associated with them.

5 The most important of the two test facilities is the Pendulum Impact Tester. This tester is shown in Figure 1-1 and consists of a pendulum with interchangeable heads, a high-mass anvil block, a piezo-electric load cell and a sample holder attached to the anvil. The pendulum head can be

released at various heights by an electro-mechanical device which also operates the camera shutter on the oscilloscope used to record the load and component change during the test.

6 The mass of the pendulum head and the sample dimensions have been chosen so that a stress/time history, which closely approximates the conditions in a test sphere, can be produced. As the impact duration of the pendulum on the sample is being compared to the stress wave reflection time, a quasistatic system is produced which can be described by the equations of simple harmonic motion. The test sample acts as a linear spring, which has a uniform stress along its length, that varies sinusoidally with time. The load pulse duration is determined by the sample spring-constant and the effective mass of the impacting pendulum head. The magnitude of the stress pulse is determined by the mass of the pendulum, the drop height and the sample spring-constant. Figures 1-2 and 1-3 show the theoretical operating curves for the Pendulum Tester based on the equation of simple harmonic motion. The average of a series of six experimental results using a 1 inch OD $\times$ 2 inch sample are plotted for comparison. The pulse times agree very closely. The discrepancies between the theoretical and practical results for the maximum stress are attributed to the heat generated at impact, the vibrations set up in the equipment, and the proportion of the load carried by the load cell mounting stud.

7 An accelerometer attached to the pendulum head is another method of determining the stress applied to the sample. The accelerometer, however, records the multiple reflections of shock waves in the pendulum head and its output must be filtered to provide a scaleable record. The filtering then produces a loss in accuracy. The reflections are not transferred to the test sample because of the mechanical impedance mismatch between the pendulum head and the sample, and therefore affect the sample under test to a very small degree. It has been estimated that only 8 per cent is transferred to the sample. This estimate is based on the diameter of the head compared to the diameter of the sample during impact and the dissimilar elastic properties of the head and sample. The errors in both systems appear to be approximately the same and for this reason the load cell has been used for all component tests. The curves shown in Figure 1-5 compare the load cell output to the composite output of two strain gauges mounted on the side of a test specimen. The top trace is the load cell and it is seen that it corresponds in time with the strain gauge record.

8 The absolute accuracy of the Computing Devices' impact tester depends on the calibration certificate supplied by the load cell manufacturer (Kistler Instrument Company). To ensure that this calibration is always valid, a check is performed from time to time using a standard aluminum sample and a standard drop height. To date, no change in load cell output has been detected.

9 The effective mass of the pendulum is the mass of the head plus the effective mass of the pendulum arm. The mass of the pendulum arm is distributed along its length and, therefore, cannot be added directly to the mass of the head. Two methods were used to determine the effective mass and the results agree to within 0.1 per cent.

10 Table 1-1 gives the pulse time and maximum stress determined experimentally for various effective pendulum weights.

EFFECTIVE WEIGHT OF HEAD (lbs)	PULSE TIME (mSec)	MAXIMUM MEASURED STRESS (psi) (drop height - 8 ft)
	1" diameter × 2" long RDD5 Sample	
3.17	0.71	11,000
8.62	1.14	17,900
15.4	1.64	17,900
	1" OD × 3/4" long RDD5 Sample	
3.17	0.53	12,000
8.62	0.77	17,900
15.4	-	-

Table 1-1. Pendulum Tester

11 The block circuit diagram of the pendulum tester is shown in Figure 1-4. The trigger circuit for the oscilloscope was completed when the pendulum head makes contact with the front surface of the test sample which was coated with conductive silver paint (Figure 1-6). The silver paint on the remaining portion of the sample was to eliminate the surface charge redistribution effects. The latter problem is discussed in a following section.

12 Since the impact test was required at various temperatures, a simple means of providing the required temperature environment during the tests was investigated. The test samples were places in a temperature oven until they have reached the desired temperature. They were then rapidly removed from the oven and placed on the sample holder, all the required electrical connections being made with a multipin connector. This simple method overcomes the need for a complex temperature test chamber to

contain the sample during the test. To check the feasibility of this method, a plastic sample was potted with two thermistors, one at the center of the sample and the other at the surface. After a uniform temperature of 140 degrees F had been reached, the sample was removed from the oven and placed on the pendulum tester. The temperature on the surface and at the center was monitored. Figure 1-7 shows the variation of temperature recorded by the two thermistors. It was apparent that there was sufficient time to remove the sample from the oven and make the required tests before appreciable cooling occurs.

COMPRESSION TESTER

13 The second test facility made available for this contract was the simple compression tester shown in Figure 1-8. The test package is held between the hydraulic ram and the load cell. The load cell is a multi-strain gauge device which has been calibrated in an accurately calibrated commercial compression machine. The load is applied to the test package by means of a hand pump.

14 The advantages of the compression tester are that somewhat greater control over the load applied to the sample is possible. The disadvantage is the difficulty in comparing the compression tester results with those from the pendulum since the plastic shows strain rate effects.

15 Since the plastic yields and the stress on the sample then varies with time, point-by-point data plots are difficult to make. The process maybe automated by applying the load cell output directly to the X-amplifier of a camera equipped oscilloscope while the compared variation data is applied to the Y-amplifier. The resultant photograph is a continuous plot of component value versus load.

COMPRESSED AIR GUN LAUNCHER

16 A six-inch compressed-air-gun is shown in Figure 1-9. The unit is similar to a larger unit developed by Computing Devices several years ago, which was used extensively to launch large rocket body models. The smaller unit is complete and all instrumentation required is available to launch 8 lb penetrometer spheres and sabots at velocities of up to 200 ft/sec. Higher velocities are possible using high-pressure bottled gas. This test facility is available for the second phase of this program.

SECTION 2

SHOCK TESTING OF ELECTRONIC COMPONENTS

INTRODUCTION

1 The component tests have been undertaken to determine the electronic stability for components while subjected to a large, short-duration mechanical stress pulse. As mentioned in the previous section only external stresses are applied to the component because of the difficulty and expense in obtaining acceleration pulses of long duration while in fact for ordinary components the external effect is much larger. Calculations show that the spherical test package to be used in the second phase of the contract will be subjected to an acceleration pulse of 1.03 milliseconds when impacted into concrete at 150 ft/sec. The pendulum tester produces a stress pulse approximately 1.2 milliseconds long. The increased pulse length subjects the component to a more rigorous test. The characteristics of the plastic encapsultant is not affected by the variation in pulse length from 0.71 to 1.64 milliseconds. The validity of this statement is discussed more fully in Section 3 of this report.

2 Encapsulation of electronic circuitry in hard plastic is the best method available to obtain high electrical and mechanical stability in a high frequency circuit such as the transmitter required for this program. For this reason, a standard test package one inch diameter and two inches long was chosen and RDD 5 plastic (a Computing Devices' nomenclature) which has good high impact characteristics, was chosen for the encapsulation of the component. Figure 1-5 shows a typical test package. The component is placed approximately 1/2 inch from the bottom of the package. After travelling 1-1/2 inches the initially spherical shock front has become sufficiently flat before it reaches the component. This is not too important, however, since the pulse duration is much longer than the time required for the shock wave to traverse the length of the package and many reflections actually occur before the maximum stress is reached. In fact, the stress build-up is sufficiently slow that it may be considered a static load except that the plastic does not have sufficient time to yield. The components to be tested are mounted, in general, in three mutually orthogonal positions. Components, such as resistors, which are symmetrical along one axis, are mounted in only two positions.

3 Some types of components, such as unpotted transistors, with metal cases are not suitable for testing in the pendulum impact tester. In the transistor, the metal case protects the semiconductor element from the external stresses to a large degree. Only acceleration tests are applicable

to this type of component. Potting of the transistor overcomes this problem, but this is not always possible with other types of components which fall into the category, such as quartz crystal resonators.

4 Many variables exist which affect the component change when it is subjected to a high-g environment and must be considered when testing components. These include, for any given class of component:

(a) Inherent mechanical variables in the component

(b) Component orientation

(c) Stress level

(d) Order of stress application if more than one test is performed on a given sample

(e) Type of plastic

(f) Temperature of plastic and sample

(g) Plastic batch

(h) Variables associated with the pendulum test
- Pulse duration
- Pulse shape

5 A number of these variables were not of immediate interest and steps were taken to exclude them from the experiments. The same type of plastic was used for all the tests (except for high temperature tests on capacitors). The mixing procedure and general control over the plastic was standardized. Plastic batch was a variable which was eventually eliminated when it was found that sufficient plastic to pot 12 samples could be mixed all at once rather than in a series of small batches. Since some testing of RDD 5 plastic had been carried out before the start of this program and since detailed mechanical tests were carried out at the initiation of this work (see Section 3), this plastic was used for all components tests.

6 Stress pulse length, stress pulse shape, and other variables associated with pendulum tester are eliminated as much as possible by using standard test conditions.

7 To determine the amount of interaction between the remaining variables, statistical methods have been applied to the information obtained from the tests. The variables considered in these tests are:

(a) Component orientation

(b) Stress level (between 2,000 and 12,000 psi)

(c) Order of applied stress pulses (increasing stress level or decreasing stress levels)

(d) Plastic batch

8 Plastic batch was eliminated during the test program as stated above by potting all components for a test series from one batch of plastic. The order of stress was eliminated from capacitor tests when it was found that breakage occurred at an unpredictable level between 6,000 to 8,000 psi.

9 The component value before and after testing was also recorded. It was found that the components which showed the highest degree of stability during the test generally had zero permanent set. A mathematical analysis of variance of the component test results requires extensive data to produce meaningful results. A minimum of three points for a given set of conditions was taken but it was found that experimental error and component variability limited the usefulness of the statistical analysis. Insufficient time was available to perform sufficient tests to exploit the analysis to its fullest.

10 An examination of the results obtained indicates that differences between various types of components in any one class can be resolved with the limited results available. It becomes apparent then which components will be most suitable for the high shock transmitter. Exact relationships of component value versus pressure are not of utmost importance since the exact magnitude of the pressure acting on any given component within the transmitter case is impossible to estimate and the exact effect any component change will have in the rf circuitry is also, in general, difficult to assess.

11 The final results must be a clear indication of which component types are obviously better for this application, and provide a reasonably degree of confidence in these conclusions. The results obtained from the tests and the analysis performed on these results does fulfill these requirements.

PREPARATION OF TEST SAMPLES

12 The preparation of the test samples containing the components was simple. A silastic mold was used to pot the components into a 1 inch by 2-1/2 inch long test package. After the necessary cure cycle, the test packages were mounted in a special adapter in a lathe so that the package

could be shortened to two inches while squaring the cylinder's ends. The end and walls were painted with conductive silver paint. Figure 1-6 shows a photo of a typical test package ready for testing.

13 The silver paint applied to the bottom portion of the sample was needed to prevent spurious signals from appearing in the test record. The effect is similar in nature to a piezo-electric voltage appearing across the component but is, in fact, a redistribution of surface charge on the test sample. Figure 2-1 is a typical record obtained from a capacitor test sample which was not treated with the silver paint. The small negative pulse at the beginning of the stress pulse and the large positive one at the end are due to the surface charge effects. The vertical scale is an order of magnitude greater than that used for normal capacitance measurements.

COMPONENT TEST RESULTS

RESISTORS

14 The circuit diagram used for the resistor tests is shown in Figure 2-2. A general Radio Type 1608A impedance bridge was used to make before/after measurements. The oscilloscope was ac coupled to the output terminals of the test circuit and monitored the variation in voltage drop across the test sample. The results from the statistical analysis although included in the monthly progress reports have been omitted from this report. The number of test samples tested was not sufficient for a complete analysis and the conclusions which could be drawn did not add greatly to the curves showing the raw data. The types of resistors tested included carbon, tin oxide, metal film, and cermet. They are discussed under individual headings below:

15 IRC CARBON 5.6K, 1/4 WATT RESISTORS. Figures 2-3 and 2-4 show the results of two sets of carbon resistors; one set was covered with a woven fiberglass tube which it was hoped would improve the characteristics of the carbon resistor. However, an increase in dynamic change in the horizontally mounted unit appears to have occurred. As an essentially constant current source is used to drive the resistor, the variation in voltage drop is proportional to the resistance change.

16 WELWYN 9.1K, 1/4 WATT TIN OXIDE RESISTORS. The plotted results are shown in Figure 2-5. It was found that these resistors were very susceptible to shock when mounted perpenducular to the direction of applied force. These resistors are typical of many tin oxide and metal film components in that they have metal caps over the end of the ceramic

core which bears the resistor film. In this instance the cap to which the lead wires are attached is actually formed on the end of the ceramic core rather than being preformed and then pressed on. This results in a continuous contact around the core rather than only at several points as is the usual case. The reason for the open circuit occurring at low stress levels is not known. It is probable that the ceramic core failed, which would bias the selection of other resistors the same basic construction. The type of failure may however be peculiar to the ceramic material used by this manufacturer. These resistors, although not suitable for the high shock transmitter, are considerably better than carbon resistors when used in a unidirectional stress field, and their cost is very low.

17 AMERICAN COMPONENTS INC. MCF 1/10 WATT METAL FILM RESISTORS. These resistors make use of conducting epoxy to form the connection between the lead wire and the resistive element. The results in Figure 2-6 indicate that although the change in resistance is low there appears to be deterioration as the component is subjected to further stress pulses.

18 AMERICAN TECHNICAL CERAMICS CERADOT 1/10 WATT RESISTORS. These resistors appear to have the best characteristic of any resistor tested. The lead wires are attached by soldering to the silvered ends of the cermet resistive element. This is probably the most reliable means of attaching the wire to the resistor of any of the types of resistors tested and repeated low stress pulse produced no change in resistance. Figure 2-7 gives the results of the tests. The before/after results are essentially zero and the dynamic change is less than 0.15 per cent in the 2,000 to 3,000 psi stress range.

CAPACITORS

19 The circuit diagram used for the shock tests on the capacitors is shown in Figure 2-8. The test capacitor was used as a frequency determining element in an oscillator. Therefore, the frequency of the oscillator is a measure of the component value. Frequency variations during the test were discriminated with an Electro Mechanical Research Inc. Tunable Discriminator, Model 97G and Variable Lowpass Output Filter, Model 95D. The frequency of the oscillator was adjusted to a predetermined value prior to the test by adjusting the power supply voltage. A frequency of 95 Kc/s was chosen for all tests. The discriminator output filter cut-off was set at 8 Kc/s.

20 Calibration of the system was accomplished by switching known capacitors across the test capacitor and adjusting the filter amplitude output to produce a specific deflection per pF. Although a number of calibration

capacitors were included in the circuit, only a one pF capacitor was needed and the filter output was adjusted to give 1 volt deviation per pF capacity variation. The output was assumed to be linear with capacitance change over this range. The assumption is acceptable since the random variations in the results were sufficiently large to make any interpolation errors insignificant.

21 Four types of capacitors have been tester - these were American Technical Ceramics Model No. ATC100, Vitramon Model VY, Corning Glass Works Models TYD6 and CY10C and Centralab DD-101. The latter type has a negative temperature coefficient.

22 The capacity variations of the ATC capacitor were generally quite large hence they do not appear suitable for the high shock transmitter, even though they are very small. Only a limited number of data points were taken since it was found that their performance was inferior to the Vitramon and Corning capacitors.

23 The Vitramon VY capacitor test results are shown in Figure 2-9. Smooth curves were drawn from point to point with no weighting on the various points. The data is presented in this manner to show the large random effects present (point scatter). Part of the variation is due to noise in the discriminator or test system which appears on the trace. A possible source of the noise is the physical movement of the test sample during and after the impact. Figure 2-10 is a typical record of a capacitor test.

24 The Corning Glass TYO6 and CY10 results are shown in Figures 2-11 and 2-12 respectively. The results are similar to those shown in Figure 2-9 for the Vitramon VY Condensers. The TYO6 is a little better at low stress levels than the CY10. Figures 2-13 and 2-14 show the results of the statistical analysis. The 90 per cent confidence limits are shown. The analysis does not consider the effect of potting batch and the order of applied stress. All the tests were performed with increasing stress levels since a catastrophic failure, possibly due to an open circuit, generally appeared at 8,000 psi, although the Corning condensers were somewhat better than the Vitramon in this respect.

25 Centralab ceramic disk capacitors have been considered because of their negative temperature coefficient and the potential need for temperature compensation in the transmitter. The results are shown in Figure 2-15. The capacitance change is orientation dependant, going positive and then negative when the plane of the disk is perpendicular to the applied force as the stress is increased and negative only, when disk is standing on edge.

26 A statistical analysis of these units was not conducted because of the lack of time and data.

R.F. COILS

27 The rf coils are the only components manufactured specifically for this application. High shock stability has been obtained by depositing a conducting film on a glass or high-alumina ceramic core.

28 High-alumina ceramic has been chosen as the core material because of its high modulus of elasticity and resulting low deformation under stress. Pyrex was considered originally. Under repeated stress pulses of 3,000 to 4,000 psi, 3/16 inch diameter by 9/16 inches long rods shattered if mounted with their axis perpendicular to the applied force. Mounted vertically they could withstand repeated stress of a high magnitude. Fiberglass reinforcing jackets around the coil did not increase the strength of the core in the horizontal position.

29 The ceramic material presently being used is a 96.6 per cent alumina manufactured by Du-Co Ceramics Co., Saxonburg, Pennsylvania. A General Electric product, "Lucalox", is presently on order and will be used in the second phase of the program. The latter material is 99.9 per cent alumina and has a modulus of elasticity of 57×10^6 psi. An estimate of the change of inductance of a helix for simple changes in length was made. An equation for the inductance of a single layer solenoid is

$$L = \frac{N^2 r^2}{9r + 10\ell}$$

where

N is number of turns
r is the radius of coil
ℓ is coil length.

for $N = 3$ $\ell = 0.5$ $r = 0.1"$

and

$$L \approx \frac{r^2}{r + \ell}$$

To determine the effect of r and ℓ on the inductance we take partial derivatives of L

$$\frac{\delta L}{L} = \frac{\delta r}{L} \times \frac{\partial L}{\partial r} + \frac{\delta \ell}{L} \times \frac{\partial L}{\partial \ell}$$

where

$$\frac{\partial L}{\partial r} = \frac{r\,(r + 2\ell)}{(r + \ell)^2}$$

and $$\frac{\partial L}{\partial \ell} = \frac{-r^2}{(r+\ell)^2}$$

substituting we get

$$\frac{\delta L}{L} = 1.8\frac{\delta r}{r} - 0.83\frac{\delta \ell}{\ell}$$

or

$$\Delta L = 1.8\,\Delta r - 0.83\,\Delta \ell$$

where ΔL, Δr and $\Delta \ell$ represent per cent change. The strains resulting from a stress directed along the axis of the coil are approximately

$$\epsilon_\ell = \frac{S_\ell}{E}$$

$$\epsilon_r = \mu\epsilon_2$$

Let
- Stress = S = 3,000 psi
- Elastic Modulus = E = 57×10^6 for Lucalox
- Poisson's Ratio = μ = 0.23
- Strain = ϵ

Therefore
- $\epsilon_\ell = 5.3 \times 10^{-5}$
- $\epsilon_r = -1.2 \times 10^{-5}$
- $\Delta \ell$ = 0.0053 per cent
- Δr = -0.0012 per cent

and ΔL = -0.0066 per cent

A change of L of +0.0062 per cent should change the frequency by approximately -0.0033 per cent which is below the required specification of 0.004 per cent. In the same manner, a stress perpendicular to the axis of the coil will cause the inductance to vary about -0.01 per cent and the frequency to vary 0.005 per cent. A decrease in stress would reduce this figure. Three thousand psi is the expected maximum stress in the transmitter package. The stresses within the transmitter are discussed in a following section. Estimates on the capacitance change which might accompany a change in physical dimensions of the coil have been made assuming that capacitance is inversely proportional to length and proportional to circumference or diameter. An axial force would produce an increase in capacitance and a force perpendicular to the axis would cause a decrease. The effect would, when added to the change in inductances calculated above, add to the frequency shift in one case and subtract in the other.

30 Impact tests conducted on the coils have given results which are an

order of magnitude greater than those indicated by the above calculations. Figure 2-16 shows the results of the impact tests. It is seen that although a trend toward higher frequency change for increasing stress level is evident there are large variations at all stress levels.

31 In an attempt to improve the experimental procedure and in particular to prevent the coil from changing position (and hence changing stray capacity) during the impact, the rf coils were tested in the compression tester. The test circuit and block diagrams of test equipment are shown in Figure 2-17.

32 The measured slopes of the curves (typical curves of frequency change versus load are shown in Figures 2-18 and 2-19) indicated no correlation between the various types of core material (ceramic and pyrex glass) nor between the different coil orientations. The percentage is seen to be approximately the same as that obtained in the dynamic tests. The difference is even less, considering the plastic is 1/2 as strong when measured statically as dunamically (see plastics section). The hysteresis effect is probably due to plastic flow occurring during the period in which the load is applied. Figure 2-20 shows the results of a ceramic coil being subjected to a series of increasing and decreasing loads. The hysteresis effect increases as the peak load increases.

33 The general conclusion, therefore, is that both tests produced roughly the same results, namely an order of magnitude greater than those calculated for the ceramic coils; coil material and orientation have had no apparent effect. The glass coils should be considerably less because its modulus of elasticity is almost half that of pure alumina.

34 The reason for the large changes and the lack of correlation for different materials and orientation is not known exactly, but the dielectric constant of the plastic appears to be a function of pressure. A literature search has failed to produce data on pressure effect, but consultation with various authorities confirm that such effects are likely. For example, the optical refractive index of a material is related to its dielectric constant, and changes in refractive index were easily observed in the stress analysis work discussed in another section of this report.

35 The problem is difficult to overcome because some form of potting material is needed to support the transmitter components during the high shock application. Fillers appear to be the best solution. "Eccospheres" are a good choice for a filler when mixed with the plastic since mechanical characteristics are preserved, the density is reduced, the dielectric constant is reduced since the "Eccospheres" are air-filled and the thermal insulation properties are improved. All these effects are desirable for this application.

36 A comparison of oscillator stability under a static stress was made on two identical oscillators, one potted with a mixture of M30 and "Eccospheres" (see Section 3) and the other with M30 alone. The tests unfortunately were inconclusive and time did not permit them to be repeated. A poor connection developed in the transmitter potted with "Eccospheres" and no useful information was obtained. The oscillator potted in solid plastic changed frequency by approximately 170 Kc/s when subjected to a load of 3,100 psi.

37 The coil design used was quite simple. The alumina substrate material was cut to the correct diameter and length. The substrate was first cleaned with aqua-regia and then thick layers of silver were built up using Hanovia liquid silver solution and a suitable bake cycle. To obtain the necessary helical coil of silver on the substrate can be removed in either of two ways.

(1) Grind the silver coating away with a suitable diamond wheel, or

(2) Etch the silver away with acid. The spiral of silver to be removed was first covered with a thin layer of tape. The complete coil was then given several thin coatings of parafin wax after which the tape was gently pulled away leaving an exposed helix of silver. Nitric acid was used as an etchant. The coils was washed in distilled water and the wax removed.

Method (2) was used in this instance. The thickness of silver was increased to 0.001 inches by silver plating. The Hanovia liquid silver solutions recommended for this application are

(1) Liquid silver #467 - the manufacturer states that three applications of this, firing each at 1,200 degrees F, will produce a silver thickness of approximately 0.001 inch. This material was recommended by the manufacturer for this application; or

(2) Liquid Silver #9375.

38 The silver material actually used for the coils produced during this program was Squeegees Silver 9091. This was used because it was immediately available. Both of the Hanovia materials are on order and will be available for Phase II of this high shock transmitter program. Initial attempts at coil making were made using a resistive platinum solution which was then silver plated. Using the Squeegee silver material as a base, raised the finished coil Q from 90 to 150.

39 Initial problems involving adhesion of the silver to the substrate have been solved by cleaning procedures. Soldering to the helix can be performed simply but silver bearing solder is recommended.

R.F. CHOKES

40 Only limited tests on micro-miniature molded rf chokes with phenolic cores were conducted because high stability is not required for their application. Two simple tests were conducted. The first was to show that no spurious voltages were produced when the inductor was subjected to a high stress pulse,and the second measured the change in resistance under the same conditions. Absolutely no spurious voltage was detected and no resistance change occurred. The units tested were made by J.W. Miller Co.

DIODES AND ZENER DIODES

41 Diodes are needed for temperature compensation and voltage regulation in the transmitter. Initial tests were made on TRW micro diodes because it was felt that their small size would be desirable not only from the point of view of available space in the transmitter, but also because they would probably not be as susceptible to the applied stress because of their small cross section and apparent ruggedness.

42 The latter, however, was not so. Only a limited number of samples were tested and the results are shown in Figure 2-21. The breakdown voltage of the PD101 is given as 50 volts in the data sheet. The average value of 10 samples was measured to be 123 volts. After a single impact of 12,000 psi, the average value was reduced to 66 volts,with 7 samples below 50 volts and one as low as 6 volts. Cracks appeared in the coating covering the active element.

43 To improve the impact characteristics, the PD 101 diodes were given a thin coating of silastic plastic. Under similar test conditions, the forward voltage change was only several millivolts and no change occurred in the breakdown voltage before and after the shock test.

44 Micro Zener diodes of the same type were tested. Three types of silastic material were used to coat them. A large variation occurred between diodes potted in the various silastic material. The best material was that which gave the most uniform coating.

45 Other diodes tested include the TI 1N457 and the Hughes 1N903A both having Type DD-7 glass cases. The majority of the samples became

open circuit during the impact test. Those samples which withstood the shock exhibited no significant change in breakdown voltage before and after testing. The glass cases showed considerable cracking. It would appear that the more common types of diodes require some form of stress relief before they are suitable for high-g applications.

46 An exception was the Hoffman 1N1313A Zener diode which is encapsulated in hard plastic. Six samples were tested and apart from a slight increase in noise, as shown in Figure 2-22, there was no change in Zener voltage at low and medium stress levels. Two diodes became momentarily open circuit when tested at 12,000 psi. It is thought that the ohmic contact to the diode crystals momentarily pulled away during the high stress level. The circuit used for these tests is given in Figure 2-22.

TRANSISTORS

47 Plastic encapsulated 2N2923 Transistors were tested on the pendulum tester using the test circuit shown in Figure 2-23. Also shown on the Figure is a typical test record. The actual results are shown in Figure 2-24, 2-25 and 2-26. The change in collector voltage reverses polarity when the transistor is mounted in one of the two horizontal positions. The transistor was cut open and it was found that in this orientation the impact force was applied along an axis perpendicular to the semi-conductor chip. A further reduction in variation of collector voltage was found to be possible by decoupling the test resistor in the emitter circuit.

48 Although the plastic-encapsulated transistors appear to be quite satisfactory, and no failures occurred in any of the units tested, the unit to be used in the transmitter oscillator will be a metal cased 2N918. The transistor case will be opened and the void filled with a hard plastic. The case of the transistor provides some stress relief.

SECTION 3

MATERIAL REVIEW

INTRODUCTION

1 A review of potentially suitable potting material was made to select a material for encapsulating the high shock transmitter and component test packages. A preliminary selection of material for use in making reinforced test spheres has also been made.

POTTING MATERIAL REQUIREMENTS

2 As the transmitter is to have the maximum possible stability, the physical deformation of the components and interconnections must be kept to a minimum under shock loads. Therefore, the encapsulating material must have a high modulus of elasticity, high shock resistance and low density. As stray capacities in the circuits have significant effects on the circuits, the dielectric constant and the dissipation factor must be small and their stress dependence a minimum. The mechanical and electrical properties must remain essentially constant over the temperature range 32 degrees F to 140 degrees F. The material must also have a low coefficient of thermal expansion, a low exotherm during potting, an adequate pot life, a low viscosity, a low shrinkage and a moderate curing temperature.

3 A knowledge of the potting and curing variables of the material which is used for component test packages is required,to ensure minimum encapsulant effect on component tests. The testing of materials was divided into the following phases:

(a) Evaluation of the mixing and curing variables of the material to be used for component test packages.

(b) Preliminary evaluation of a number of commercially available resin systems which might satisfy the transmitter requirements.

(c) Final evaluation of the material chosen from (b).

4 The material survey was limited to epoxies, as their low shrinkage, good adhesion, and good shock resistance when in a rigid form appeared best suited to the transmitter requirements. The selection of materials

for testing, was based on data from:

(a) Users of high impact materials
(b) Resin suppliers
(c) Available literature (References 1, 2, 3, 4, 5)
(d) Past experience in encapsulating high-g electronics.

MATERIAL FOR COMPONENT TEST PACKAGES

5 The schedule of work required that the component test program be initiated as soon as the contract was awarded. It was decided that the plastic designated as RDD5,which had previously been developed at Computing Devices, be used for producing component test packages. The RDD5 plastic had been evaluated using only room temperature qualitative tests and no quantitative data was known regarding the dynamic mechanical properties. As it was desirable to remove the encapsulant variables from the component test results, information regarding the mechanical properties versus loading time, curing and test temperature was required for the RDD5 material.

ELASTIC PROPERTIES OF RDD5

6 DYNAMIC PROPERTIES. An experiment has been performed to determine the effect of: individual batches, curing temperature, curing time, stress pulse duration and sample temperature on the dynamic elastic properties of RDD5.

(a) Three batches of plastic were mixed and four samples (1-1/8 inch OD × 3 inches long) poured from each batch. These samples were given different cure cycles and machined to a 1 inch OD × 2 inches standard size. Strain gauges were applied, and the samples tested on the pendulum tester. One-eighth inch gauge length foil strain gauges were mounted on both sides of the sample using Eastman 910 cement. These gauges were wired in series so that any bending effects due to unsymmetrical impact of the pendulum hammer on the sample would be eliminated.

(b) The strain gauge output and the load cell output were recorded on a photograph of an oscilloscope trace. Figure 1-5 shows an example of an oscilloscope trace of strain gauge and load cell outputs. Some of the samples were tested using different pendulum heads, giving stress pulse lengths of 0.71, 1.14 and 1.64 milliseconds. This was done to determine whether strain rate effects were significant over this range. Figure 3-1 shows an outline of the experiment in schematic form. The results of these experiments

are plotted in Figure 3-2. Figures 3-3, 3-4, 3-5, 3-6 and 3-7 show the individual plots of the curves in Figure 3-2.

(c) After testing at room temperature, the 14-day cure samples were tested at 150 degrees F, 128 degrees F, 100 degrees F and 26 degrees F. The testing at other than room temperature was accomplished by removing the sample from the temperature chamber, quickly attaching the sample to the pendulum tester anvil and completing the test within 2 minutes. To check the feasibility of this approach, 2 thermistors were potted in a sample: one just under the surface and one in the center. The sample temperature versus time was monitored. The results of this test are shown in Figure 1-7. During the initial two minute period the surface temperature dropped from 63 degrees C to 51 degrees C but the internal temperature dropped only 0.5 degrees C. The results of the testing at various temperatures are shown in Figure 3-8.

(d) The dynamic Poisson's ratio of RDD5 was measured using two longitudinal strain gauges and two circumferential strain gauges. The relative strain during impact of the pendulum head was measured; the results of this test are shown in Figure 3-9.

7 STATIC PROPERTIES. The static stress/strain curve and Poisson's ratio was obtained from strain gauge readings similar to the dynamic Poisson's ratio tests. Results of the static stress/strain curve and Poisson's ratio tests are shown in Figure 3-10.

8 DISCUSSION OF RESULTS.

(a) Figure 3-2 shows that the material continued curing at room temperature during the two week test period and also that elevated curing temperatures provide a small improvement in cure time (curves B and D). The results indicate that if the curing time is kept constant, the normal room temperature variations will not significantly alter the curing of the final product.

(b) The load pulse variation of 0.7 milliseconds to 1.6 milliseconds does not alter the mechanical properties significantly (see scatter of points on Figure 3-3). As the variation in stress pulse duration did not produce a significant change in mechanical properties, further testing of material samples was performed using the 1.2 millisecond pulse (the 8.62 lb head).

(c) Figure 3-8 shows that RDD5 has excellent mechanical properties from 25 degrees F to 75 degrees F but a significant reduction in strength is observed above 100 degrees F.

(d) The testing on the RDD5 material indicated that it should have consistent mechanical properties for different batches cured at normal room temperature if the curing time is held constant.

(e) A comparison of the static and dynamic properties shows a modulus increase from 4.2×10^5 to 5.1×10^5 and a decrease in Poisson's ratio from 0.47 to 0.42 respectively. The loading rate has a pronounced effect on the plastic parameters.

PRELIMINARY MATERIAL SURVEY

9 Table 3-1 lists the materials obtained, the mixing proportions and the curing schedule used for the resins and hardners obtained for evaluation.

10 A series of tests have been performed to evaluate the strength, elastic modulus, dielectric strength, and dissipation factor over the temperature range of 32 degrees F to 200 degrees F.

11 Three individual samples (1-1/8 inch OD × 3 inches) of each material were poured. Care was taken not to introduce air into the mixture and general observations as to the handling properties, handling time and exothermic reaction were noted. After curing,the samples were machined to 1 inch OD × 2 inches long standard size.

12 All samples were tested on the pendulum tester using the 8.62 lb head. Table 3-2 shows the results of these tests.

13 The elastic modulus was calculated from the stress pulse duration; the pulse length is determined by the elastic properties of the sample. As indicated in Section 1, the stress pulse produced by the pendulum tester is given by

$$t = \pi\sqrt{K/M}$$

where
t = pulse time in seconds
k = spring constant of sample
m = mass of pendulum

The spring constant k is determined by the elastic modulus of the material and the sample dimensions. Thus, the elastic modulus is given by:

$$E = 0.56/t^2 \quad \text{for a 1 inch OD} \times \text{2 inch long sample}$$

Figure 3-11 shows two examples of traces showing load pulse records.

Table 3-1.

Plastic Designation	MANUFACTURER	RESIN		HARDENER		FLEXIBILIZER		MINIMUM CURE
		Designation	Proportions	Designation	Proportions	Designation	Proportions	
M4	Ciba Co. Ltd.	502 508	80 20	951	12	RD1	2	7 days at room temperature
M5	Ciba Co. Ltd.	502 508	90 10	DP-138	20	-	-	4 hours at room temperature
M6	Ciba Co. Ltd.	502	100	951	12	-	-	7 days at room temperature
M7	Emerson & Cummings (Stycast)	1090	100	#9	9	-	-	7 days at room temperature
M8	Emerson & Cummings (Stycast)	1090SI	100	#11	12	-	-	16 hours at 167 degrees F
M9	Emerson & Cummings (Stycast)	2850FT	100	#11	5	-	-	16 hours at 167 degrees F
M10	Emerson & Cummings (Stycast)	2850FT	100	#11	5	-	-	16 hours at 167 degrees F
M11	Emerson & Cummings (Stycast)	1090SI	100	24LV	23	-	-	24 hours at room temperature
M12	Emerson & Cummings (Stycast)	2850GT	100	#9	3	-	-	24 hours at room temperature
M13	Emerson & Cummings (Stycast)	2850FT	100	#9	3	-	-	24 hours at room temperature
M14	Shell Chemical Co. (Epon)	815	100	U	10	Versamid 140	25	24 hours at room temperature

Table 3-1. List of Resin Systems

M15	Shell Chemical Co. (Epon)	815	100	U	25	-	-	24 hours at room temperature
M16	Shell Chemical Co. (Epon)	828	100	U	25	-	-	24 hours at room temperature
M17	Hysol Co. Ltd.	4362	100	3404	7	-	-	24 hours at room temperature
M18	Emerson & Cummings (Stycast)	1090	100	#11	12	-	-	2 hours at 212 degrees F
M19	Dow Chemical	DER	100	DETA	3	#3483.2	40	Material not available
M20	Shell Chemical Co. (Epon)	828	100	AEP	22	(Exothermid runaway)		
M22	Shell Chemical Co. (Epon)	828	100	Tonox	28	-	-	4 hours at 200 degrees F
M23	Dow Chemical Co.	331	100	DETA	8	-	-	4 hours at 200 degrees F
M24	Dow Chemical Co.	331	100	DETA	10	-	-	4 hours at 200 degrees F
M25	Dow Chemical Co.	331	100	DETA	12	-	-	4 hours at 200 degrees F
M26	Dow Chemical Co.	331	100	Tonox	28	-	-	4 hours at 200 degrees F
M28	Shell Chemical Co.	828	100	AEP	18	-	-	4 hours at 200 degrees F
M29	Dow Chemical Co.	331	100	AEP	20	-	-	4 hours at 200 degrees F
M30	Shell Chemical Co.	828	100	U	20	-	-	24 hours at room temperature

Table 3-1.

Sample No.	M4 (RDD5)	M5	M6	M7	M8
Resin Manufacturer	Ciba	Ciba	Ciba	----	----
Sample Composition					
Resin	502-80	502-90	502-100	1090-100	1090SI-100
Resin	508-20	508-10	---	---	---
Hardner	951-12	DP-138-20	951-12	#9-9	#11-12
Flexibilizer	RDl-2	---	---	---	---
Density lbs/in^3	0.043	0.043	0.043	0.032	0.023
Colour	Clear	Clear Light yellow	Clear	Black	Black
Elastic Modulus psi					
at 200°F	0.79x10^5	0.14x10^5	2.5x10^5	4.4x10^5	---
75°F	5.8x10^5	5.3x10^5	5.3x10^5	5.5x10^5	7.4x10^5
26°F	6.6x10^5	8.3x10^5	7.0x10^5	6.8x10^5	6.9x10^5
Maximum Stress psi					
at 200°F	2350	1,368	6,620	7,790	---
75°F	16,875	14,970	18,780	12,610	4,530
26°F	21,020	20,700	19,000	15,600	6,370
Sample Condition at maximum stress					
at 200°F	Unchanged	Unchanged	Unchanged	Shattered	---
75°F	"	"	"	Crushed	Crushed
26°F	"	"	---	"	Shattered
Pourability	excellent	good	good	fair	fair
Exotherm	acceptable	acceptable	acceptable	acceptable	acceptable

CDC 273A

Table 3-2.

M9	M10	M11	M12	M13	M14
Emerson	And	Cummings	---	---	Shell
2850FT-100	2850GT-100	1090SI-100	2850GT-100	2850FT-100	815-100
---	---	---	---	---	---
#11-5	#11-5	24LV-23	#9-3	#9-3	U-10
		---			Versamid 140-25
0.084	0.086	0.026	0.080	0.085	0.041
Black	Grey-Black	Black	Grey-Black	Grey-Black	Clear Yellow
16.8×10^5	22.0×10^5	0.4×10^5	13.4×10^5	26×10^5	3.2×10^5
21.2×10^5	$23,7 \times 10^5$	4.7×10^5	22.7×10^5	29×10^5	5.7×10^5
28×10^5	17.3×10^5	5.2×10^5	28.5×10^5	32×10^5	5.2×10^5
24,000	20,700	828	24,200	24,800	8,920
30,600	34,400	9,230	24,850	33,100	17,070
33,700	37,000	11,080	26,100	34,400	19,100
Unchanged	Unchanged	Unchanged	Cracked	Unchanged	Unchanged
"	"	Crushed	Shattered and split	Sample Cracked	"
"	"	Shattered	Shattered	Unchanged	"
poor	not acceptable	fair	not acceptable	not acceptable	good
acceptable	acceptable	acceptable	acceptable	acceptable	acceptable

Table 3-2. Results of Preliminary Material Survey (Sheet 1 of 2)

Sample No.	M15	M16	M17	M18	M22
Resin Manufacturer	Shell Chemical Co.		Hysol	Emerson & Cummings	Shell
Sample Composition					
Resin	815-100	828-100	4362-100	1090-100	828-100
Resin	---	---	---	---	---
Hardner	U-25	U-25	3404-7	#11-12	Tonox-29
Flexibilizer	---	---	---	---	---
Density lbs/in^3	0.043	0.043	0.051	0.032	0.040
Colour	Clear	Clear	Grey	Black	Clear yellow
Elastic Modulus psi					
at 200°F	3.5×10^5	4.0×10^5	3.2×10^5	4.6×10^5	4.9×10^5
75°F	5.9×10^5	5.8×10^5	8.5×10^5	5.6×10^5	5.1×10^5
26°F	8.2×10^5	8.3×10^5	10.5×10^5	6.2×10^5	6.2×10^5
Maximum Stress psi					
at 200°F	9,940	13,900	8,920	10,200	14,700
75°F	18,450	16,875	21,030	12,100	17,200
26°F	19,750	19,750	23,600	14,000	16,800
Sample Condition at maximum stress					
at 200°F	Unchanged	Unchanged	Unchanged	Shattered	Unchanged
75°F	"	"	"	"	"
26°F	"	"	"		"
Pourability	good	fair	fair	poor	good
Exotherm	acceptable	acceptable	acceptable	acceptable	acceptable

CDC 273A

Table 3-2.

M23	M24	M25	M26	M27	M28	M29
Dow	Dow	Dow	Dow	Shell	Shell	Dow
331-100	331-100	331-100	331-100	828-100	828-100	331-100
---	---	---	---	---	---	
Deta-8	Deta-10	Deta-12	Tonox-28	AEP-20	AEP-18	AEP-20
---	---	---	---	---	---	---
0.040	0.040	---	0.039	0.040	0.039	0.039
Clear light yellow	Clear light yellow	porous bubbles	Clear yellow	Clear yellow	Clear yellow	clear yellow
3.8×10^5	4.6×10^5	2.6×10^5	4.3×10^5	4.2×10^5	3.6×10^5	4.2×10^5
5.1×10^5	6.5×10^5	4.6×10^5	6.2×10^5	4.6×10^5	4.7×10^5	5.1×10^5
5.8×10^5	5.4×10^5	5.8×10^5	5.6×10^5	5.5×10^5	5.5×10^5	6.1×10^5
13,500	16,300	7,990	14,500	11,700	11,500	13,000
17,200	16,500	12,200	17,200	15,300	15,300	14,000
17,600	17,300	12,500	16,800	16,600	15,800	16,300
Unchanged	Unchanged	Shattered	Unchanged	Unchanged	Unchanged	Unchanged
"	"	"	"	"	"	"
"	"	"	"			
good	good	good	good	good	good	good
high	high	excessive	high	high	high	high

Table 3-2. Results of Preliminary Material Survey (Sheet 2 of 2)

The pulse is slightly unsymmetrical due to the strain lag or "memory effect" in the plastic sample. Because of this effect, the pulse time used for modulus determination was measured from the start of the pulse to its peak value, and then multiplied by two.

14 The modulus of elasticity for the material is calculated from the average of at least three stress levels which occur on the linear portion of the stress-strain curve. The stress at which yielding occurs can be detected from the total pulse length. As the sample yields, the total pulse length increases. As an indication of the accuracy of this method, the modulus of elasticity for the RDD5 samples was measured from Figures 3-5 and 3-6, and also from the pulse duration. The modulus, as measured direct from Figures 3-5 and 3-6, are 5.32×10^5 psi and 5.75×10^5 psi respectively. The modulus calculated from the average of the nine stress pulse durations indicated a modulus of 5.2×10^5 psi and 5.6×10^5 psi or a difference from the previous method of 2.3 per cent and 2.6 per cent respectively.

15 The maximum stress tabulated in Table 3-2 does not necessarily indicate the yield stress of the material. It gives either the stress at which the sample broke or the maximum stress obtained when the pendulum head was dropped from 8 feet. As the area under the force/time curve is equal to the kinetic energy of the pendulum, material with a lower modulus will have a longer pulse time but lower stress for any given drop height. However, the stress indicated shows a minimum ultimate strength of the materials at the various temperatures.

DETERMINATION OF THE ELECTRICAL PROPERTIES OF PLASTICS

16 The two important electrical properties of the plastic used to encapsulate the transmitter are:

(a) THE DIELECTRIC CONSTANT (K). Because of the high frequency and close spacing of components, stray capacitance will have a significant effect upon the resonant frequencies of tuned circuits in the transmitter. When the circuit is encapsulated the effective stray capacitances will change. To minimize the retuning necessary after encapsulation, the dielectric constant of the plastic chosen should be as small as possible.

(b) DISSIPATION FACTOR (D). As the stray capacitances form part of the tuned circuits the losses should be kept as small as possible in order to keep the Q's of the tuned circuits close to their original value in air. The dissipation factor of the encapsulating plastic should therefore be as small as possible.

17 The dielectric constant and dissipation factor were measured initially with the jig shown in Figure 3-12 and remeasured on a Marconi dielectric loss jig, Type TJ 155b/1.

18 Disks of material 1 inch diameter by 0.02 to 0.03 inch thick were taken from the 1 inch diameter samples used in the pendulum impact tester. A small thickness is necessary to produce a measureable capacity. However, errors are introduced because of thickness variations in each sample and the pressure exerted by the jig. In most cases three samples of each plastic were used and the results averaged.

19 For tests at low frequencies (1 Kc/s to 100 Kc/s), the measurements were taken with a General Radio 1608A bridge and at high frequencies (90 Mc/s to 180 Mc/s), a Marconi Type TF1245 Q-meter was used.

20 The test jig was calibrated at low frequency using polyethylene sheets of known thickness as the dielectric. The dielectric constant of polyethylene was taken to be 2.26, (Reference data for Electrical Engineers, 4th edition ITT). Figure 3-13 compares the theoretical with actual capacitances obtained for various thicknesses of polyethylene. The results compare closely.

21 As the electrical properties of the plastics were also expected to be dependent on temperature some of the tests were carried out at different temperatures.

22 Samples M4, M7 and M16 were tested at temperatures between 40 degrees F and 140 degrees F and although large variations in test data were obtained the trend indicated an increase in dielectric constant with temperature.

23 Values of dielectric constant varied between 3.8 and 6.4 and dissipation factor varied between 0.005 and 0.04 for the materials listed in Table 3-2. The results of these tests showed large variation between samples of the same material, and between individual tests on the same sample, especially at the higher frequencies.

24 As changes in the dielectric constant of the encapsulating material with stress would adversely affect the transmitter operation during impact, the stress dependency of dielectric constant should be investigated. The refractive index "n" of a material is related to the dielectric constant "K" by the relation

$$n = \sqrt{K}$$

25 At visible optical frequencies all transparent epoxy materials exhibit

a bi-refringent or photoelastic effect which is directly related to stress, and it is likely that the dielectric constant is dependant on stress at the lower uhf frequencies.

26 The stress dependency of the dielectric constant was investigated using the ac bridge, and a sample compressed between a parallel plate capacitor in the compression tester. No great effect was detected and the random nature of the data obtained indicated that more sophisticated equipment would be required to measure this effect.

RESULTS OF THE PRELIMINARY SURVEY

27 Of the material tested in the preliminary survey, samples M7, M16 and M18 were considered as possible encapsulants for the transmitter. M16 and M7 are both systems which cure at room temperature. M16 has a very short working life and a higher exotherm than M7 and M18. M16 also has the lowest viscosity at room temperature, and cures to a transparent material. The M18 material has the advantage of a long working time, but it must be poured at approximately 140 degrees F to lower the viscosity to an acceptable level. A reactive diluent "Mod-Epoxy" manufactured by Monsanto Corporation was tried, to reduce the viscosity of M18 system, but the filler separated and the high temperature properties were destroyed. A summary of the results is shown in Table 3-3.

SYSTEM	M7	M16	M18
Pour Temperature	75 degrees F	75 degrees F	140 degrees F
Viscosity	Fair	Fair	Good
Working Life	30 minutes	15 minutes	120 minutes
Exotherm	Low	High	Low
Curing Temperature	75 degrees F	75 degrees F	200 degrees F

Table 3-3. Possible Encapsulants for Transmitter

28 As mentioned before, the electrical testing gave inconclusive results and could not be used to differentiate between the plastics. However, the manufacturers' specifications for M16 and M18 indicate that the latter system has slightly better properties.

29 A modified M16 system was chosen for further evaluation using strain gauges to confirm the results of the preliminary survey. The amount of hardener was reduced to 20 phr (parts per hundred) from 25 phr to increase the working life, and the material was designated M30. The material was chosen because of its good mechanical properties, transparency, and reasonable viscosity at room temperature.

30 The dynamic mechanical properties of M30 material were evaluated at 28 degrees F, 75 degrees F, 149 degrees F and 200 degrees F using strain-gauged samples and the pendulum tester. The static properties were also measured at room temperature.

31 A summary of the test results are plotted in Figure 3-14 and the individual tests are shown in Figures 3-15, 3-16, 3-17, 3-18 and 3-19. The properties of RDD5 are included for comparison.

SAMPLE	TYPE OF TEST	TEST TEMPERATURE	ELASTIC MODULUS	POISSON'S RATIO
M30	Dynamic	28 degrees F	5.8×10^5	0.42
	Dynamic	75 degrees F	5.8×10^5	0.41
	Dynamic	149 degrees F	5.2×10^5	0.44
	Dynamic	202 degrees F	4.4×10^5	0.45
	Static	75 degrees F	5.5×10^5	-
RDD5	Dynamic	75 degrees F	5.8×10^5	0.42
	Static	75 degrees F	4.2×10^5	0.47

Table 3-4. Mechanical Properties of M30 and RDD5

32 Table 3-4 indicates that the M30 material has good mechanical properties over the temperature range of 28 degrees F to 202 degrees F and therefore would satisfy the mechanical properties required for the transmitter. After these tests had been made on the M30 material, the problem of the stress dependence of the dielectric constant of encapsulants was investigated. Although the magnitude of this effect is not known, the material which had the lowest dielectric constant should have a minimum effect on the circuit under stress. Manufacturers data indicated that the M18 material had slightly better electrical properties than the M30 plastic and it was felt that the hollow glass sphere used as a filler would reduce the stress dependency of the dielectric constant in the M18 material. The viscosity of

the M18 plastic was reduced to a useable value by heating the material to 140 degrees F before pouring. Low density and long working life of this material were also advantageous for this application.

33 Because of the test results and the above reasons, Computing Devices has chosen the M18 plastic for encapsulating the prototype transmitter.

MATERIAL FOR TEST SPHERES

34 The RDD5 plastic was chosen for the production of reinforced test spheres. The material exhibits excellent room temperature and low temperature properties and has a low viscosity. One 3-1/2 inch test sphere was produced by packing a spherical mould with milled fiberglass and drawing the RDD5 material into the mould with a vacuum system. A sphere with a density of 0.047 lbs/in^3 was produced with a 26 per cent fiberglass content. No problems were encountered with the potting or curing of this test ball.

SECTION 4

STRESS ANALYSIS

INTRODUCTION

1 Components for the transmitter must be capable of satisfactory operation when the transmitter is potted in a 3-1/2 inch test sphere impacting concrete at velocities up to 150 ft/sec. In order that components may be qualified for use in the transmitter, an estimate of the stresses expected in the transmitter package during impact of the test sphere was required.

2 The impact force and duration resulting from the impact of two hard elastic bodies may be calculated from the Hertz laws of contact. The work of McCarty and Carden (Reference 6) indicates that the impact of steel on concrete approximates an elastic impact. However, the maximum acceleration measured on impact was found to be approximately 30 per cent less than that predicted by the Hertz laws. The explanation given attributes the difference to local pulverization at the contact point and non-perfect elastic collision. NASA photographs L-65-3978 to L-65-3985 inclusive, illustrate epoxy balls which have impacted concrete at up to 218 ft/sec and there appears to be no pulverization or permanent deformation at the contact point. From the above it was concluded that the impact of epoxy on concrete should approximate an elastic collision.

3 The coefficient of restitution of the epoxy ball - concrete collision is not known, it will be assumed to be one. The assumption will give a conservative estimate of the maximum acceleration loads acting on the ball, and the actual acceleration value may be in the order of 30 per cent less than the value calculated from the Hertz law.

THE ACCELERATION OF SPHERE ON IMPACT

4 Assume the ball impacts concrete at 150 ft/sec. The Elastic Properties of Ball and Target are:

	EPOXY	CONCRETE
μ = Poisson's Ratio	0.41	0.2
E = Modulus of Elasticity	5.8×10^5 psi	3.5×10^6 psi
$\delta = \frac{1 - u^2}{E}$	143×10^{-8} in^2/lb	8.74×10^{-8} in^2/lb

NOTE: The epoxy to be used for producing test spheres is material RDD5, and its properties are outlined in the material selection section of this report.

Maximum acceleration

$$a_m = \frac{1}{386}\left[\frac{0.173\ DV_i^6}{m^2(\delta_p + \delta_t)^2}\right]^{0.2} = 41,400\ g$$

where D = diameter of sphere = 3.5 inches
V_i = impact velocity = 1,800 in/sec
m = mass of ball = 2.92×10^{-3} lb sec^2/in

Impact duration

$$t = 5.208\left[\frac{(\delta_p + \delta_t)\ m}{\sqrt{DV_i}}\right]^{0.4} = 1.3 \times 10^{-3}\ \text{seconds}.$$

STRESS DISTRIBUTION IN AN IMPACTING SPHERE

5 A literature survey was made to obtain the stress distribution in an impacting elastic sphere. A report entitled "The Distribution of Stress in a Decelerating Elastic Sphere" by Dean, Sneddon and Parsons (Reference 7) was obtained. This work gives a solution for the problem of an elastic sphere impacting on a soft surface where the area of contact is assumed to be quite large. Although the report has limited application to the problem at hand it is interesting to note that the authors found no major tensile hoop stresses in the impacting sphere.

6 To obtain a more precise estimate of the stress distribution in an elastic sphere, a computer program was written to evaluate the basic equilibrium and compatibility equations. The inputs to the program include the diameter of the sphere, the elastic modulus, density and Poisson's ratio of any number of concentric spheres, and the velocity of impact. The output gives a cross section of the stresses and displacements throughout the sphere. Some difficulty has been encountered with the stability of the finite difference portion of the program used to solve this problem and computation results will not be available by the completion date for Phase I.

7 The stress distribution in the sphere may be approximated by calculating the impact acceleration loads using the Hertz laws and assuming a cylinder equal in length to the diameter of the sphere. Figure 4-1 illustrate the epoxy cylinder and transmitter case for the two orientations considered. The density of the reinforced epoxy is $\rho = 0.047$ lb/in^3. The weight of the transmitter is 2 oz = 0.125 lbs.

8 FORCES ON THE TRANSMITTER PACKAGE LOADED ALONG ITS CYLINDRICAL AXIS.

Weight of epoxy A or C $= \frac{\pi (1.375)^2}{4} \times 1.25 \times 0.047$

$= 0.872$ lbs

Weight of transmitter $= 0.125$ lbs

Force required to accelerate A $= 41,400 \times 0.0869 = 3,600$ lbs

Force required to accelerate A and B $= 41,400 \times 0.212 = 8,780$ lbs

The maximum compressive load on the transmitter in this orientation is 8,780 lbs and the average compressive load is 6,190 lbs.

9 FORCES ON THE TRANSMITTER PACKAGE LOADED PERPENDICULAR TO ITS CYLINDRICAL AXIS.

Weight of epoxy D or F $= 0.0785$ lbs

Weight of transmitter $= 0.125$ lbs

Force required to accelerate D $= 41,400 \times 0.0785 = 3,250$ psi

Force required to accelerate D and E $= 41,400 \times 0.203 = 8,400$ lbs

The maximum compressive load on the transmitter in this orientation is 8,400 lbs and the average compressive load on the transmitter is 5,825 lbs.

THE TRANSMITTER CASE

10 The design of the transmitter case illustrated in Figure 4-2 was based on the following considerations:

(a) Work statement limitations on dimensions and weight.

(b) Structural rigidity required to keep the external test sphere stresses from loading the electronic components.

(c) Electrical isolation of the various transmitter stages.

(d) Good thermal conductivity of the partitions to reduce internal hot spots.

(e) Good rf conductivity.

(f) Ease of assembly of components.

11 The material chosen for the transmitter case is high strength aluminum (75ST6) with a 0.0005 to 0.00075 inch thick silver plate. Aluminum was chosen because of its high strength-to-weight ratio and its good thermal conductivity. The case was silver plated to increase the surface conductivity and to facilitate soldering.

STRESSES IN TRANSMITTER CASE AND POTTED COMPONENTS

12 The stresses in the case and in the components must be determined differently for the axial and perpendicular loadings of the transmitter case. The stresses produced when the transmitter is loaded parallel to its cylindrical axis can be calculated theoretically. However, the loading of the transmitter perpendicular to its cylindrical axis is a very complicated calculation. In the latter case an experiment was performed using strain gauges potted inside a dummy transmitter case,and loads applied using the Compression Tester.

13 LOADING OF TRANSMITTER CASE ALONG THE CYLINDRICAL AXIS. The maximum load on the transmitter case calculated previously was 8,780 lbs. This is equivalent to a stress of 5,950 psi on the ends of the transmitter case. See Figure 4-1.

Density of Potted electronics = $0.04\ lb/in^3$

Area of aluminum in compression A_{Al} = $0.632\ in^2$

Area of plastic in compression A_{Pl} = $0.853\ in^2$

Elastic modules of aluminum E_{Al} = 10×10^6 psi

Elastic modules of plastic E_{Pl} = 5×10^5 psi

S_{Al} and S_{Pl} represent the stress in the aluminum and plastic respectively.

$$S_{Al} = S_{Pl} + \frac{E_{Al}}{E_{Pl}}$$

$$S_{Al} + S_{Pl} = 5,950 \text{ psi}$$

$$S_{A1} = (5,950 - S_{A1}) \frac{10 \times 10^6}{5 \times 10^5}$$

$$S_{A1} = 5,670 \text{ psi}$$

$$S_{P1} = 280 \text{ psi}$$

The stress in the plastic due to the acceleration loading on its own weight

$$= 0.04 \times 41,400 \times 0.75$$
$$= 1,240 \text{ psi}$$

Therefore the total loading on the encapsulated components equals 1,520 psi.

14 LOADING OF TRANSMITTER CASE PERPENDICULAR TO ITS CYLINDRICAL AXIS. It is assumed that the internal partitions of the transmitter case add no strength to the assembly. A transmitter case was produced as shown in Figure 4-2 except that the partitions were not included. Three strain gauges designated A, B and C, were potted in the case in mutually perpendicular planes as shown in Figure 4-3. A load P was applied through the curved blocks which distributed the load along the length of the cylinder. Figure 4-4 gives the strain readings of gauges A, B and C versus load. Strain A is negative and strains B and C are positive. The compressive stresses due to the load P was calculated from

$$S_A = \frac{E}{(1 - 2\mu)(1 + \mu)} \left[(1 - \mu)\, \epsilon_A + \mu\, (\epsilon_B + \epsilon_C) \right]$$

where $E = 5.8 \times 10^5$

$\mu = 0.41$

and the maximum compressive stress versus load, in the transmitter case is shown in Figure 4-5. Under the action of the compressive load of 8,400 lbs, as calculated previously, the maximum compressive stress inside the transmitter case will be 1,500 psi (see Figure 4-5). Added to this will be the stress produced by the "g" loading on the plastic itself.

$$S = 0.75 \text{ inches} \times 0.04 \text{ inches} \times 41,400 = 1,240 \text{ psi}$$

The maximum stress in the transmitter will be 2,740 psi when loaded perpendicular to its cylindrical axis. It is expected that loading of the package on an axis other than parallel or perpendicular to the cylindrical axis will produce stresses intermediate to the previously calculated stress. The maximum stress calculated for loading parallel to, or perpendicular to, the axis of the transmitter case will be 1,520 and 2,740 psi respectively. Thus, the absolute maximum stress to which any component could possibly be subjected, will never exceed 2,740 psi.

SECTION 5

TRANSMITTER CIRCUIT DESIGN

INTRODUCTION

1 Various systems were considered for the high-shock FM transmitter. These included:

(a) A single transistor operating as an LC oscillator. The required output (100 mW) with an efficiency greater than the minimum (15 per cent) specified could easily have been obtained. However, the frequency stability of such a circuit is greatly dependent upon the load, and would not meet stability requirements (±0.03 per cent) for open or short circuit load.

(b) A crystal controlled low power oscillator followed by multiplying and amplifying stages. The stability requirements would be easily met with such a system, but the efficiency requirements might not be. Such a system would be very complex, little experience is available with regard to crystal packaging at the environmental levels dictated by the work statement and there is some doubt as to the frequency stability of an oscillator controlled by a piezoelectric device under varying strain.

(c) An oscillator operating at a lower frequency and followed by multiplying and amplifying stages. Although a crystal is not used, the buffering action of the multiplying and amplifying stages would reduce the effect of load changes on the oscillator frequency. The circuit would be complex, however, and would require careful tuning. Efficiency could also be a problem.

(d) A single transistor oscillating at 250 Mc/s followed by amplifying and buffering stages. Attentuator pads or mismatching may be used to provide buffering but would require a corresponding increase in amplifier gain. The number of amplifying and buffering stages used would be a compromise between frequency stability and efficiency requirements. The circuit would probably need fewer components than systems (b) and (c) and would therefore require the smallest volume.

2 System (d) was considered to be most promising for this application. Initial designs used a single transistor oscillator coupled through an attentuator pad to a single-transistor amplifier. Tests showed (Reference 8) that this circuit was not sufficiently stable and therefore an extra rf amplifying and buffering stage was added. The final circuit is now shown in Figure 5-1. The four stages are a modulator, an oscillator, a buffer amplifier and power amplifier.

THE OSCILLATOR CIRCUITS

3 The frequency stability of the system is primarily determined by the oscillator. A Colpitts configuration is used to obviate the use of tapped inductors. The frequency of oscillation (f) is determined to a first order by

$$f = \frac{1}{2\pi\sqrt{LC}}$$

where L is the inductance of L_1 plus stray inductances, and the associated stray capacities C is the parallel capacitance comprising the series combination of C_3 and C_4. The ratio of C_1 to C_2 determines the feedback applied to the transistor. A rigorous analysis of the circuit is very difficult at these frequencies; partly because the circuit elements are not truly lumped elements and the importance of stray capacity, but principally because the transistor parameters are variable from device to device and most are dependent on frequency and operating conditions. However, consideration of the low-frequency, small-signal analyses that have been applied to the circuit can provide a good insight into the modes of operation and the effects of component variations.

4 Cote (Reference 9) has shown that the frequency of an oscillator having the configuration used is given by

$$(2\pi f)^2 = \frac{1 + n\,(1 + L/C\,\Delta y)}{LC}$$

where $\Delta y = y_i y_o - y_r y_f$

and $n = C_3/C_4$

and y_i, y_o, y_r and y_f are the two-part parameters of the transistor. The analysis assumes that the imaginary components of Δy are negligible.

5 The equation indicates that the ratio L/C should be low so that the effects of variations in the transistor parameters upon the frequency will be minimized.

6 The qualitative analysis of large signal oscillators (References 10 and 11) suggests that a high circuit Q (where $Q = 2\pi fL/R$) is the prime requirement for stability. In view of the nature of Q, the use of large inductances to get a large Q is normally dictated. The net result is at variance with Cote's analysis.

7 A high-Q circuit infers that the frequency shift required to compensate

for a phase change in the feedback loop is small. Since the transistor must have limiting action to constrain the oscillation to some final amplitude, harmonic generation occurs. The net result of these harmonics and their intermodulation products is a phase shift in the fundamental frequency, which varies since the limiting parameters are a function of operating point (Reference 10). It can thus be seen that no hard and fast rule can be applied to the determination of an optimum L/C ratio where transistor parameter variations are concerned.

8 Consideration must also be given to the effect on the frequency of changes in the L and C portions of the circuit under conditions of shock. Calculations in a previous section indicate that the alumina cored inductors should be very stable under shock; similarly, the capacitors are stable components. As the changes under shock to be expected from the stray capacitances and inductances are at present unkonwn, it was decided as an initial compromise to keep the ratios of stray to fixed capacitance, and stray to fixed inductance approximately equal.

9 A comparison of the frequency before and after potting of the oscillator indicated that the stray capacity was about 1 to 2 pF. Calculations of the lead inductance show that it will probably be about 0.005 μH. A reasonable choice then appears to be C = 10 pF and L = 0.05 μH approximately. The inductance value quoted represents about three turns on the alumina cores used.

10 Cote (Reference 9) also gives an equation for the ratio n; where

$$n = \frac{y_i}{y_k + y_i}\left[1 + \sqrt{1 + \frac{y_k + y_i}{y_o}}\right]$$

where $y_k = y_f + y_r$

Substitution of the real parts of the y parameters taken from the data sheets for the transistor used (2N3663) gives a value of $n = 1.3$, however this is only an approximate value.

11 In practice, it was found that the values shown in the circuit diagram (Figure 5-1) produced the most satisfactory results. The ratio of capacity however, was not critical as oscillations were provided using a wide variation in ratios. The capacitance of C_3 and C_4, together with the output capacitance of the transistor, the tuning capacitance and the stray capacitance bring C up to 12 pF (approximately) which is close to the stated desired value.

12 The output is loosely coupled to the next stage via C_5 such that 2.5 mW of power would be delivered into a 50 ohm load.

MODULATOR

13 In order to frequency modulate the transmitter, a variable reactance element is required. A varactor was considered for this application but it was decided that the associated circuitry would be too complex and bulky for this application. A simpler method is to utilize the dependence of the transistor output capacity upon its collector-to-base voltage. A curve of the obtainable variation is shown in Figure 5-2. To provide linear modulation, a square-law relationship of capacity to voltage is required if

$$f \propto \frac{1}{\sqrt{C}} \propto V_m$$

where V_m = modulation voltage

then $$C = \frac{K}{V_m^2}$$

where K is a constant. The collector-base capacity variation is sufficiently close to this relationship to give negligible errors under small-signal conditions.

14 During the bread-board stages of the design, a ramp generator was used to check the linearity of modulation. The use of the generator is described in the first progress report, and although the circuit is straight forward, a brief description will be included here for the sake of completeness. One half of the ramp generator (Figure 5-3) uses a bootstrapped unijunction transistor to provide a linear sawtooth waveform which is available at output 1. The other half provides a constant voltage source for use as a bias supply for experimental oscillators. The voltage amplitude may be varied by VR2. A small portion of the ramp voltage is superimposed on the bias voltage in order to check modulation sensitivities and linearities. The ramp waveform is shown in Figure 5-4.

15 The specifications call for the frequency response to be 3 dB down at 5 c/s and 10 Kc/s. If the modulator were ac-coupled, high-value capacitors would be required to provide sufficient low-frequency response (for an input impedance of 100 K the series capacitor would need a value greater than 0.32 μF). Since large-value ceramic or glass capacitors are not available, some other type of capacitor would be required. Such types have not yet been fully environmentally tested but it is suspected that they might show considerable parameter changes under stress. However, stable resistors have been found and it was decided to dc-couple the modulator to the oscillator. The operation of the modulator circuit is described in Paragraphs 16 and 17 with references made to Figure 5-1.

16 MODULATOR CIRCUIT. Transistor Q_1 provides a nominally constant current through R_8 and thus defines the base voltage of the oscillator transistor Q_2. Any modulation voltage applied to the input resistors R_1 and R_2 will vary the current through R_8 and thus will vary the base voltage of Q_2. As only a few hundred millivolts of signal are required at the base of Q_2, the overall gain of the modulator is much less than one. High-value input resistors can thus be used together with some negative feedback (via R_4 and R_5) which tends to make the amplifier independent of transistor parameters. Since the bias voltage must be stable and independent of power supply voltages, both the modulator and oscillator require a regulated supply. The Zener diode CR_1 provides a regulated 8.2 v. The Zener is supplied via the voltage dropping resistors R_{10}, R_{11} and R_{12}. In earlier designs, the buffer amplifier was used to provide the voltage drop, but problems were encountered in decoupling the amplifier and oscillator since the regulated rail was then a virtual ground. The present configuration alleviates the decoupling problem. The efficiency of the overall transmitter is relatively unchanged since the current to the buffer amplifier has been reduced and the principal power dissipation takes place in the power amplifier. The diodes D_1 and D_2 provide temperature compensation for changes in the base-emitter voltages of Q_1 and Q_2.

17 BUFFER AND POWER AMPLIFIER CIRCUITS. The rf amplifier stages are connected in common-emitter configurations. This configuration was chosen because of the greater stability obtainable at this frequency compared to that of common-base stages. Larger amplifier gains than are obtained in the present circuit, have been obtained on breadboards using common-base stages, but these prototype stages were critical with regard to tuning and layout and were not satisfactory for this application. The required gain was obtained from the amplifiers by tuning the emitter lead inductances with the bypass capacitors (C_8 and C_{12}) so that the combination formed a series resonant circuit at the operating frequency. The capacitor values were chosen to produce the maximum gain. A 2N3663 transistor is used for the first amplifying stage, since the power levels involved are low. About 15 mW of rf is available when connected to a 50 ohms load. A 2N3866 transistor is used in the last stage. It is a high-gain overlay type and is run well within its specified ratings. The diodes (D_3, D_4 and D_5) in its base circuit are used to provide a constant base-potential so that the emitter current is stabilized against temperature variations. Approximately 20 mA (at 16 volts) are drawn by this stage. At 24 volts about 35 mA are drawn. The increase is chiefly due to extra biasing arising from the increased power from the buffer amplifier. The power amplifier is coupled to the buffer amplifier via the capacitive divider C_9 and C_{10}. The load is coupled to the power amplifier via C_{13} and C_{14}. These capacitors were all chosen to provide optimum power output and optimum buffering.

TEMPERATURE RISE IN TRANSMITTER CASE

18 To determine whether the transmitter could be operated in a vacuum of 10^{-6} mm of mercury without exceeding the maximum case temperature of 140 degrees F, two hollow aluminum cases having the specified transmitter dimensions of 1-3/8 inch diameter by 1 inch long were manufactured. The outside surface of one unit was black anodized while the other was polished. Two-watt resistors were potted in RDD5 into each case along with thermistors to measure the temperature on the inside surface of the resistor.

19 The two cases were mounted, in turn, in a vacuum chamber and the internal and case temperatures were monitored when 1.5 watts of power dissipated in each case. The results are shown in Figure 5-5 and 5-6. A vacuum of 1/2 mm was the capability of the available system but it was found that the pressure could be increased to 40 mm before there was any noticeable change in the case temperature. This result showed that the effect of convection cooling was negligible at 0.5 mm pressures and thus that the test data is valid and represents the performance of the system.

20 To provide a closer approximation to an isothermal enclosure the inside surface of the bell jar was blackened. The reduction in the case temperature was not great and it is shown in Figures 5-5 and 5-6.

21 Figure 5-7 shows the temperature rise due to plastic exotherm at the center and/or the surface when the above cases were potted with RDD5 plastic.

CONSTRUCTION OF THE TRANSMITTER

22 The physical layout of the transmitter can be seen in the Figures 5-8 to 5-13 inclusive.

23 Each section (modulator, oscillator, buffer amplifier and power amplifier) was constructed in a separate compartment. This reduces undesirable interactions between sections. The diodes were thinly coated with RTV silastic rubber before potting. The 2N3663 transistor cases were filed down to half their original size. Filing the cases does not affect their electrical properties and considerably eased the problem of mounting them in the available space. The other transistors were pre-potted with M16 plastic and their size was then reduced. In particular, the 2N3866 transistor was converted to a disk approximately 1/8 inch thick. It would have been desirable to mount this transistor in one of the partitions or in the base of the transmitter case in order to improve heat dissipation, however,

the collector is electrically connected to the case and electrical insulation would have had to be provided. Sufficient heat conduction through the plastic to the case walls has been provided by positioning the transistor close to a partition. Cooling is also assisted by the relatively large surface area of the transistor case.

24 An alumina-cored coil is used in the oscillator and wire-wound coils are used in the amplifying stages. The coils are mounted as far from the compartment walls as possible to reduce stray capacity and to minimize magnetic interaction with the walls.

25 Ground connections are made to brass terminals which are mounted in and soldered to the silver-plated partitions and base. DC supply lines between compartments are carried via rf chokes. Output and input cables are brought in through holes in the base.

26 The initial tuning of the transmitter was performed with variable capacitors in place of C_1, C_6, C_7, C_{10} and C_{11} and with the case removed. The variable capacitors were then replaced by the equivalent fixed capacitors. During potting, which was performed on one section at a time, the tuning capacitor was replaced with a silastic rubber plug. When the plastic had cured, the silastic plug was replaced with a fixed capacitor of the correct value. A guide to this value was given by the final setting of the variable capacitor, but did not correspond exactly as the tuning was affected by the potting.

27 The last adjustment that was made was to the value of R_1 to produce the correct value of modulation sensitivity. When that resistor had been chosen and mounted, the modulator section was potted, together with the small spaces around the tuning capacitors in the other compartments. The final operation was to place the transmitter into its case and tighten the fixing screws.

SECTION 6

TRANSMITTER ELECTRICAL TESTS

TEST EQUIPMENT

1 The equipment used for the tests, was as follows:

Manufacturer	Instrument	Type No.
Polarad	Signal Analyzer	SA-84
Hewlett Packard	Frequency Counter	5245L
Hewlett Packard	Frequency Converter	52538
Hewlett Packard	Digital Voltmeter	3440A
Hewlett Packard	Vacuum Tube Voltmeter	400D
Hewlett Packard	Vacuum Tube Voltmeter	410C
Hewlett Packard	Bolometer	430C
General Radio	Attenuators	874
Communication Elect. Inc.	Receiver	501
General Radio	Impedance Bridge	1608A
Fisher	Thermometer (0 to 200 degrees F)	

TESTING

2 Each of the following tests was performed at three different temperatures, at atmospheric pressure. Each test was also performed at 140 degrees F in a vacuum of better than 10^{-5} mm of mercury.

3 The case temperature was measured by a thermistor which was glued to the case. During the tests the thermistor resistance was measured with the impedance bridge. The thermistor was calibrated against the thermistor by placing both in a thermostatically controlled oven.

4 During the tests the case temperature tended to increase due to the heat dissipation from the transmitter. This was obviated by reducing the oven temperature sufficiently to maintain the case temperature to within ±2 degrees F of the required value. In the vacuum tests the case temperature was maintained at the correct value by using radiant heat from two heat-lamps.

5 WARM-UP TESTS. After the temperature had stabilized, the transmitter was switched on. A power supply voltage of 20.00 volts was used for all tests. The results showed a maximum warm-up time of 1.5 minutes (see Figure 6-1) time was defined as the time between switch on and that time

when the frequency drift was less than 10 Kc/s per 5 minutes.

6 FREQUENCY CHANGE WITH TEMPERATURE. Figure 6-2 (upper curve) shows the variation of transmitter frequency with variation in temperature. This test was not required in the work statement but was added for completeness.

7 FREQUENCY CHANGE WITH VOLTAGE. Figure 6-2 (lower curve) shows the variation of transmitter frequency with variation of power supply voltage at three different ambient temperatures and at the highest temperature in a vacuum. These results are much better than those called for in the work statement.

8 POWER OUTPUT Vs POWER SUPPLY VOLTAGE. Figure 6-3 (upper curve) shows the variations in output power with variation of power supply voltage. The power output was lower than would normally be the case as the transmitter became slightly detuned during the final potting process and no time was available in which to make the necessary corrections. The values in the vacuum were lower than those in air at 140 degrees F. The cause of this was a mismatch in the cable connector in the wall of the vacuum chamber; a pressure-tight coaxial connector was not available.

9 EFFICIENCY Vs POWER SUPPLY VOLTAGE. Curves showing the variations in efficiency with power supply voltage are shown in Figure 6-3 (lower curve). The efficiency was lower than normal for the same reasons that the power output was low.

10 EFFECT OF LOAD VARIATIONS. Table 6-1 shows the effect of open-circuit and short-circuit loads at three power supply voltages under the four environmental conditions. The detuning of the transmitter mentioned earlier (Paragraph 8) had an adverse effect upon these results. The mismatch in the connector also affected the characteristics under vacuum conditions.

11 MODULATION SENSITIVITY. The modulation sensitivity was determined by applying a sinosoidal voltage to the modulation input and measuring the output voltage of the receiver. The two voltages were both measured with the same VTVM. An incorrect figure was used for the receiver discriminator voltage/frequency characteristic and there was also a slight shift in modulation sensitivity during the final potting process. For these reasons the modulation sensitivity of this transmitter was higher than is required by the work study. However, deviations from this value will have the same significance as if the exact sensitivity required had been obtained. The results are given in Figure 6-4. The change in modulation sensitivity at lower supply voltages is due to an increase in the Zener diode impedance

Temperature (°F)	V_{PS}	Frequency Shift (Kc/s)	
		Short Circuit	Open Circuit
32	16	+280	-180
	20	+270	-60
	24	+270	-60
69	16	+250	-100
	20	+200	-80
	24	+430	0
140	16	+210	-70
	20	+140	-40
	24	+120	-120
140 in vacuum	16	-30	+290
	20	0	+350
	24	+10	+230

Table 6-1. Frequency Shift with Change in Load

thereby causing a reduction in gain of the modulation circuit. On later models the zener impedance can be held to a sufficiently low value merely by increasing the bias by one milliamp. The efficiency of the transmitter will be only slightly degraded. During final construction of the transmitter a problem was encountered with feedback from the amplifiers into the modulator section. The problem is one of decoupling and ground currents, and can be solved by modifying the layout. The feedback caused large variations in modulation sensitivity with voltage and temperature. It was confirmed that feedback was the cause by disconnecting the amplifiers. When tested alone and together,the modulator and oscillator showed no noticeable change in modulation sensitivity with either voltage or temperature.

12 MODULATION LINEARITY. Figure 6-5 shows the excellent linearity of the modulation mechanism. The linearity was measured with the same equipment that was used to measure the modulation sensitivity.

13 MODULATION BANDWIDTH. The bandwidth was determined by applying a constant-amplitude, variable-frequency signal to the input of the transmitter, and comparing the ratio of the output voltage from the receiver

discriminator with the input voltage to the modulator. The results are shown in Figure 6-6. The low frequency roll-off is due to the voltmeter since the modulator possessed a flat response to dc.

14 SPURIOUS RADIATIONS. The results of tests on the transmitter using the spectrum analyzer are shown in Table 6-2. The transmitter was terminated in a loss pad which served to present the spectrum analyzer with a signal at a level below its saturation point.

Fundamental Power = 0 dB

SPURIOUS RADIATIONS	POWER SUPPLY VOLTAGE	
	16 v	24 v
Spurious FM of fundamental	< -50 dB	-50 dB
Second Harmonic	-53 dB	-50 dB
Third Harmonic	-63 dB	-60 dB

Table 6-2. Fundamental Radiations

15 INPUT IMPEDANCE. The input impedance was measured by increasing the source impedance of the signal generator feeding the modulator, until the measured output from the receiver dropped to half value. At 1 kc/s the input impedance was found to be 140 kilohms.

SUMMARY OF RESULTS

16 The results described in the preceeding sections were obtained from one completed engineering model. As described above, its performance differed from that predicted from breadboard test results. The causes of the differences have been determined and, with the experience gained in the construction of this transmitter, future transmitters shall meet all specifications. The transmitter is well within specification in most respects, and breadboard models have proved capable of meeting all specifications. For example, with minimum power outputs of 120 mW and minimum efficiencies of 18 per cent.

SECTION 7

CONCLUSIONS

1 The Phase I component-qualification program has evaluated the shock-resistance of a large number of components over a wide range of dynamic shock conditions. From this work a number of components have been selected as having maximum stability, and are therefore considered suitable for the final evaluation program of the transmitter under shock conditions. A brief summary of the test results is given in Table 7-1. Although stable components are now available the actual stability of the transmitter can only be assessed under the shock condition specified in Phase II of the program since an analysis of the transmitter circuit with small variations in component value is difficult, and the stress distribution within the transmitter package is unpredictable.

2 The plastic survey and testing program was conducted with a broad scope and two plastics emerged: one suitable as an encapsulant for the transmitter and the other for manufacturing Phase II test spheres. Emerson and Cummings 1090 plastic with its high "Eccosphere" content has good mechanical properties at all temperatures, low density, good electrical properties and, because of its low plastic content, is thought to possess more stable electrical characteristics in a high stress environment.

3 RDD5 plastic with a viscosity improver has been chosen for the manufacture of the reinforced spheres required for Phase II testing. One sphere has been constructed and, although incomplete wiring of the fiberglass reinforcement occurred, the problems associated with sphere manufacture are understood. The six-inch compressed-air-gun is available, with suitable instrumentation, to launch the Phase II test spheres.

4 The transmitter in its breadboard form has met all the specifications for Phase I; in the final prototype transmitter, only characteristics associated with rf decoupling between stages and final tuning techniques are slightly below these specifications. The necessary modifications would have been included in the final potted prototype had time permitted. The experience gained by Computing Devices' personnel in rf technology and materials, during the assembly of the final prototype, will ensure the success of the transmitter needed for the Phase II testing program.

5 In conclusion, all aspects of the work carried out in Phase I indicate the excellent chances of success in the shock and vibration testing required in Phase II. Components, plastics, transmitter design, impact test facilities and instrumentation, and Company experience are presently available for Phase II.

Component	Manufacturer	Type	Effect of Orientation	Change under 2500 psi stress pulse	Remarks
Resistor	American Technical Ceramics	Ceradot 1/10 watt	Very small	0.1%	
Capacitor	Vitramon Corning Glass Works	VY CY10	Very small Small	0.04% 0.04%	
Diode	TRW	PD101	None	Forward voltage change very small	Silastic coated
Zener diode	TRW	PD6014	None	Zener voltage change 0.002%	Typical Zener silastic coated
Transistor	General Electric	2N2933	Very small	Collector voltage changed 10 millivolts	A typical Encapsulated transistor
R.F. Choke	J.W. Millar Co.	9230	-	No change in dc resistance	Only tested for dc reliability

Table 7-1. Summary of Component Test Results

REFERENCES

1. C.A. Harper "Resins for Embedding Microelectronic Devices" I.E.E.E. Transactions on Component Parts, March 1964.

2. H.P. Tardif and H. Marquis, "Some Dynamic Properties of Plastics" Canadian Aeronautics and Space Journal, September 1963.

3. Lester A. Cohen, "Are You Evaluating Thermoplastics Properly" Materials in Design Engineering, June 1964.

4. G.H. Sherrard and C.A. Murray, "High Performance Reinforced Plastics", Machine Design, May 23, 1963.

5. William J. Ehner, "Thermoplastic Parts" Machine Design, August 29, 1963.

6. John Locke McCarty and Huey D. Carden, "Impact Characteristics of Various Materials Obtained by an Acceleration-Time-History Technique Applicable To Evaluating Remote Targets", Langley Research Center, Langley Station, Hampton, Va. NASA Technical Note TND-1269.

7. W.R. Dean, I.N. Sneddon and H.W. Parsons, "The Distribution of Stress in a Decelerating Elastic Sphere", Theoretical Research Report No. 33/44. Armament Research Department, Fort Halstead, Kent, England

8. "High-Shock FM Transmitter Progress Report No.PR-1" issued by Space Sciences Division of Computing Devices of Canada Limited.

9. A.J. Cote, "Matrix Analysis of Oscillators and Transistor Applications". IRE trains on circuit theory. P181, September 1958.

10. "A handbook of selected semiconductor circuits". No. bsr 73231. Bureau of Ships, Department of the Navy.

11. "Transistor circuit design", Texas Instruments Limited. McGraw-Hill Book Co. Ltd. Lib. of Congress Cat. Card No. 62-19766.

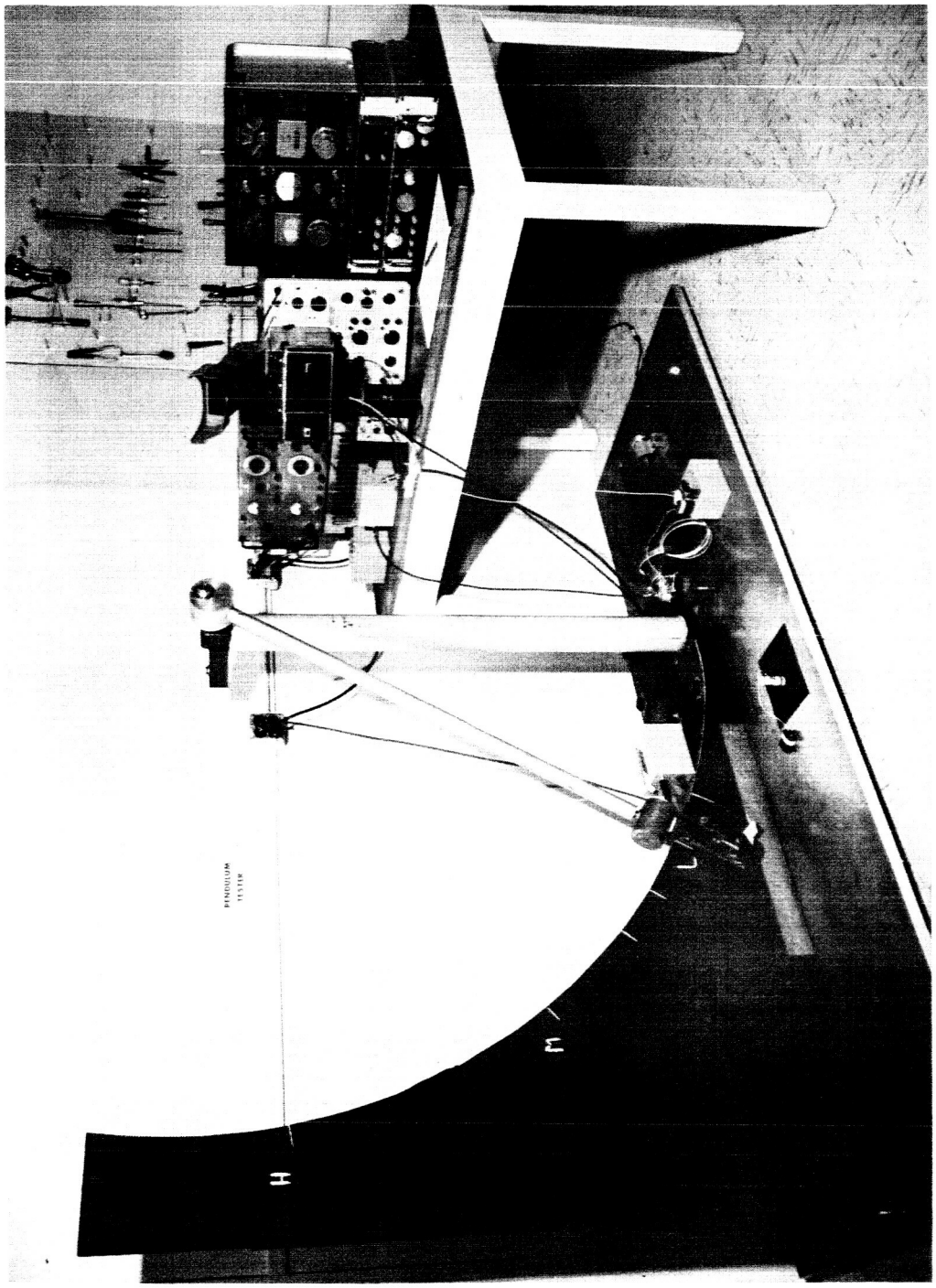

Figure 1-1. Pendulum Impact Tester

Figure 1-1.

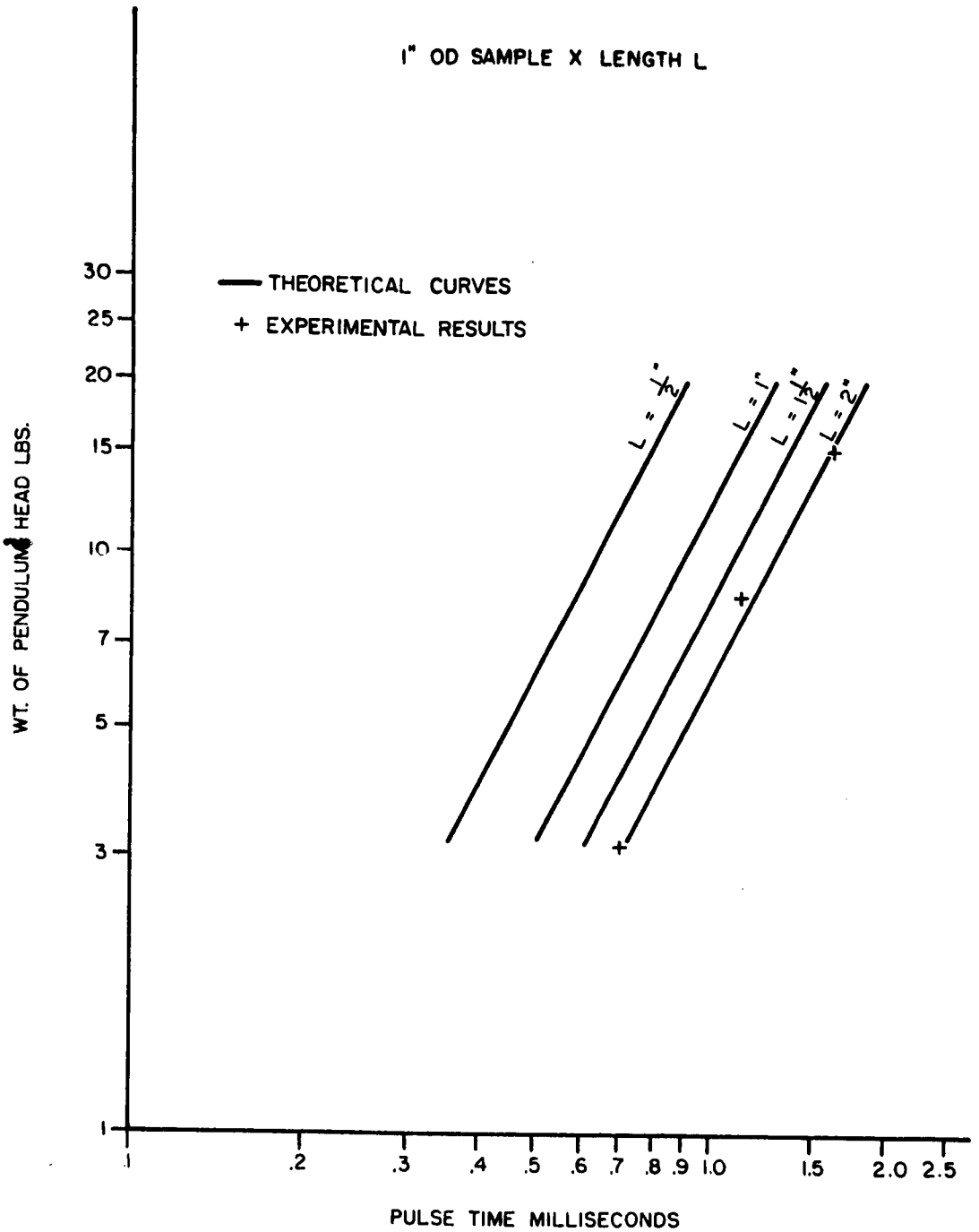

Figure 1-2. Stress Duration Curves for Pendulum Impact Tester

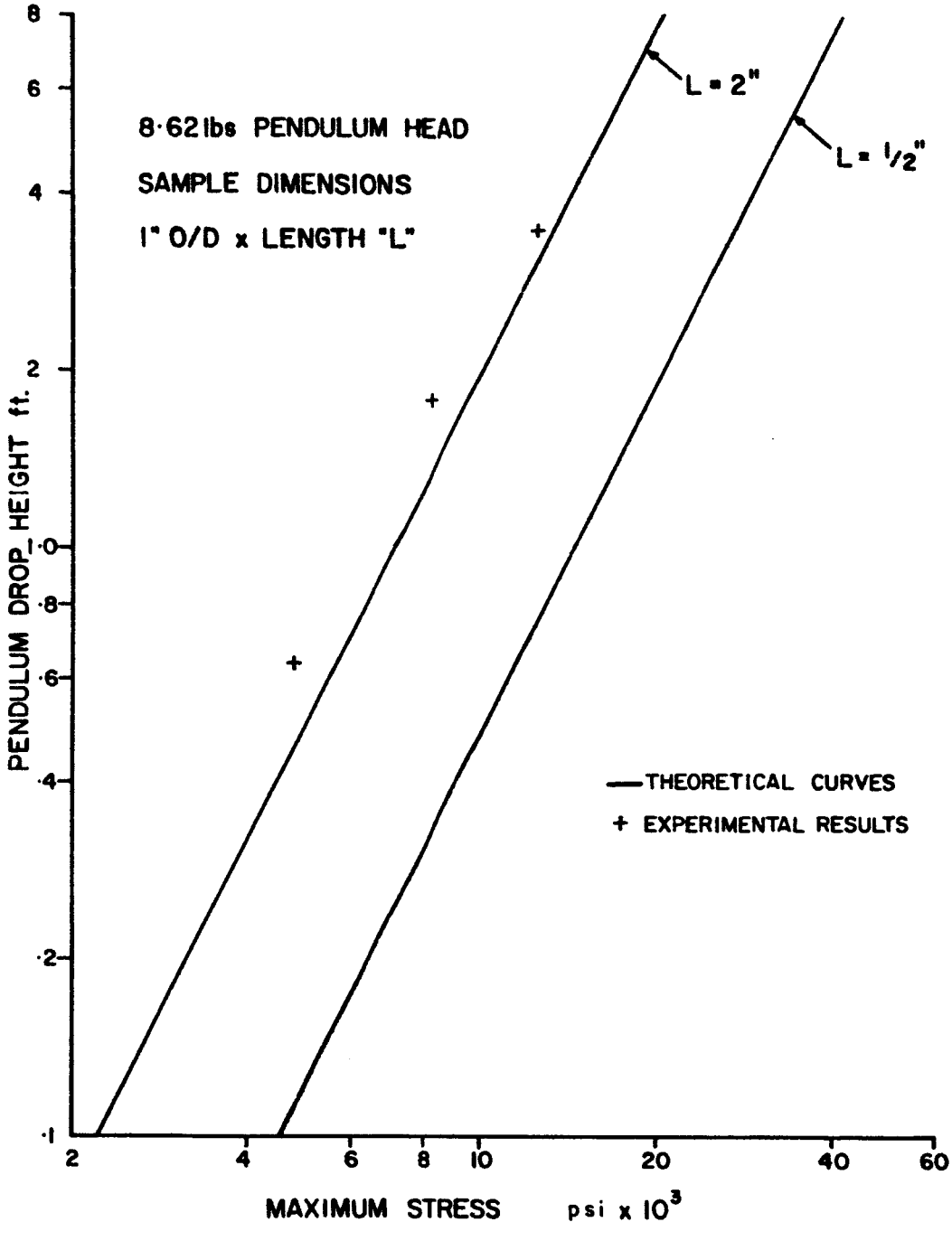

Figure 1-3. Peak Dynamic Stress Curves for Pendulum Impact Tester

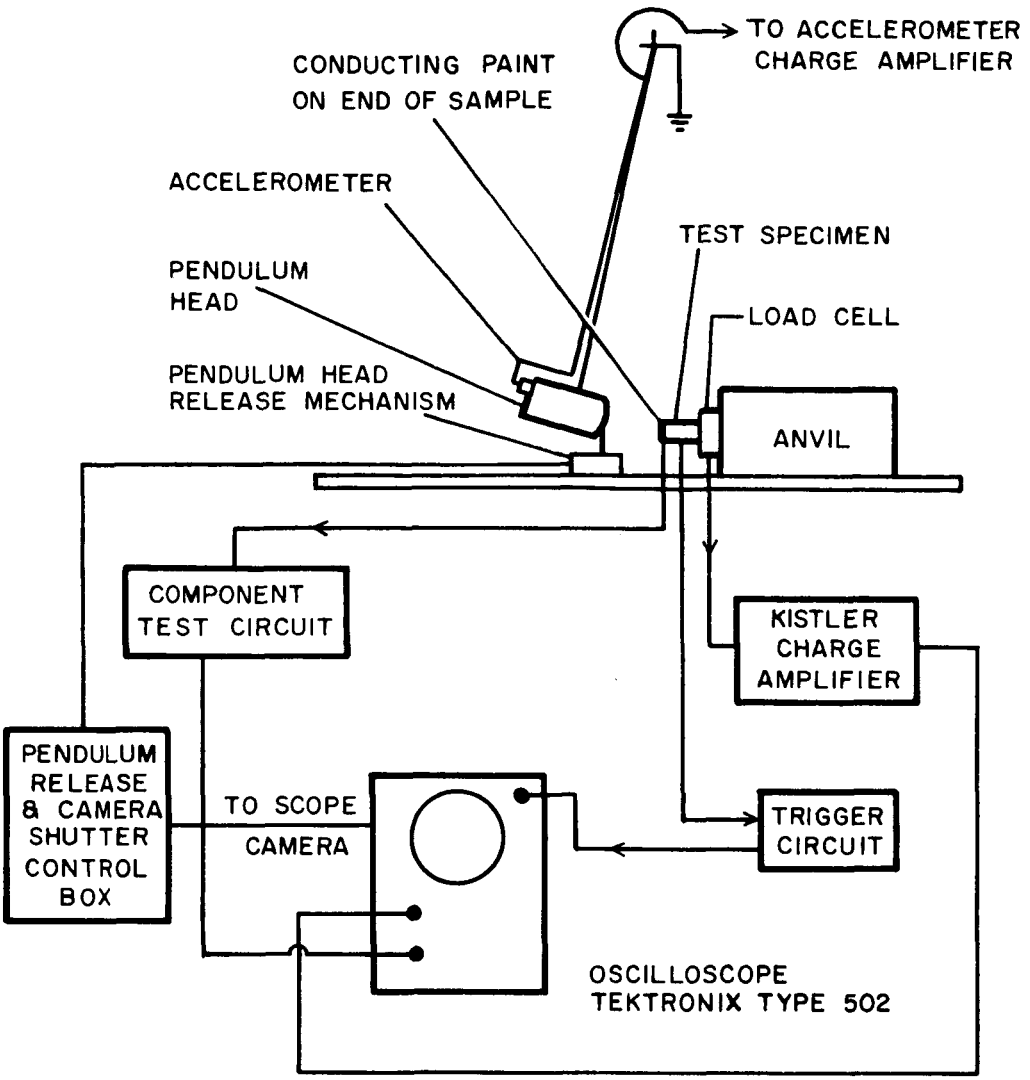

Figure 1-4. Block Diagram of Pendulum Impact Tester

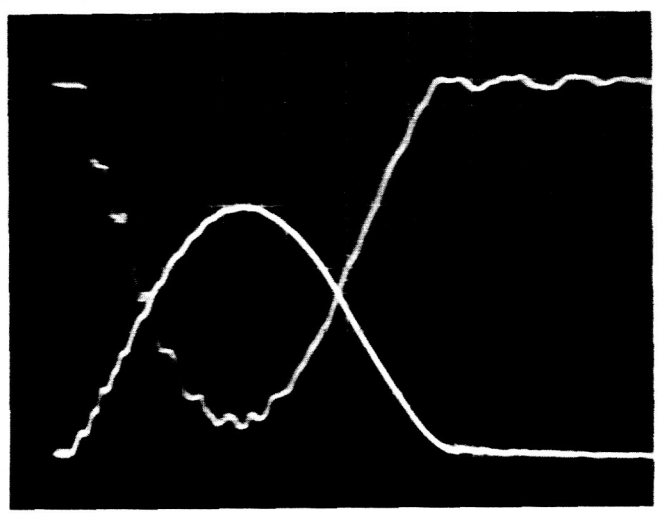

Dynamic Properties of RDD5

Hood strain output from pendulum tester
Upper trace load 2,000 lbs/cm
Sweep time 0.2 milliseconds/cm

Figure 1-5. Load Cell - Strain Gauge Comparison

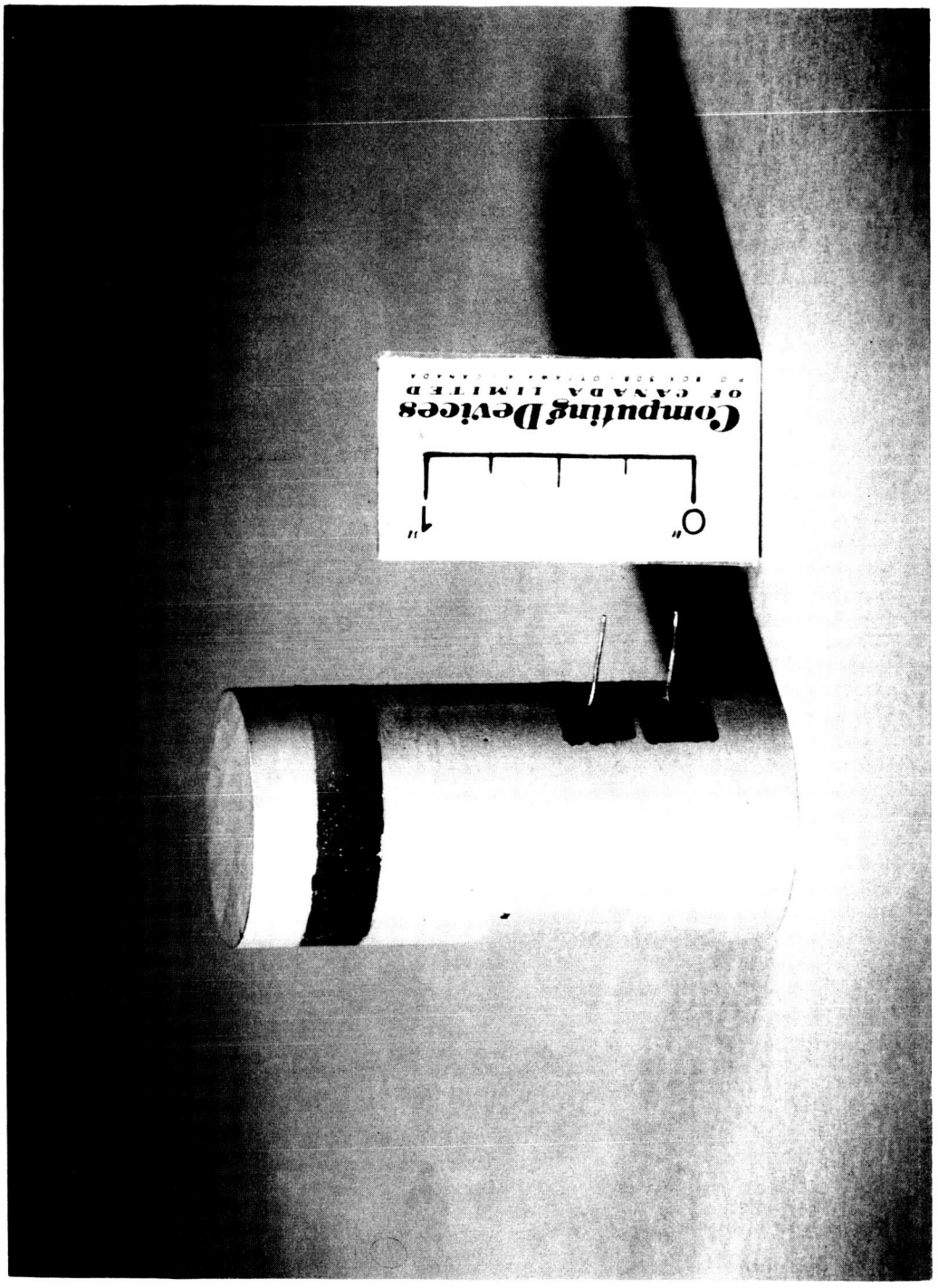

Figure 1-6. Typical Test Package

Figure 1-6.

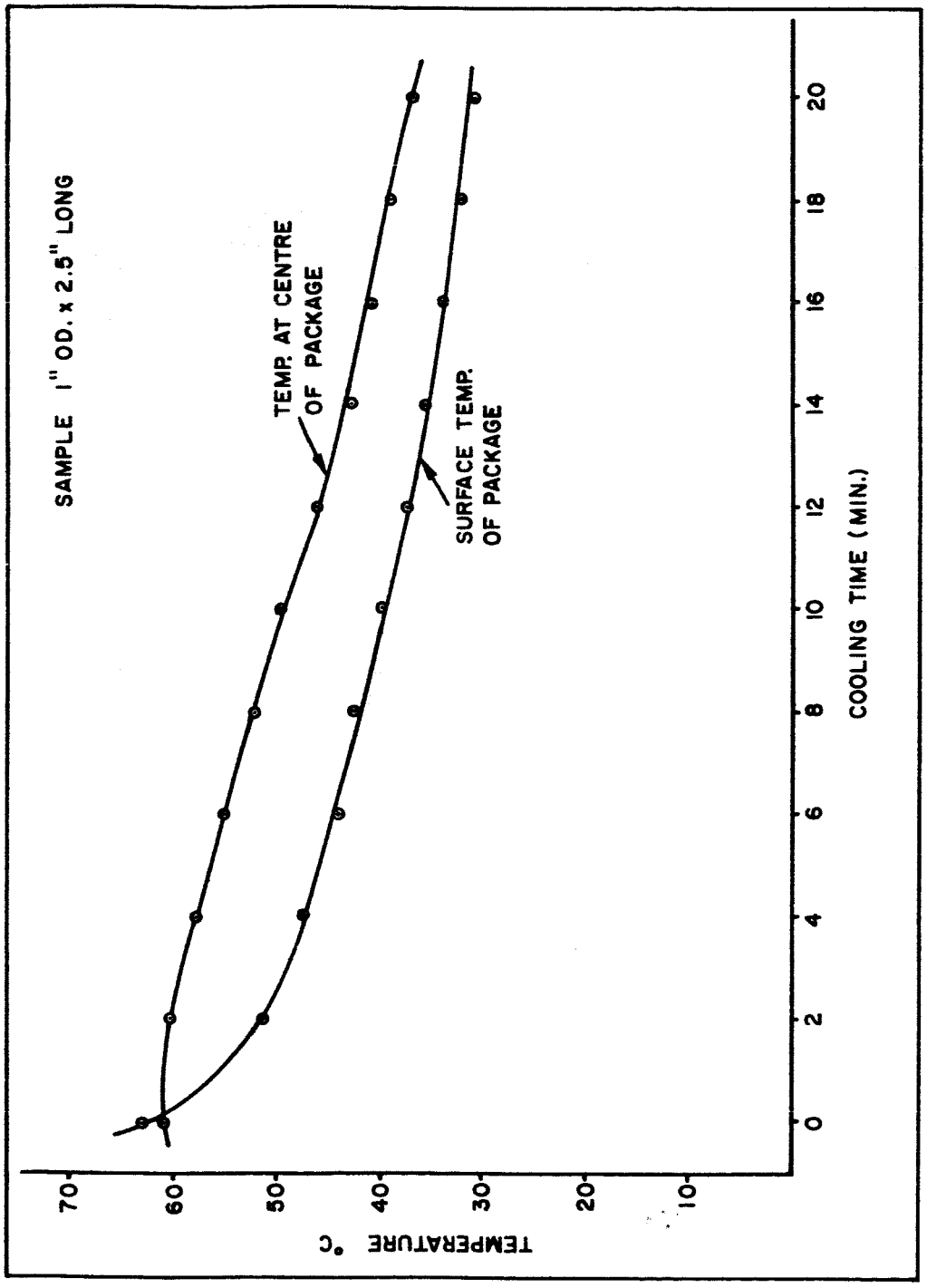

Figure 1-7. Cooling Rate of RDD5 Test Package

Figure 1-7.

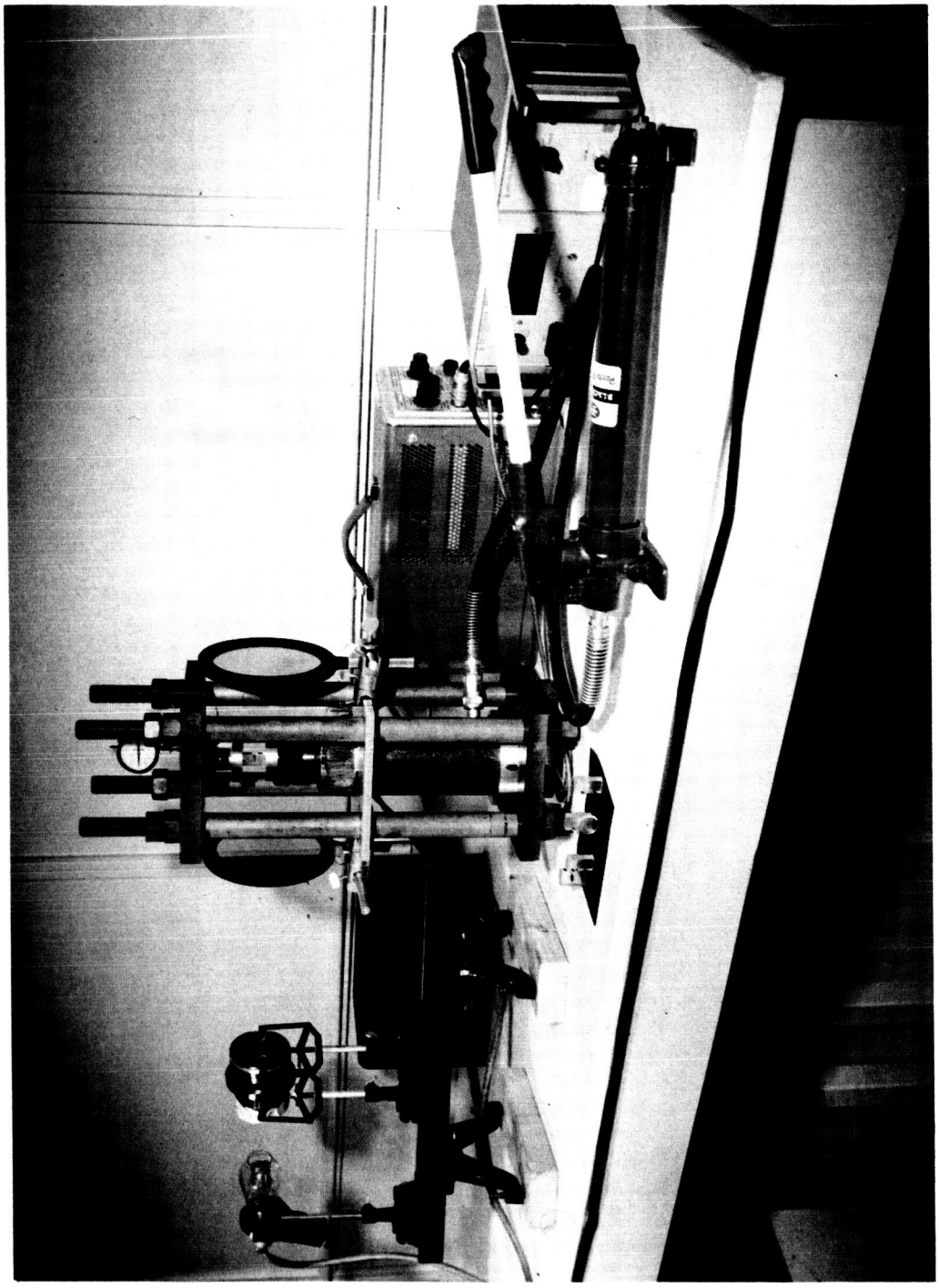

Figure 1-8. Compression Tester with Photo stress Instrumentation

Figure 1-8.

Figure 1-9. Six-inch Compressed Air Gun

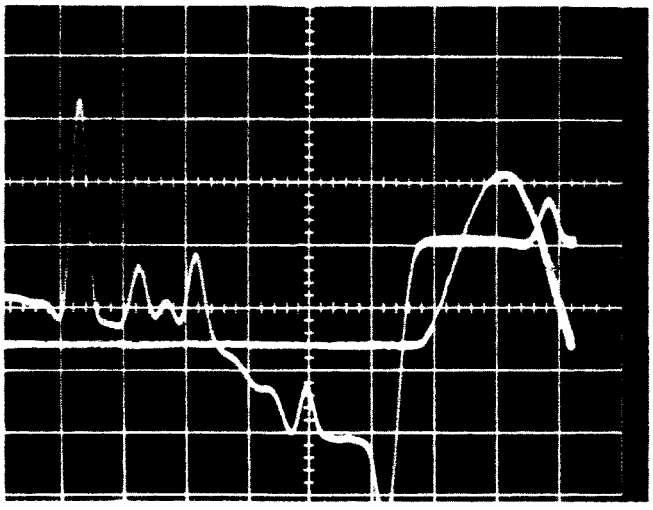

Figure 2-1. Capacitor Test Record Showing Stray Surface Charge Effect

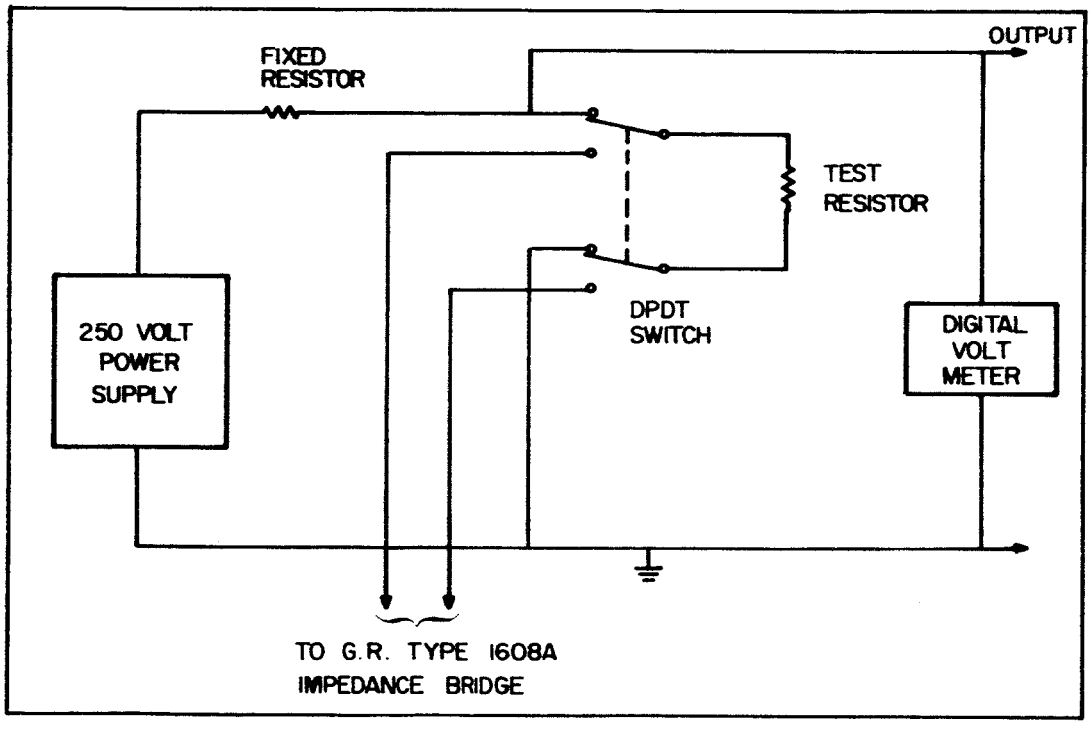

Figure 2-2. Circuit Diagram for Resistor Tests

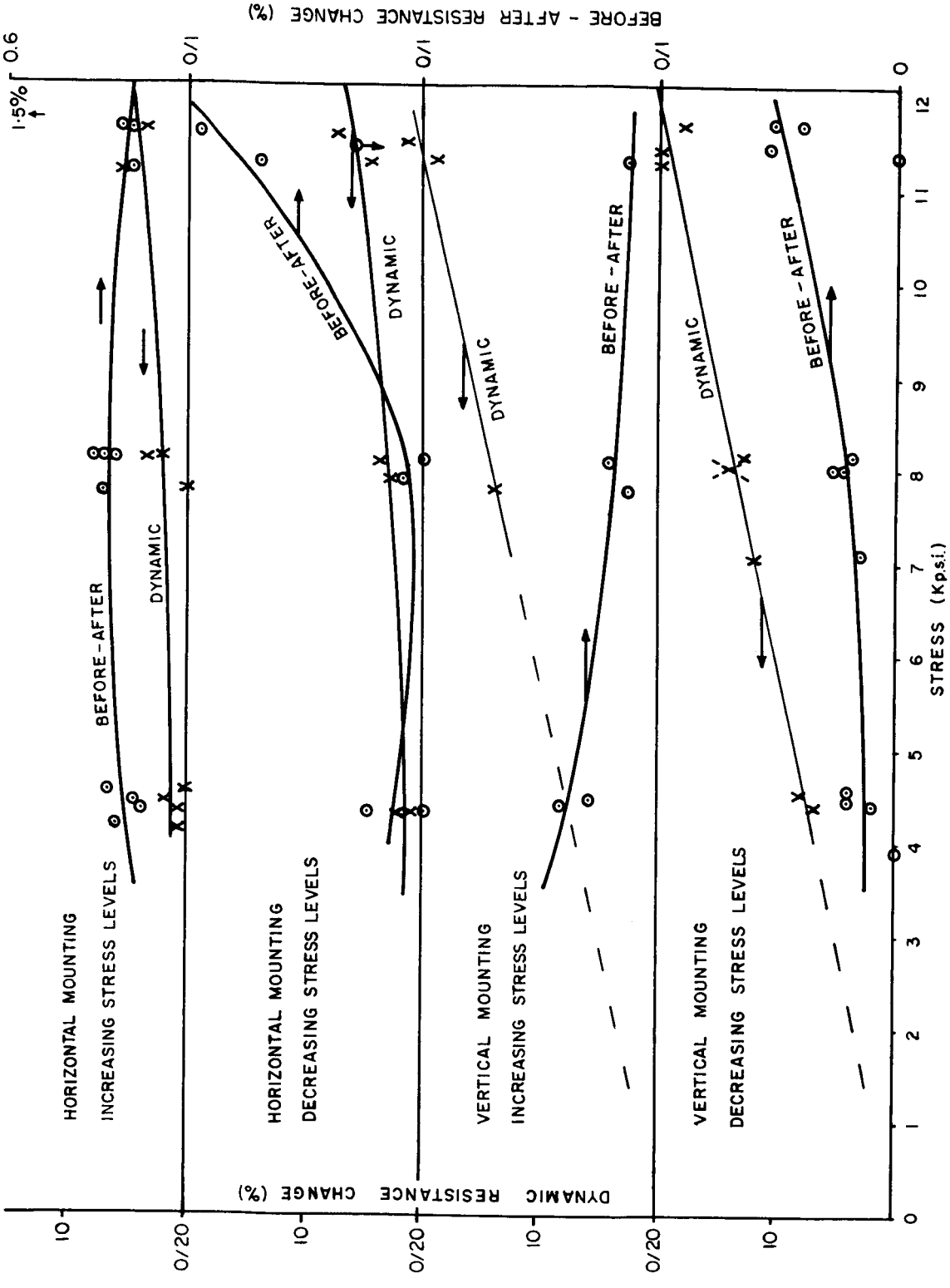

Figure 2-3. Impact Tests on IRC Carbon 1/4 Watt Resistor at Room Temperature

Figure 2-3.

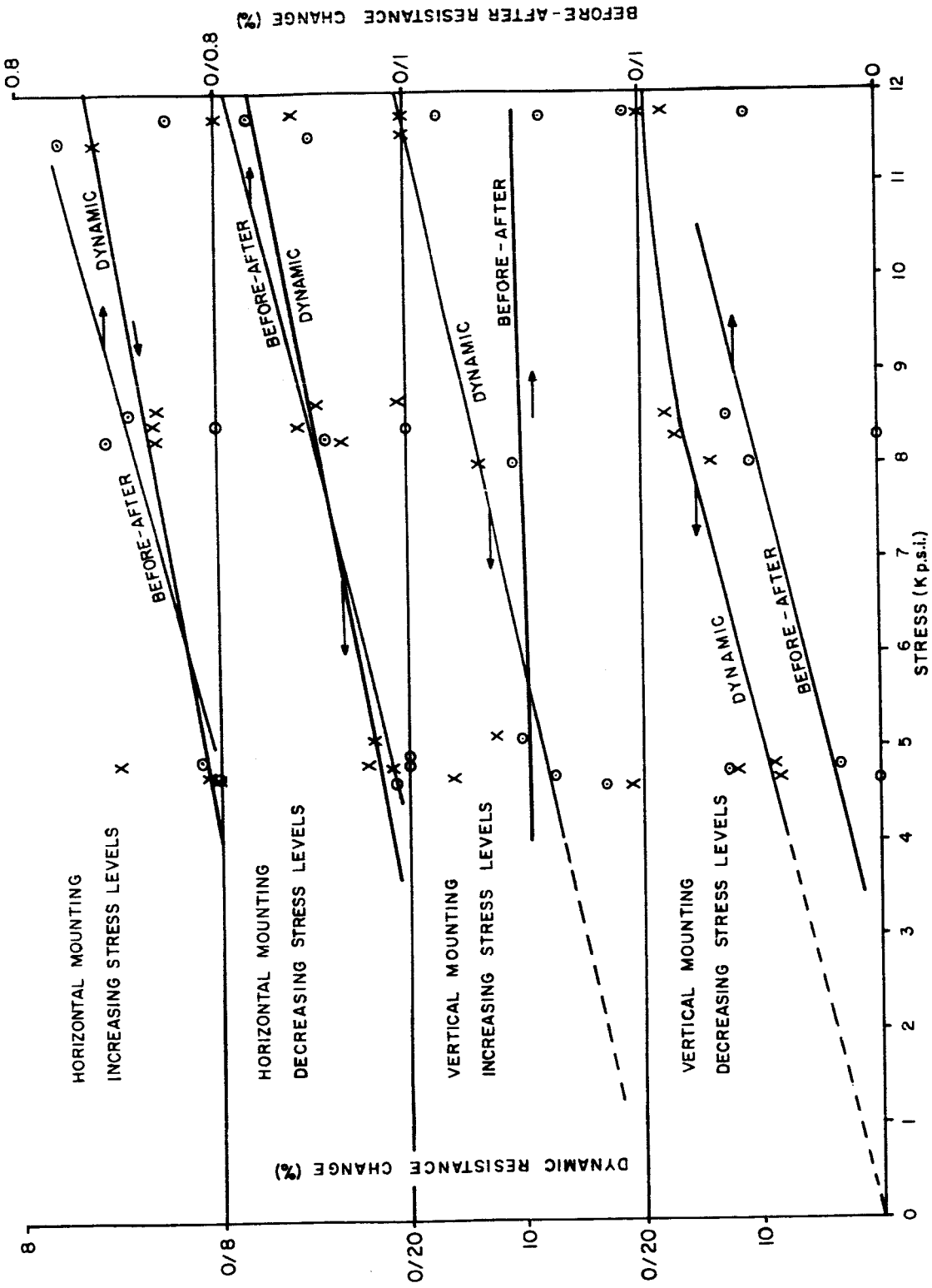

Figure 2-4. Impact Tests on IRC Carbon 1/4 Watt Resistor (with fiberglass sleeve) at Room Temperature

Figure 2-4.

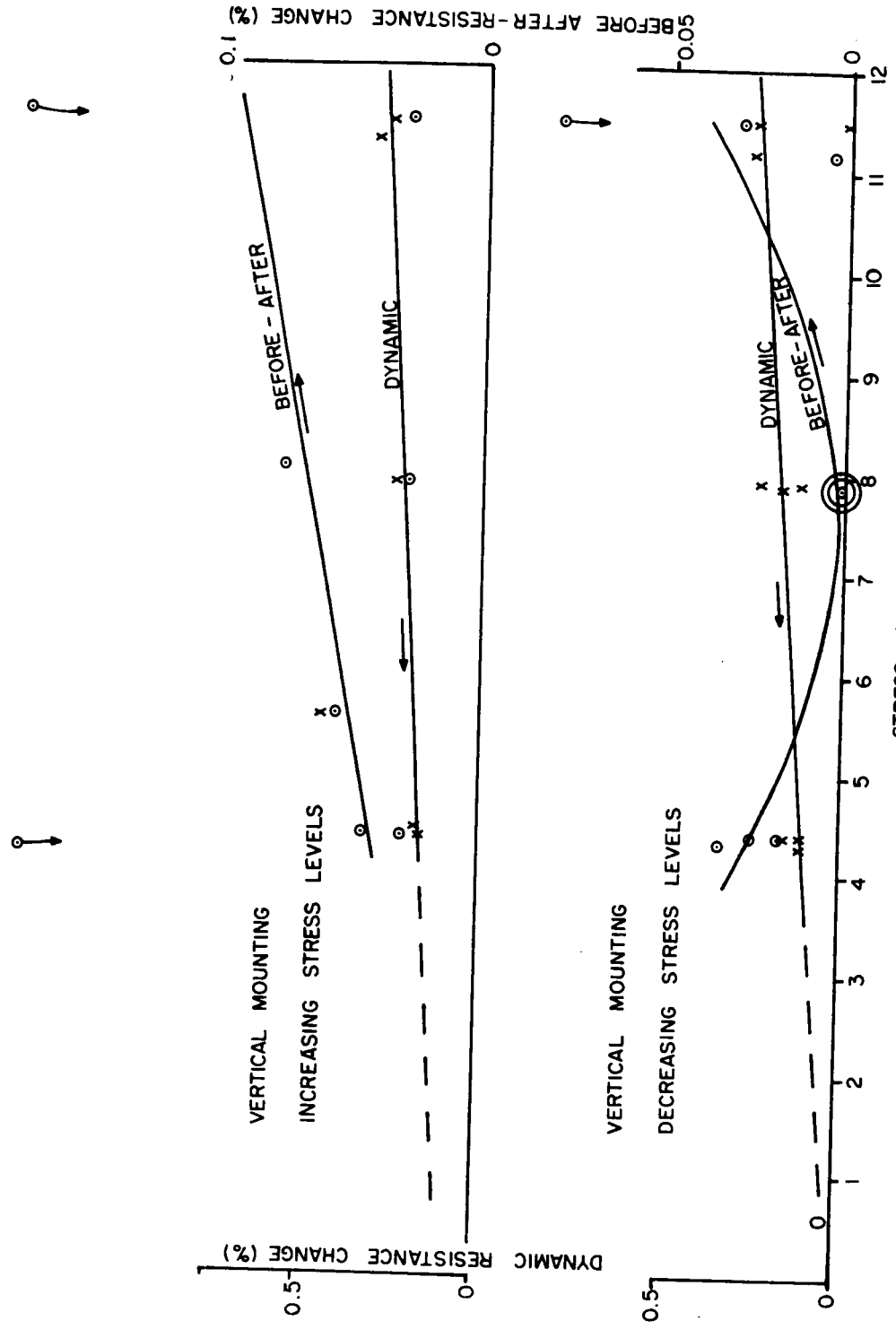

Figure 2-5. Impact Tests on Welwyn Tin-Oxide, F25, 1/4 Watt Resistor at Room Temperature

Figure 2-5.

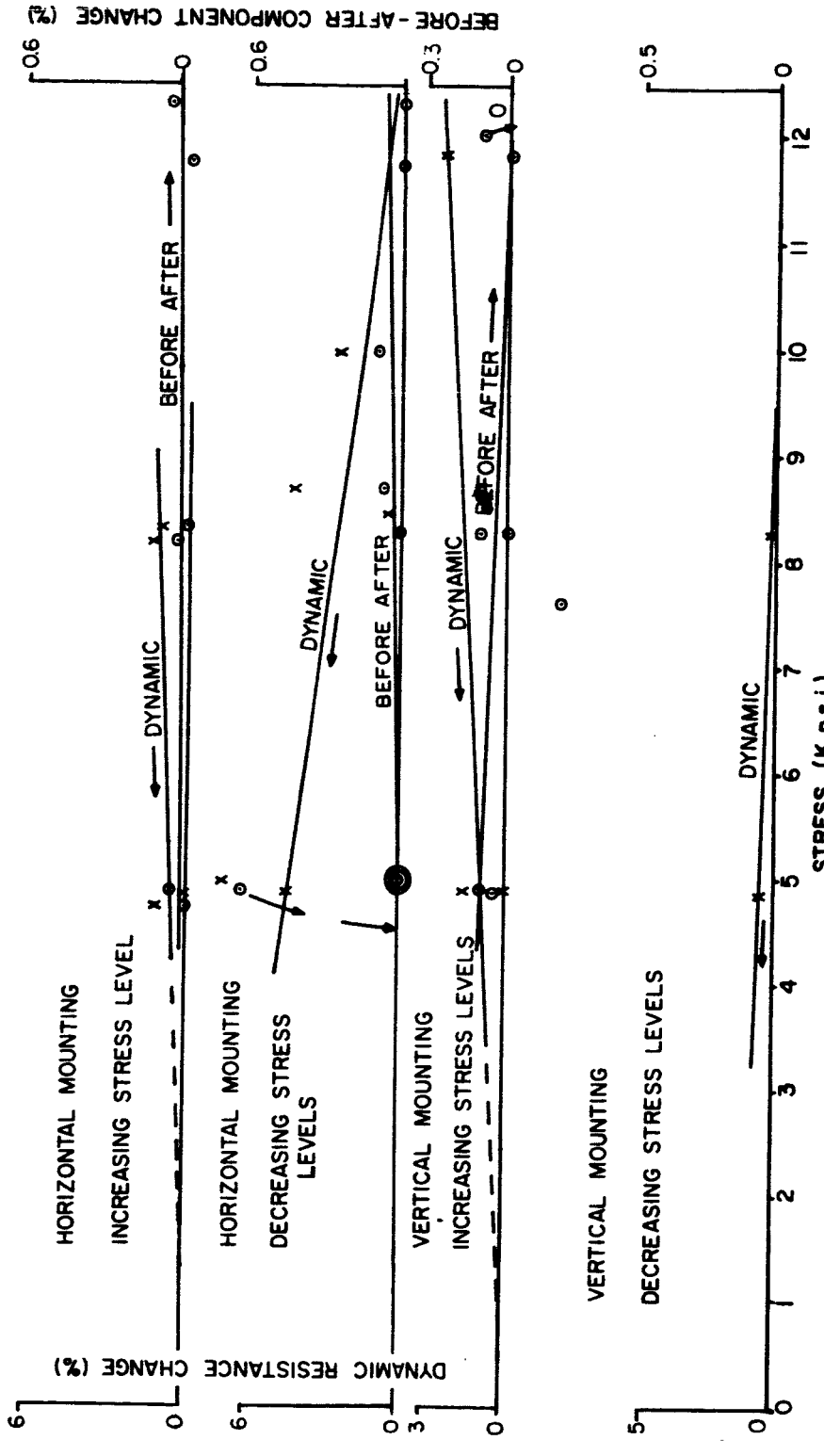

Figure 2-6. Impact Tests on American Components Inc. Metalfilm MCF 1/10 Watt Resistors at Room Temperature

Figure 2-6.

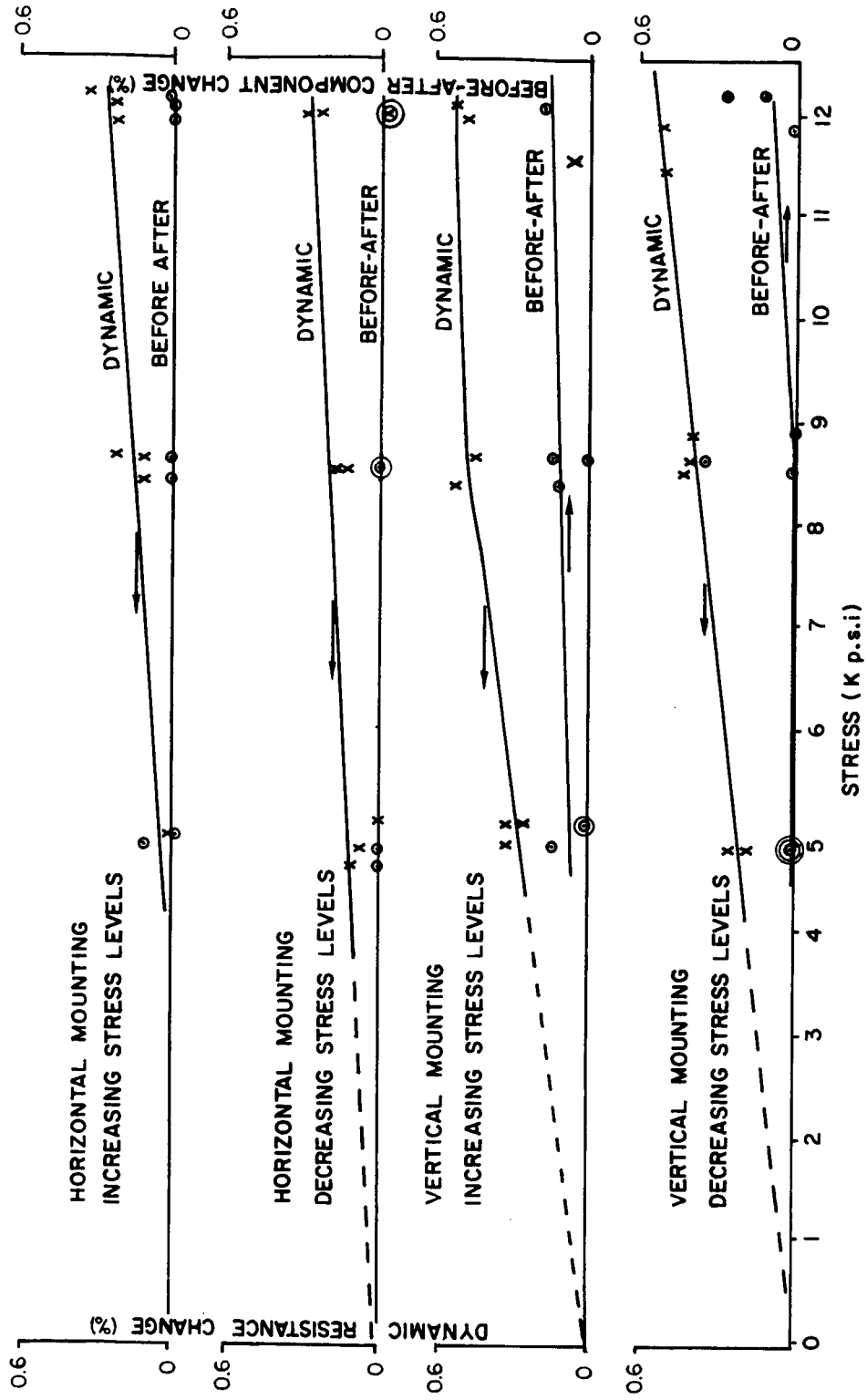

Figure 2-7. Impact Tests on American Technical Ceramics Ceradot 1/10 Watt Resistors at Room Temperature

Figure 2-7.

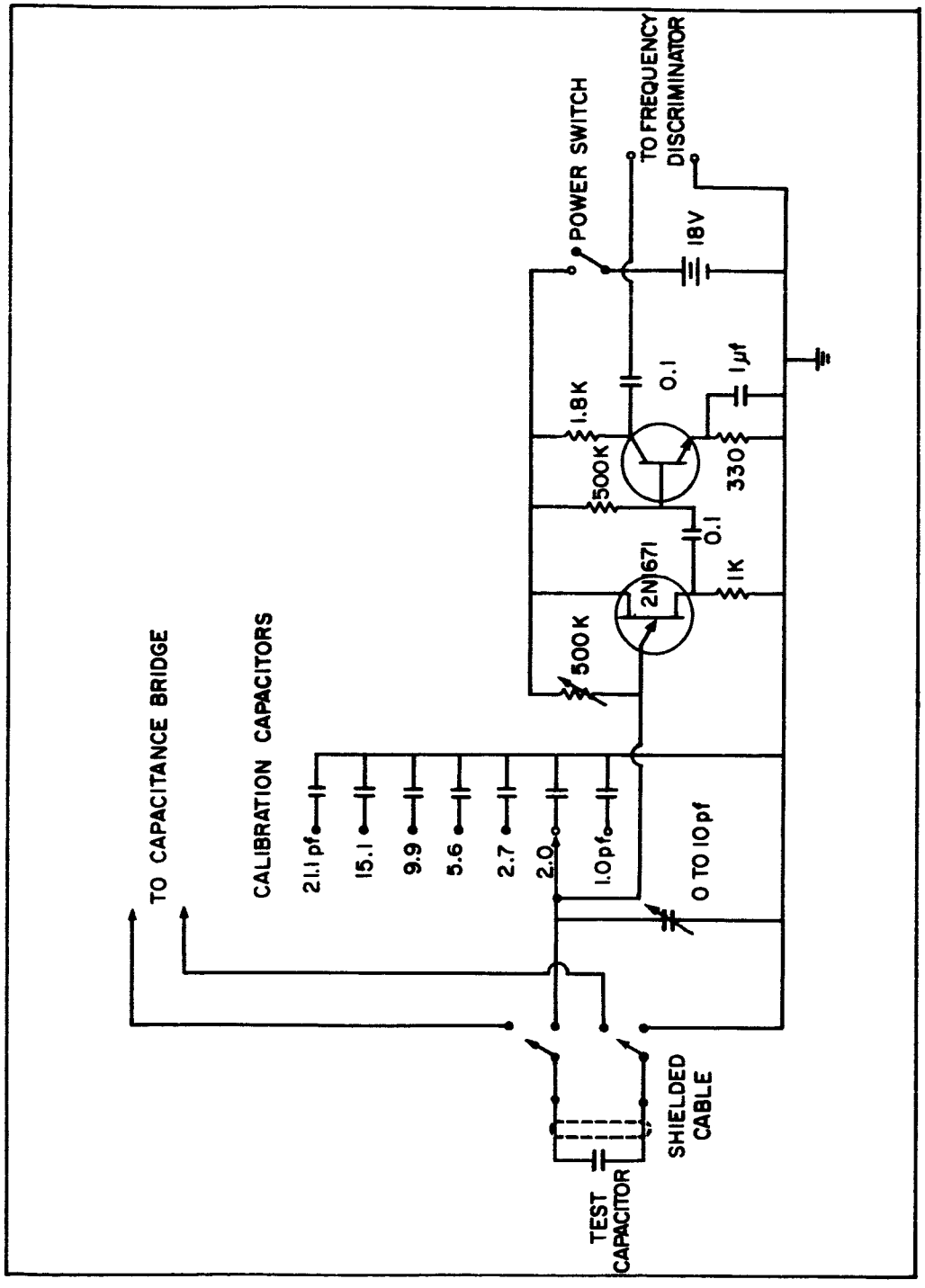

Figure 2-8. Circuit Diagram for Capacitor Tests

Figure 2-8.

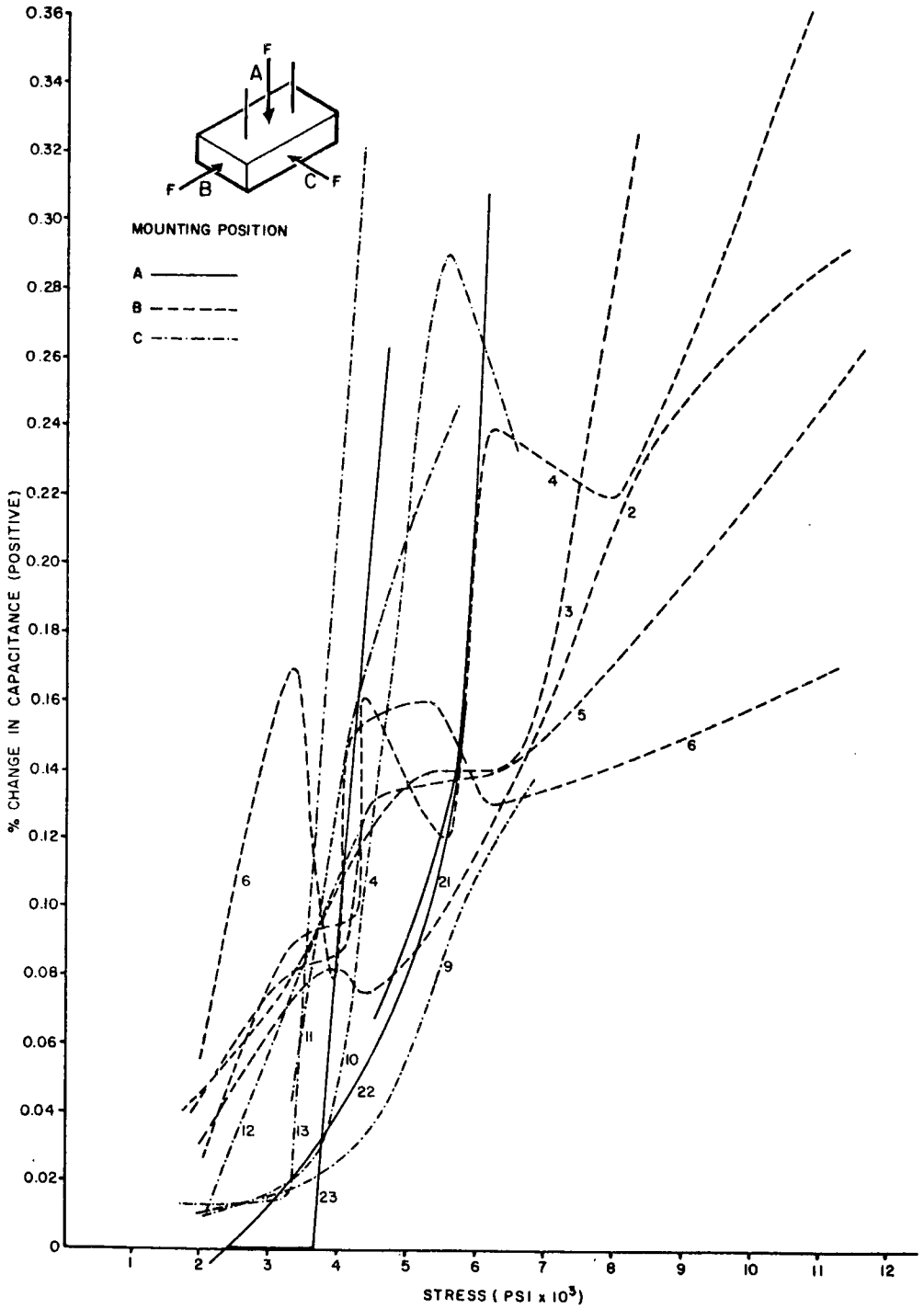

Figure 2-9. Impact Tests on Vitramon VY Capacitors at Room Temperature

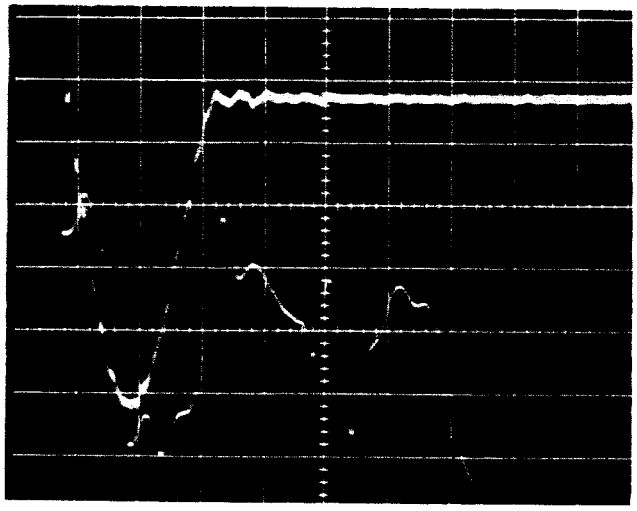

Stress 12,400 psi, Component change 1.3 pF

Figure 2-10. Typical Vitramon VY Capacitor Test Record

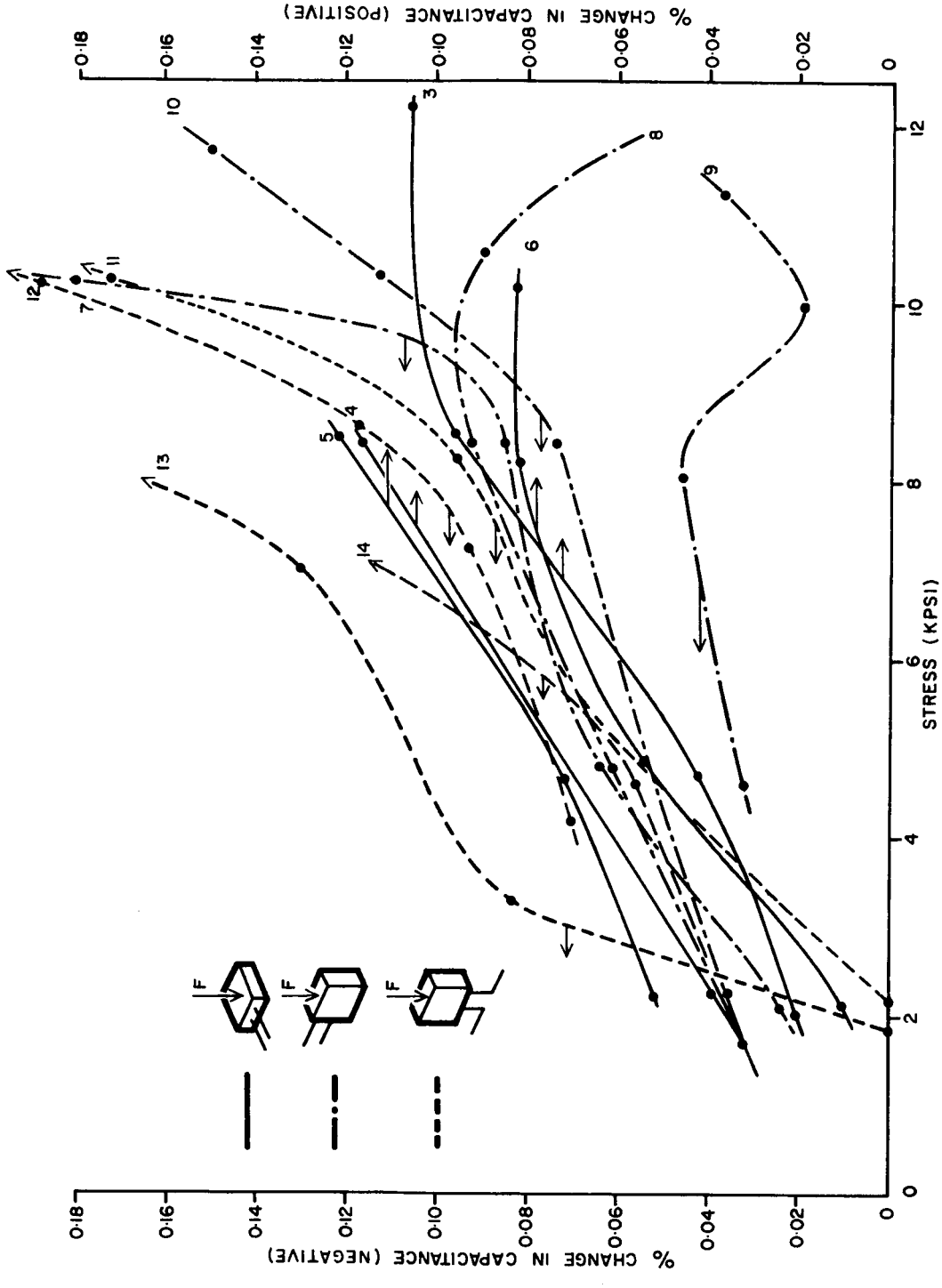

Figure 2-11. Impact Tests on Corning Glass TY06 Capacitors at Room Temperature

Figure 2-11.

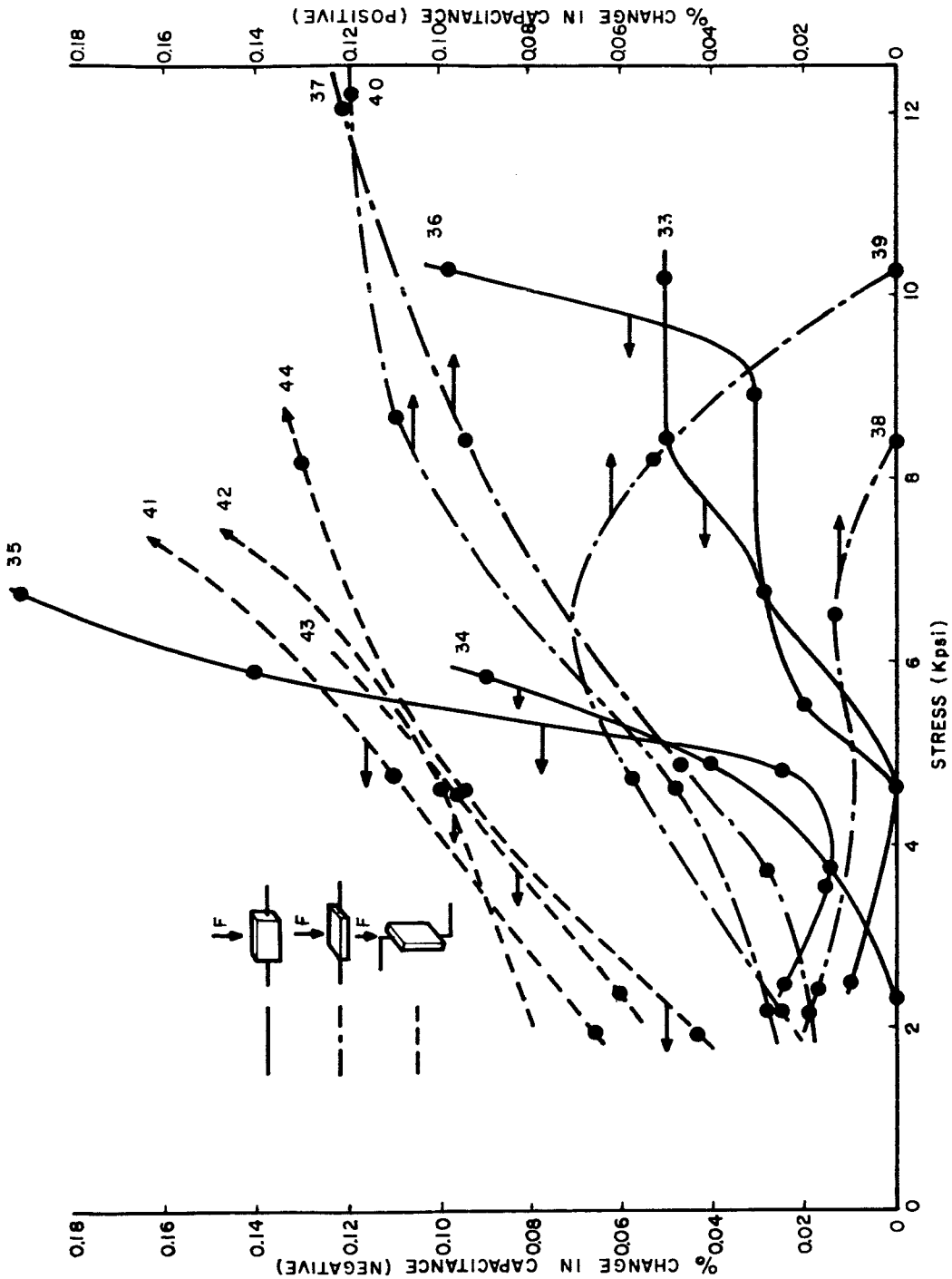

Figure 2-12. Impact Tests on Corning Glass CY10 Capacitors at Room Temperature

Figure 2-12.

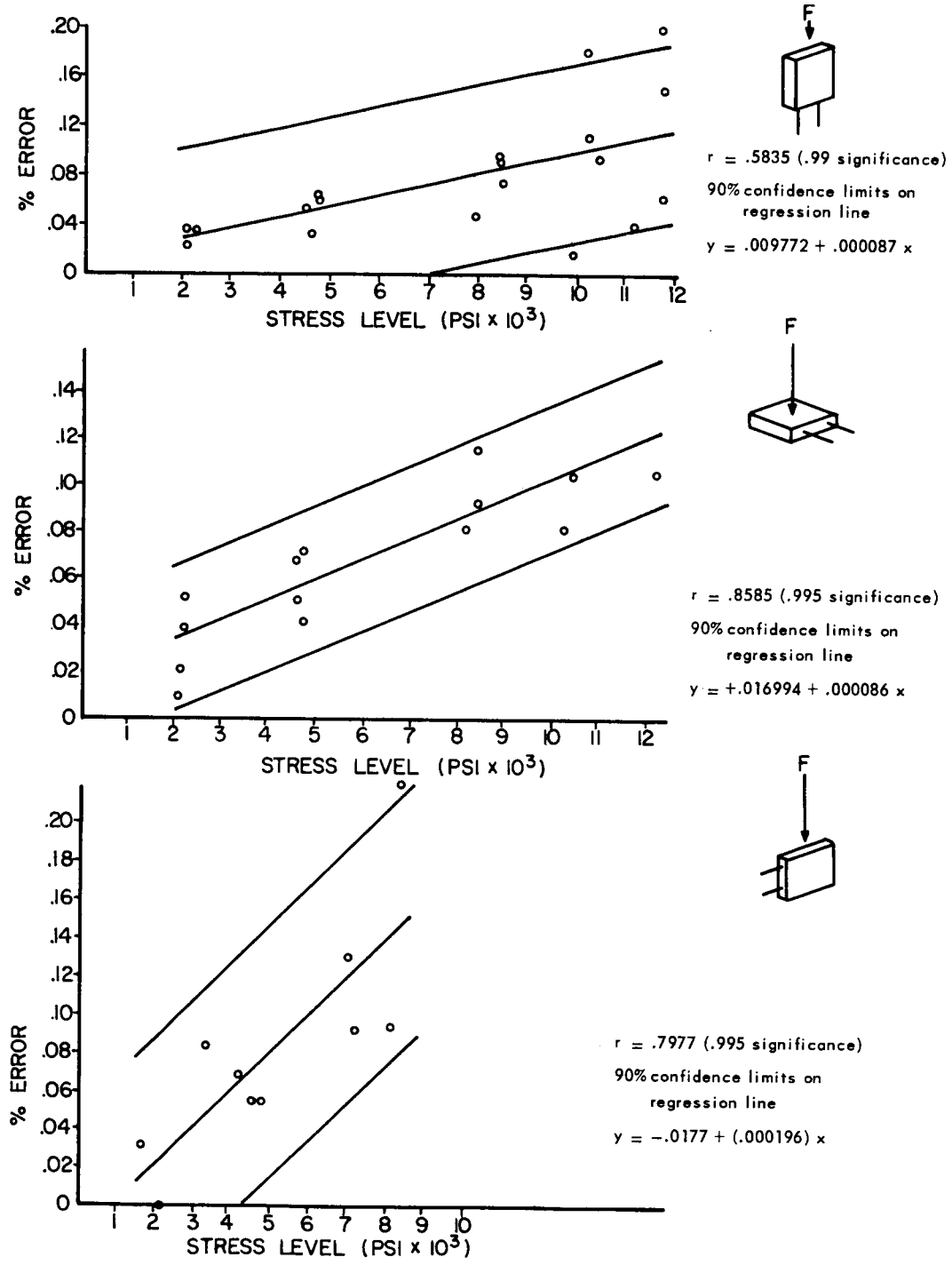

Figure 2-13. Analysis of Corning Glass TY06 Capacitors

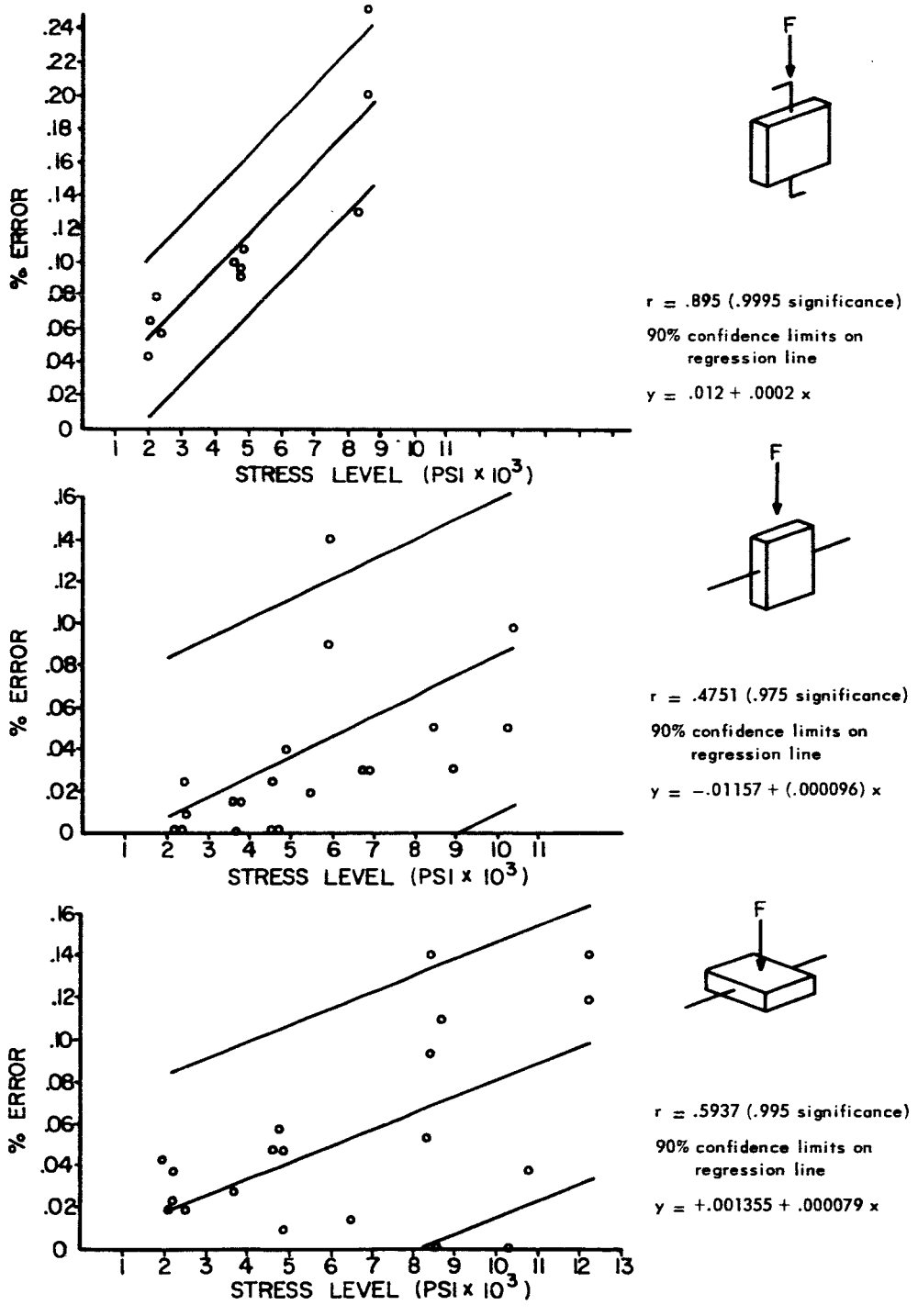

Figure 2-14. Analysis of Corning Glass CY10 Capacitors

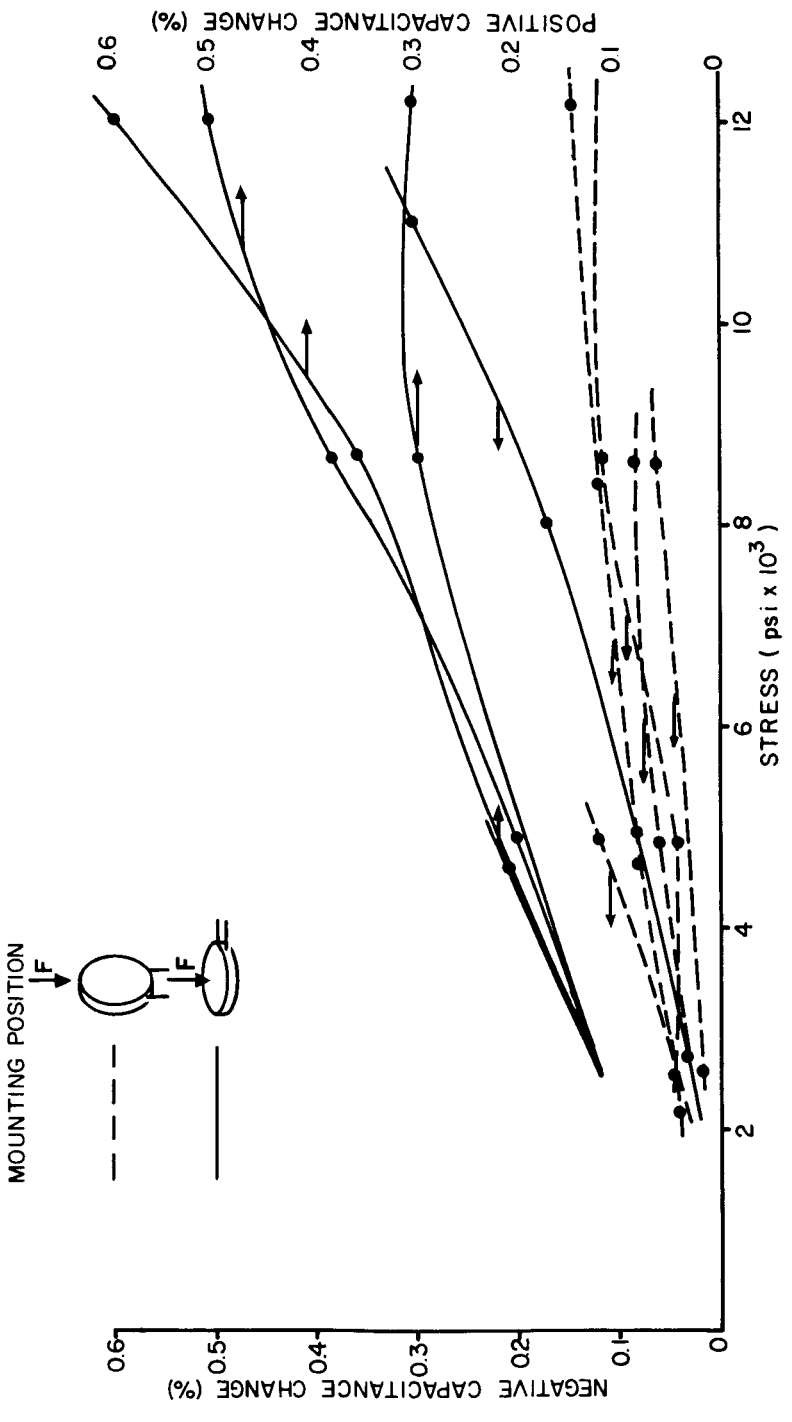

Figure 2-15. Impact Tests on Centralab Disk Capacitors at Room Temperature

Figure 2-15.

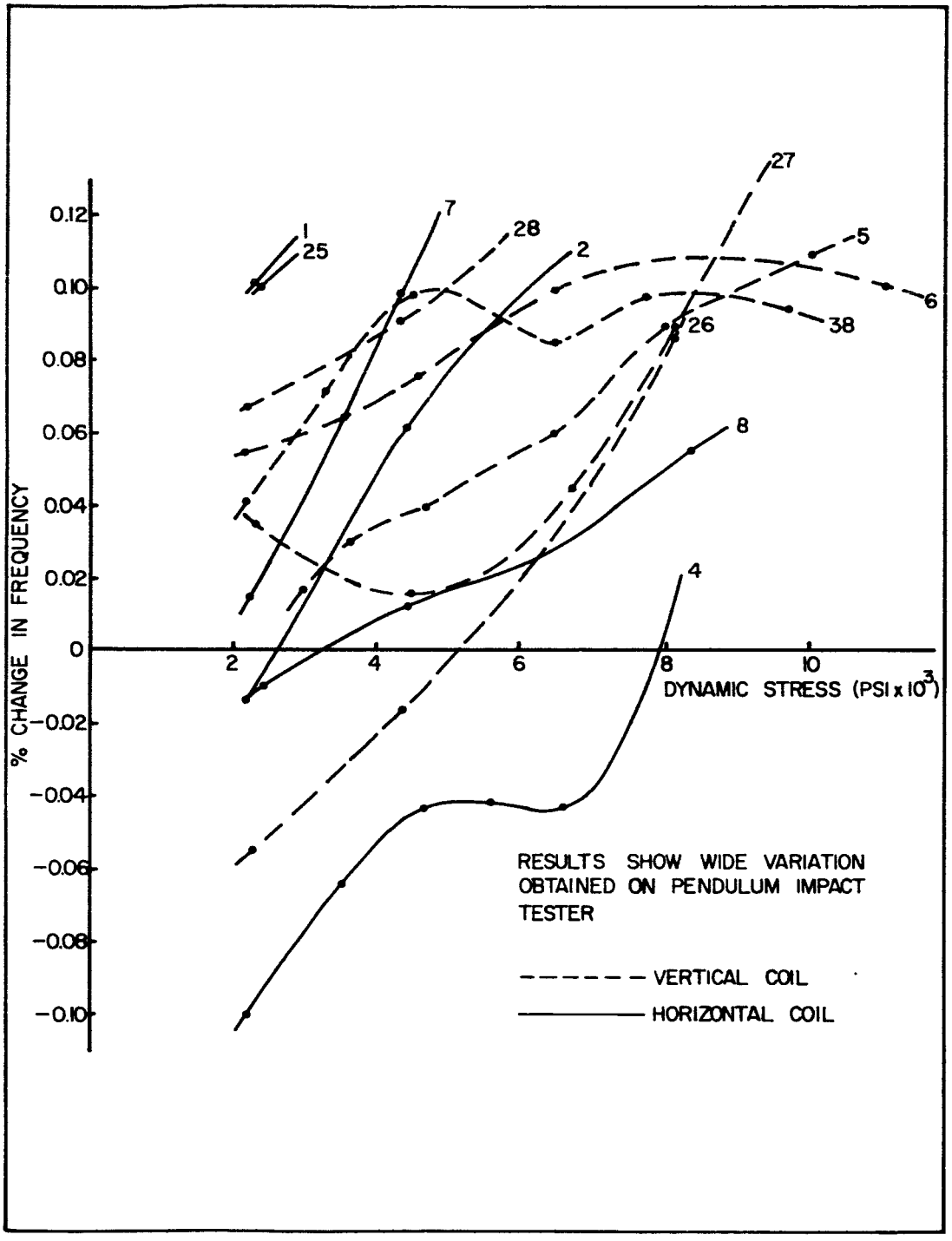

Figure 2-16. Impact Tests of RF Coils measured at 180 Mc/s

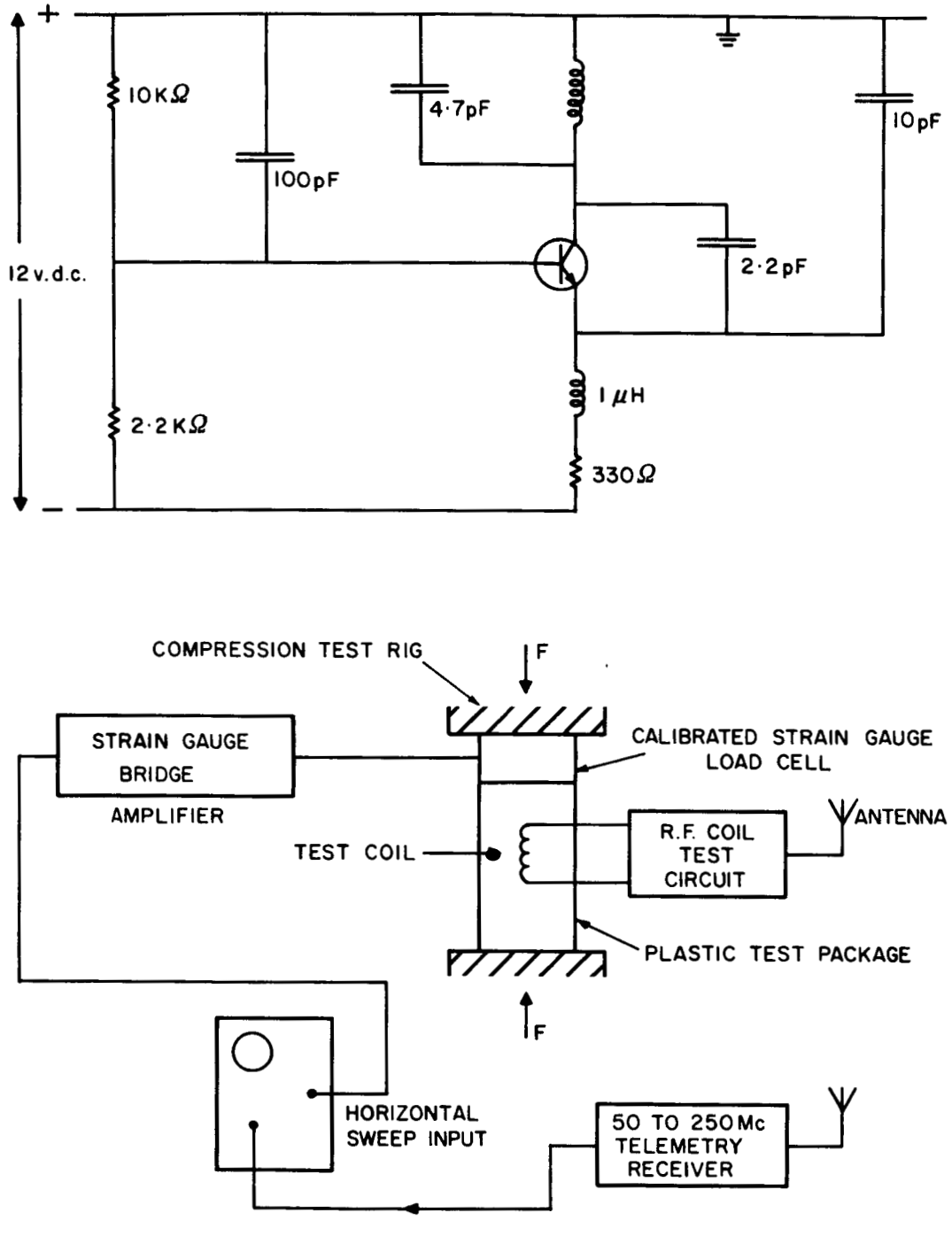

Figure 2-17. RF Coil Test Circuit and Block Diagram of Compression Tester

Figure 2-18. Compression Test on Pyrex RF Coil

Figure 2-18.

Figure 2-19. Compression Test on Alumina Ceramic RF Coil

Figure 2-19.

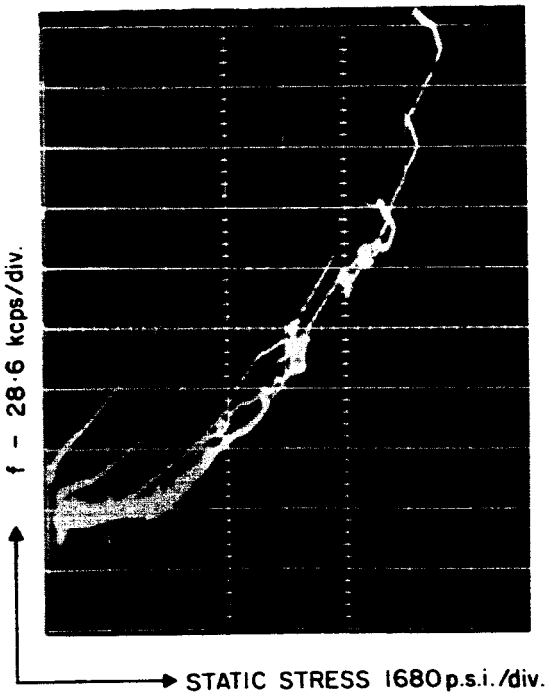

Ceramic rf coil

Figure 2-20. Variation of Frequency Hysteresis with Peak Load

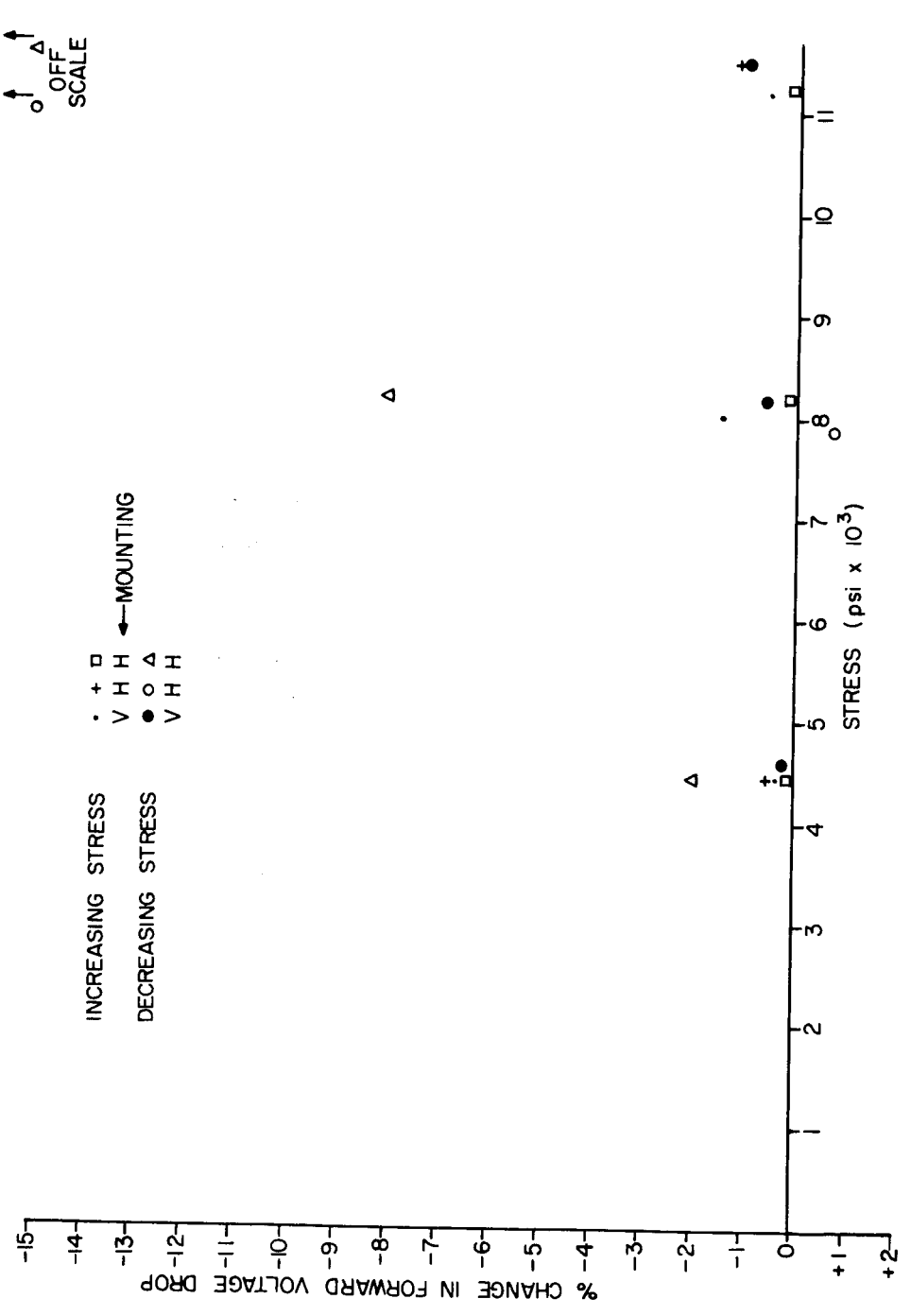

Figure 2-21. Impact Tests on PD101 Diodes without Silastic Coating

Figure 2-21.

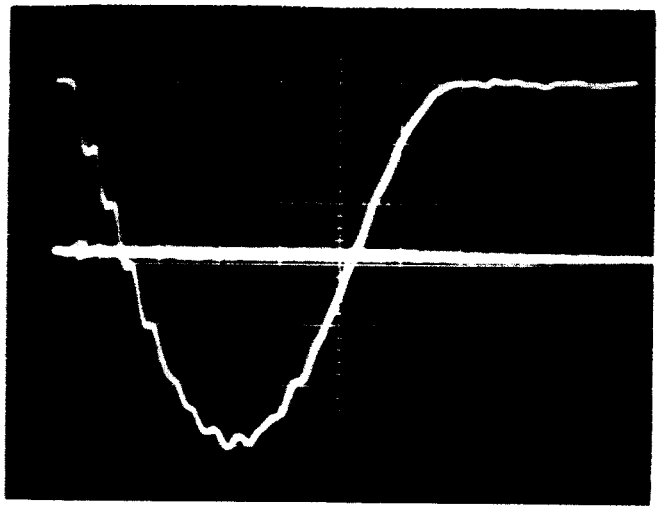

Upper Trace Stress 1,000 psi per cm
Lower Trace Zener voltage change 10 mV per cm

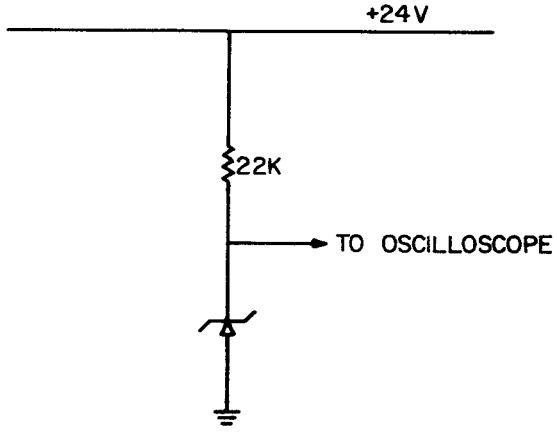

Figure 2-22. Zener Diode Test Circuit and Typical Record

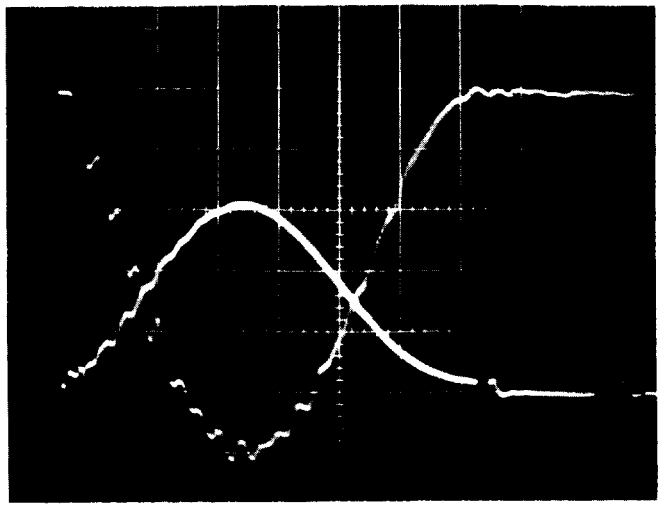

Upper trace stress 1,000 psi per cm
Lower trace change in collector voltage 10 mV per cm

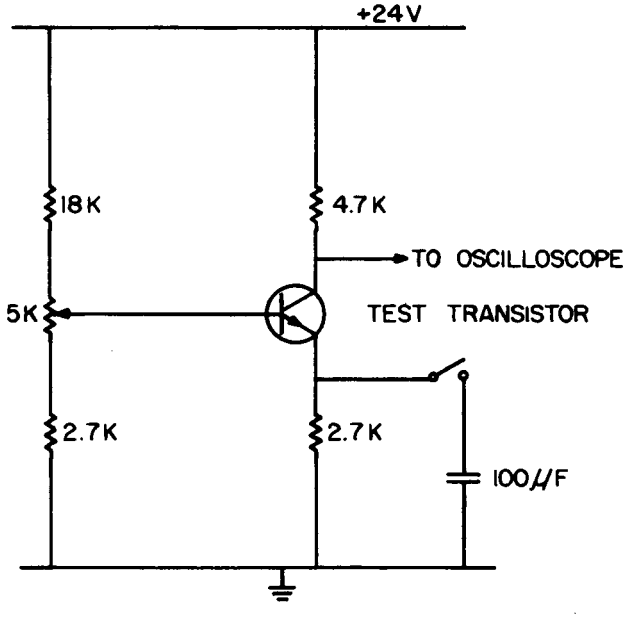

Figure 2-23. Transistor Test Circuit and Typical Record

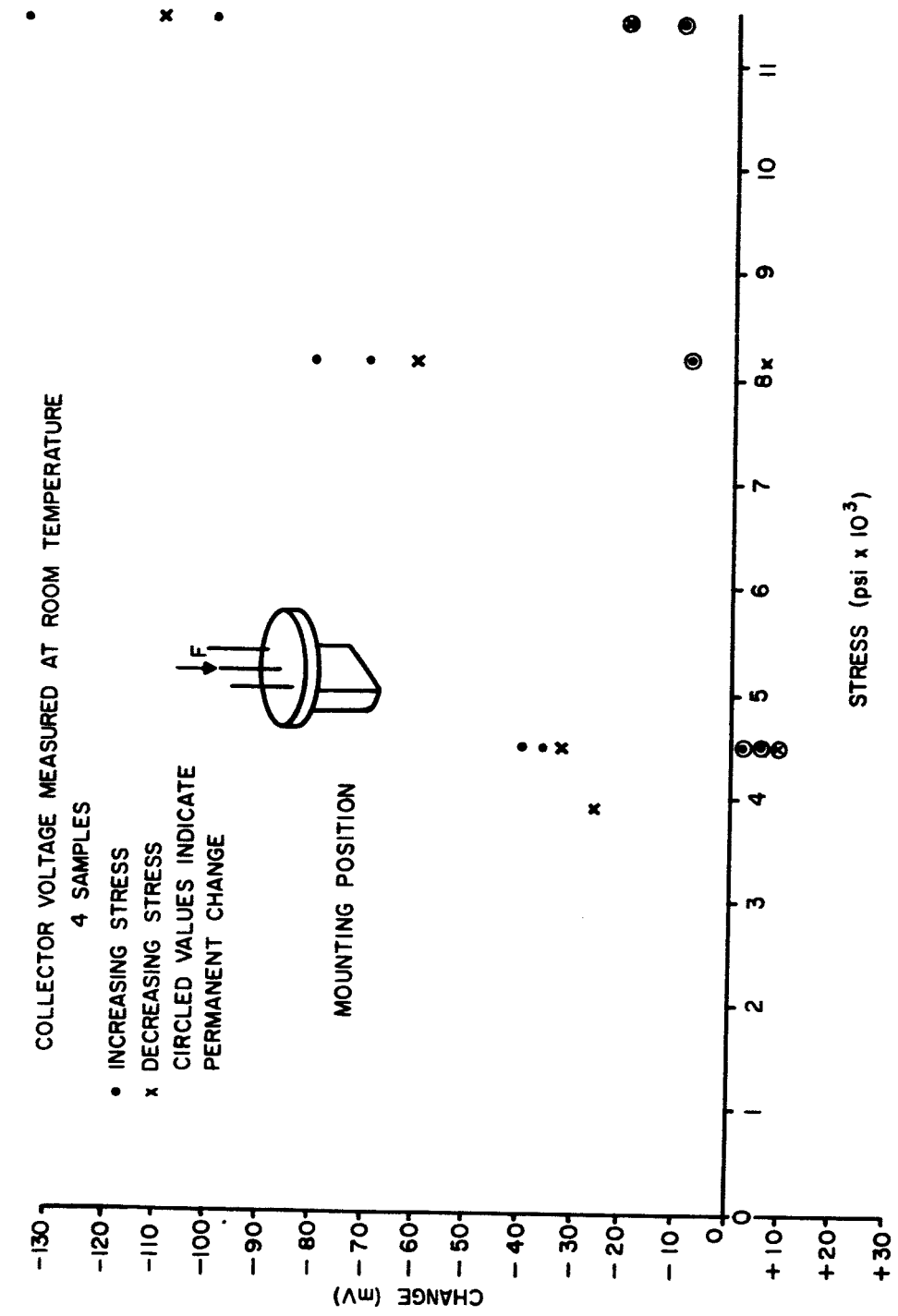

Figure 2-24. Impact Test Results on Encapsulated Transistors

Figure 2-24.

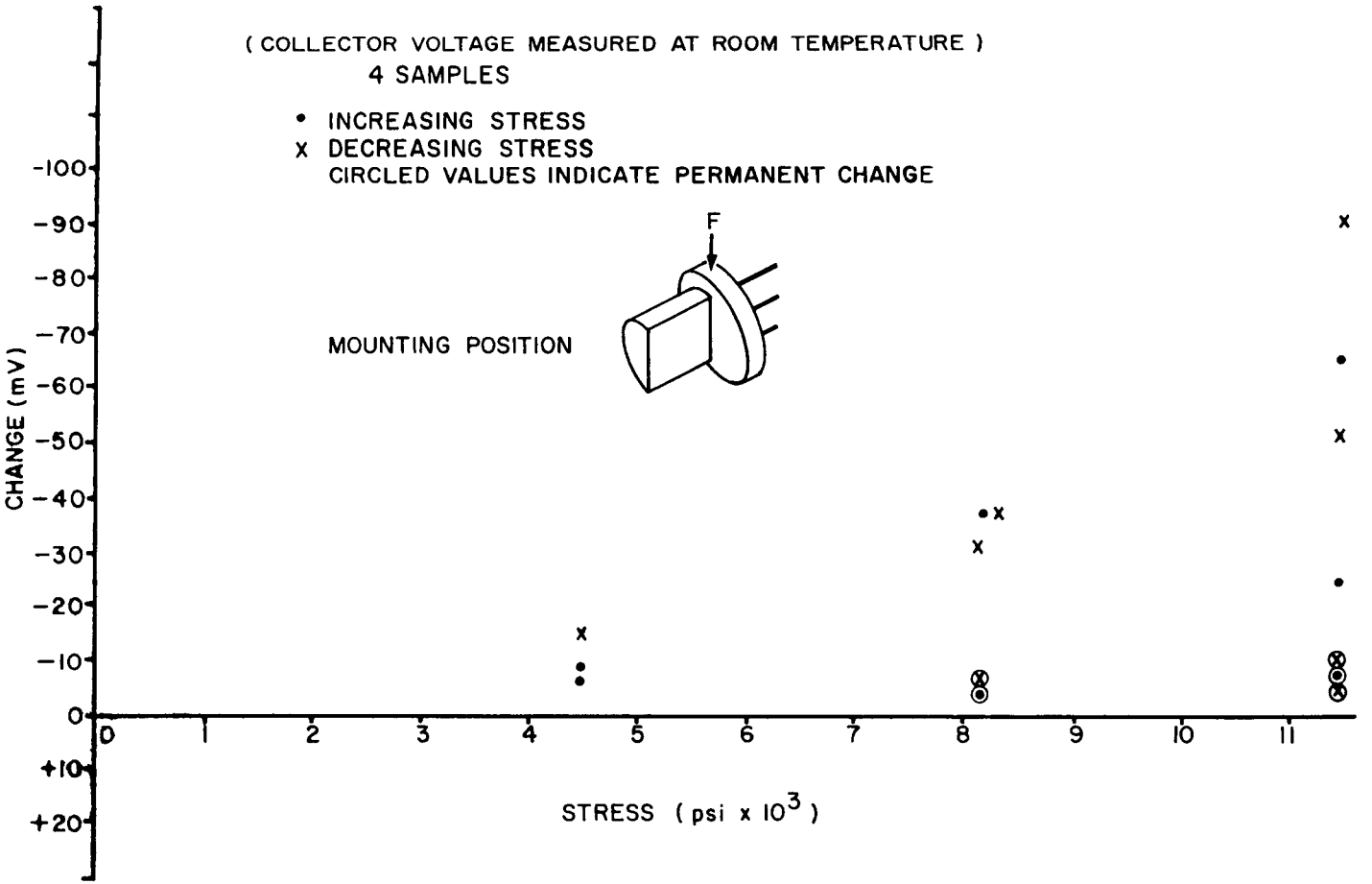

Figure 2-25. Impact Test Results on Encapsulated Transistors

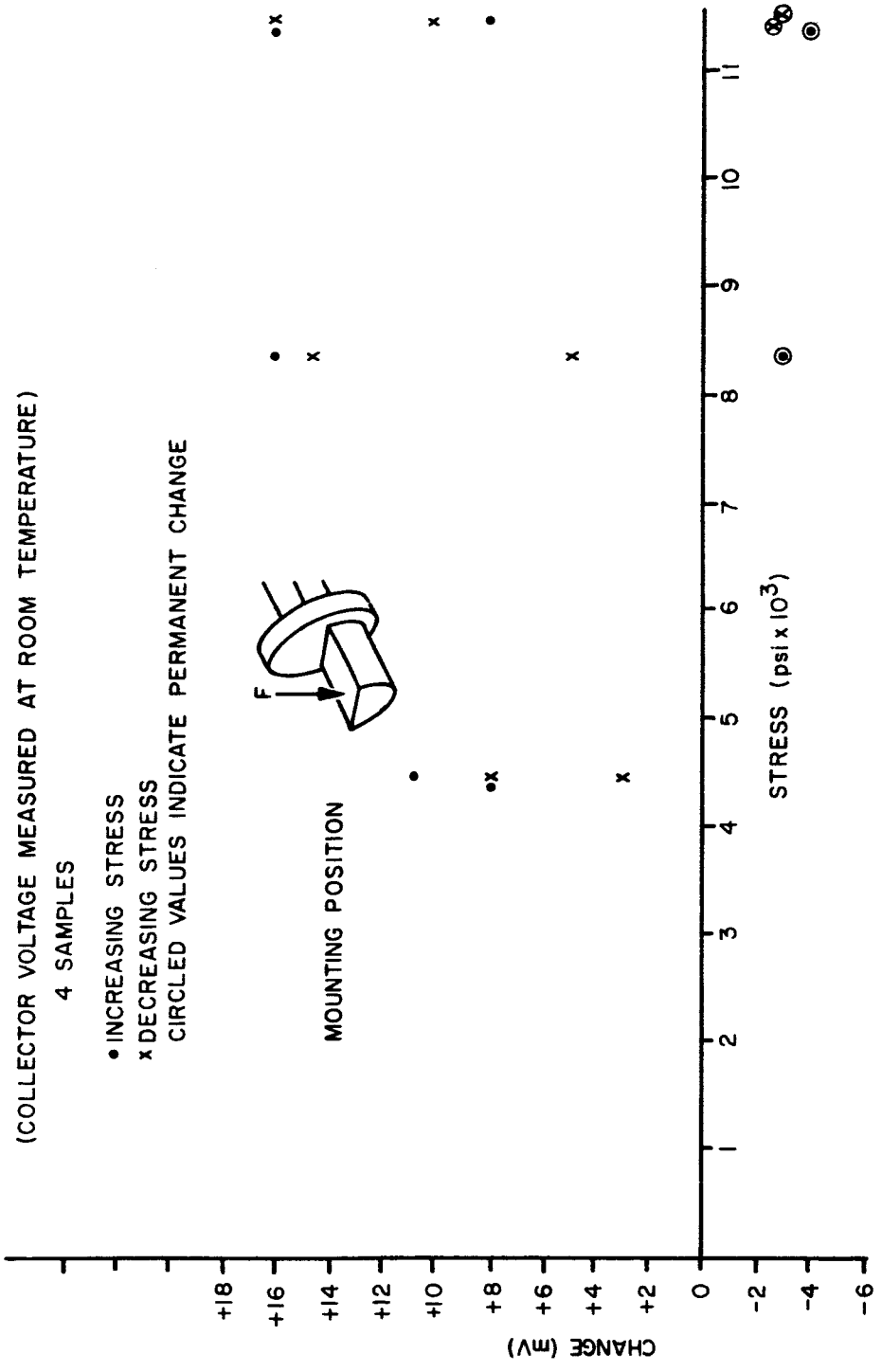

Figure 2-26. Impact Test Results on Encapsulated Transistors

Figure 2-26.

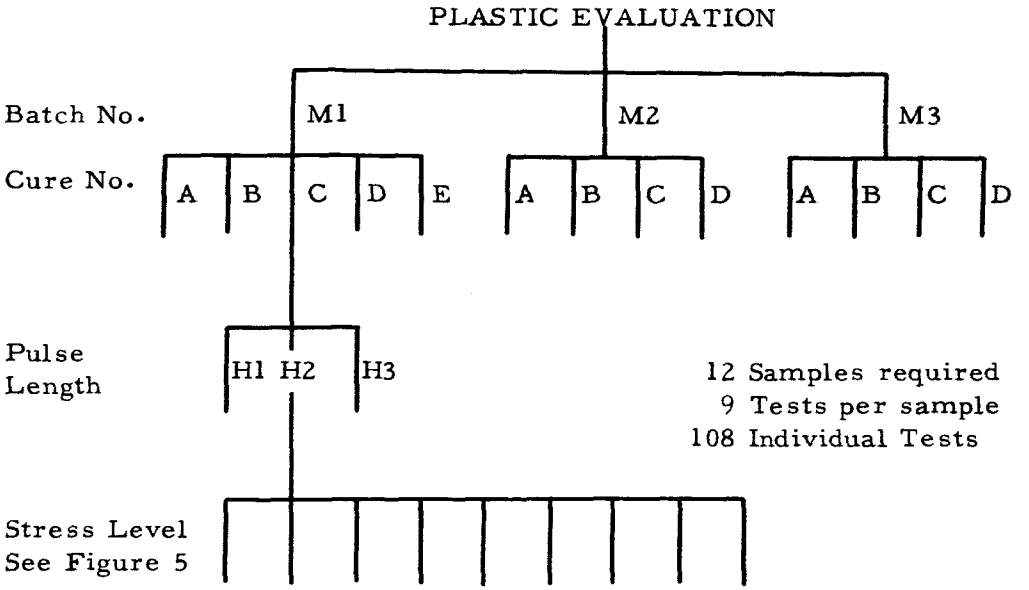

Batch Numbers - M1, M2, M3.

Cure No.	Cure Cycle		
	75°F (in mold)	105°F	75°F
A	1	2	-
B	1	2	5
C	1	-	14
D	1	-	7
E	1	-	120

Head Number	Stress Pulse Time	Effective Head Weight
H3	0.71 milliseconds	3.17 lbs.
H4	1.14 milliseconds	8.62 lbs.
H5	1.64	15.4 lbs.

Stress Levels - These are shown in Figure 3-2

Figure 3-1. Schematic Diagram of Dynamic Mechanical Properties Experiment (Araldite RDD5)

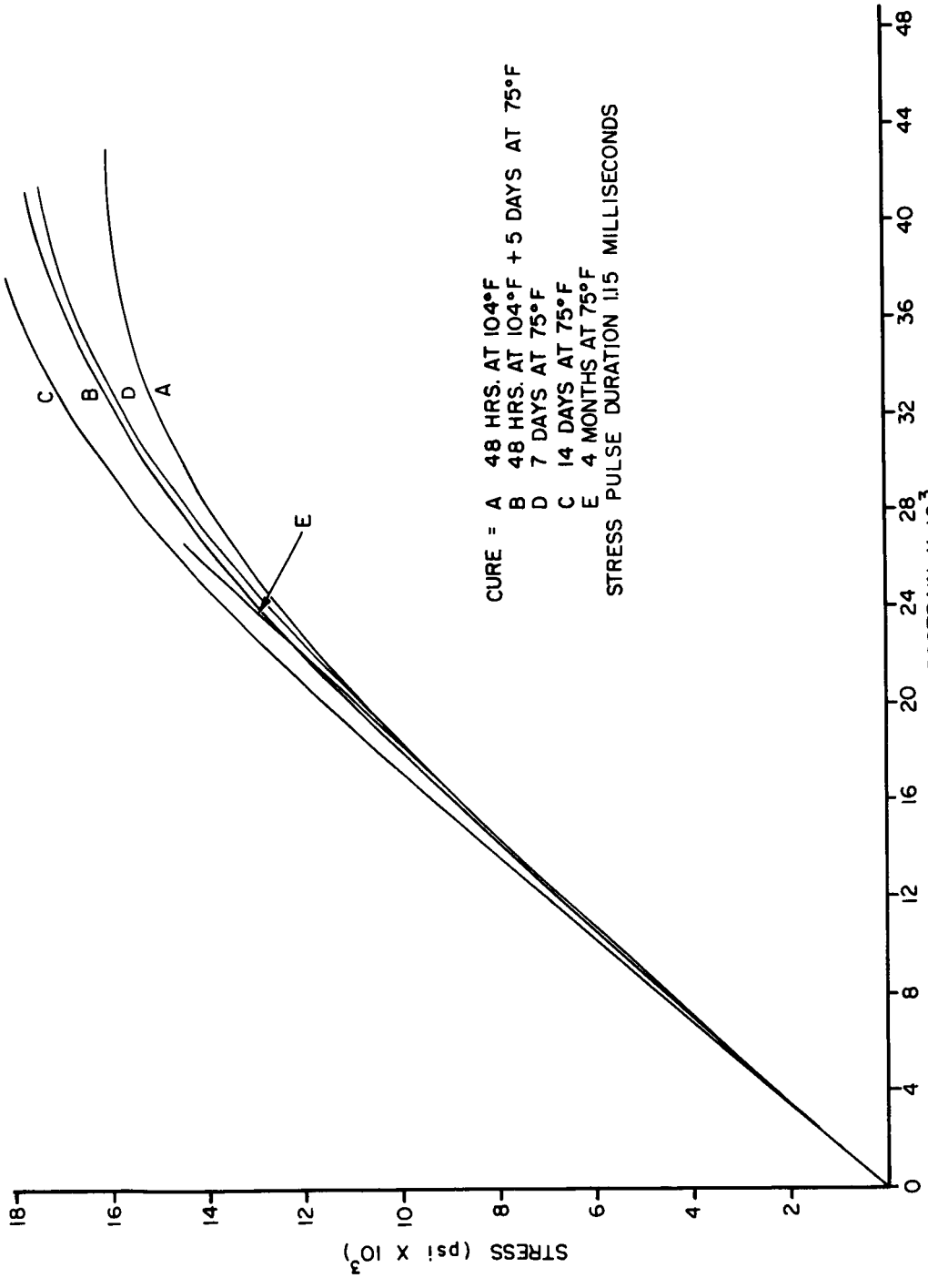

Figure 3-2. Dynamic Properties of RDD5 (Comparison of Cure Cycles)

Figure 3-2.

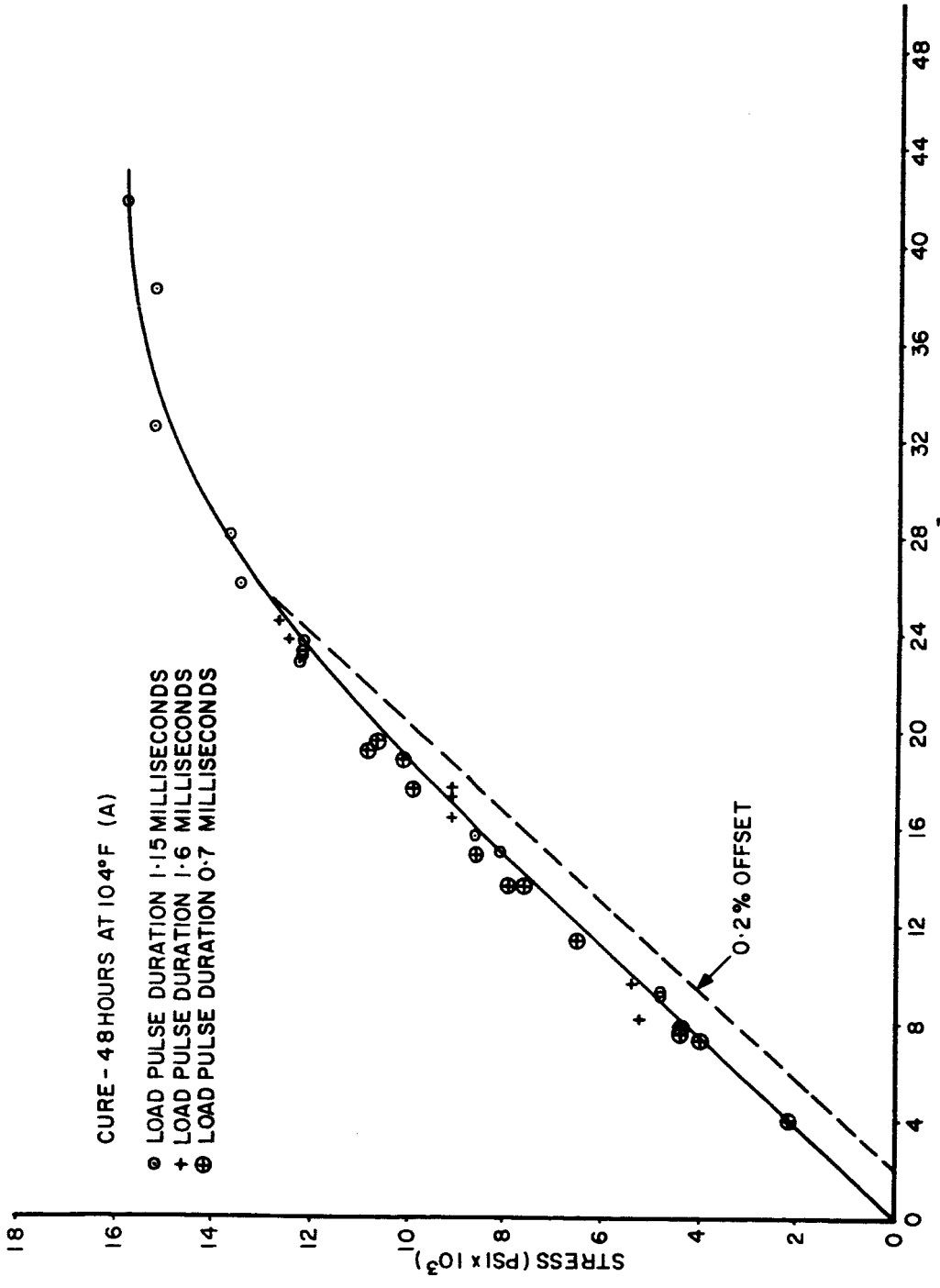

Figure 3-3. Dynamic Properties of RDD5 (Cure 48 hours at 104 degrees F)

Figure 3-3.

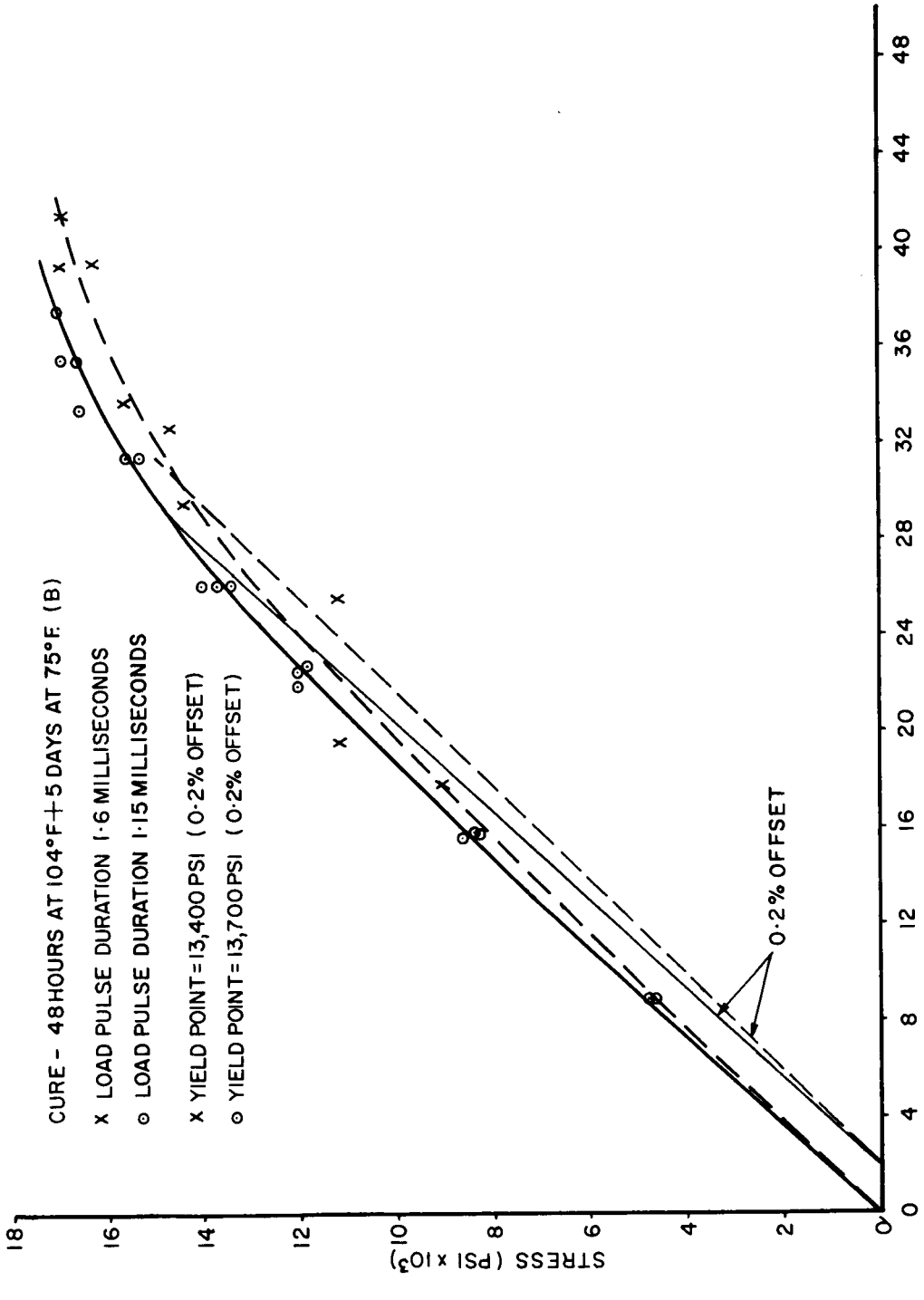

Figure 3-4. Dynamic Properties of RDD5 (Cure 48 hours at 104 degrees F plus 5 days at 75 degrees F)

Figure 3-4.

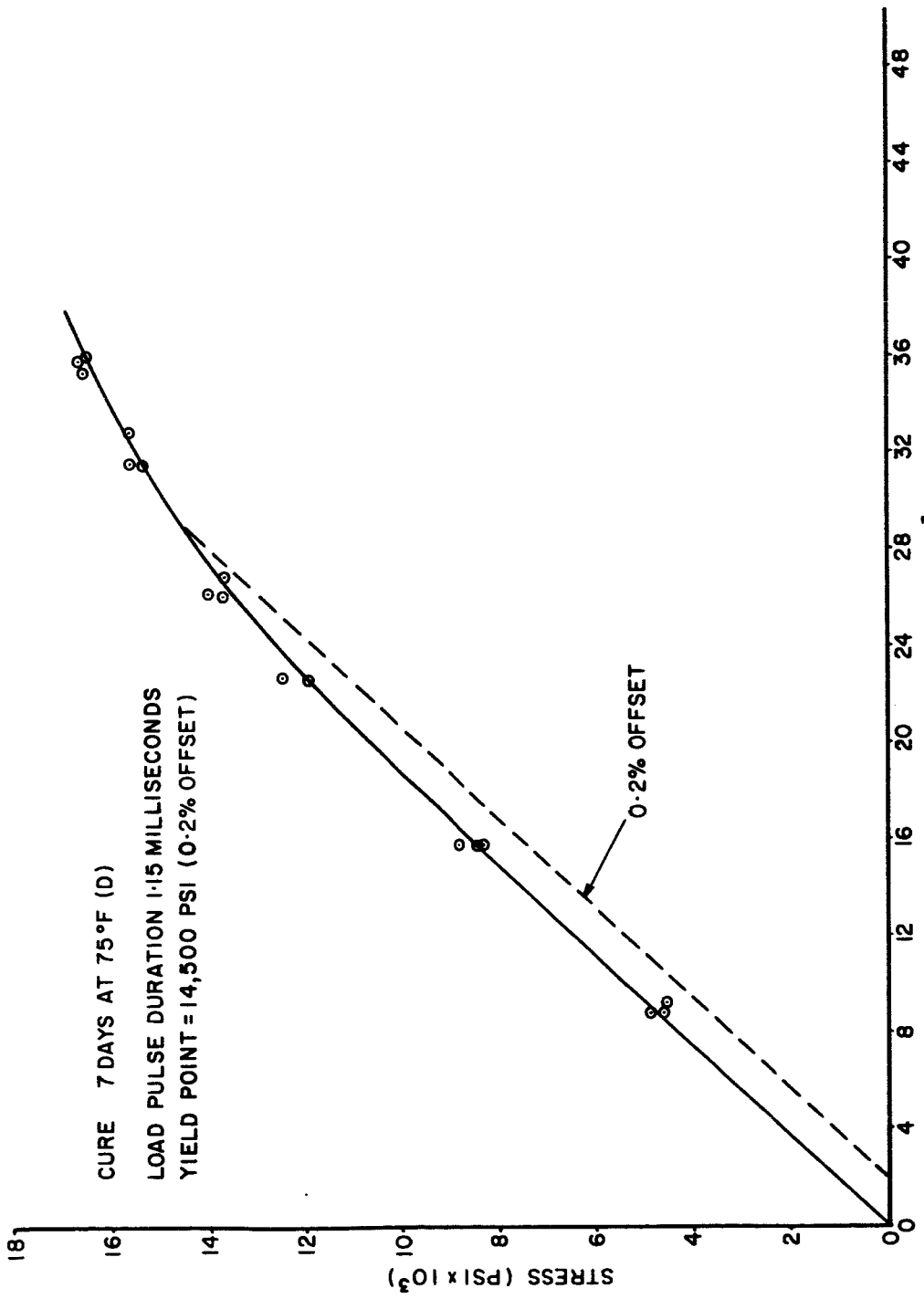

Figure 3-5. Dynamic Properties of RDD5 (Cure 7 days at 75 degrees F)

Figure 3-5.

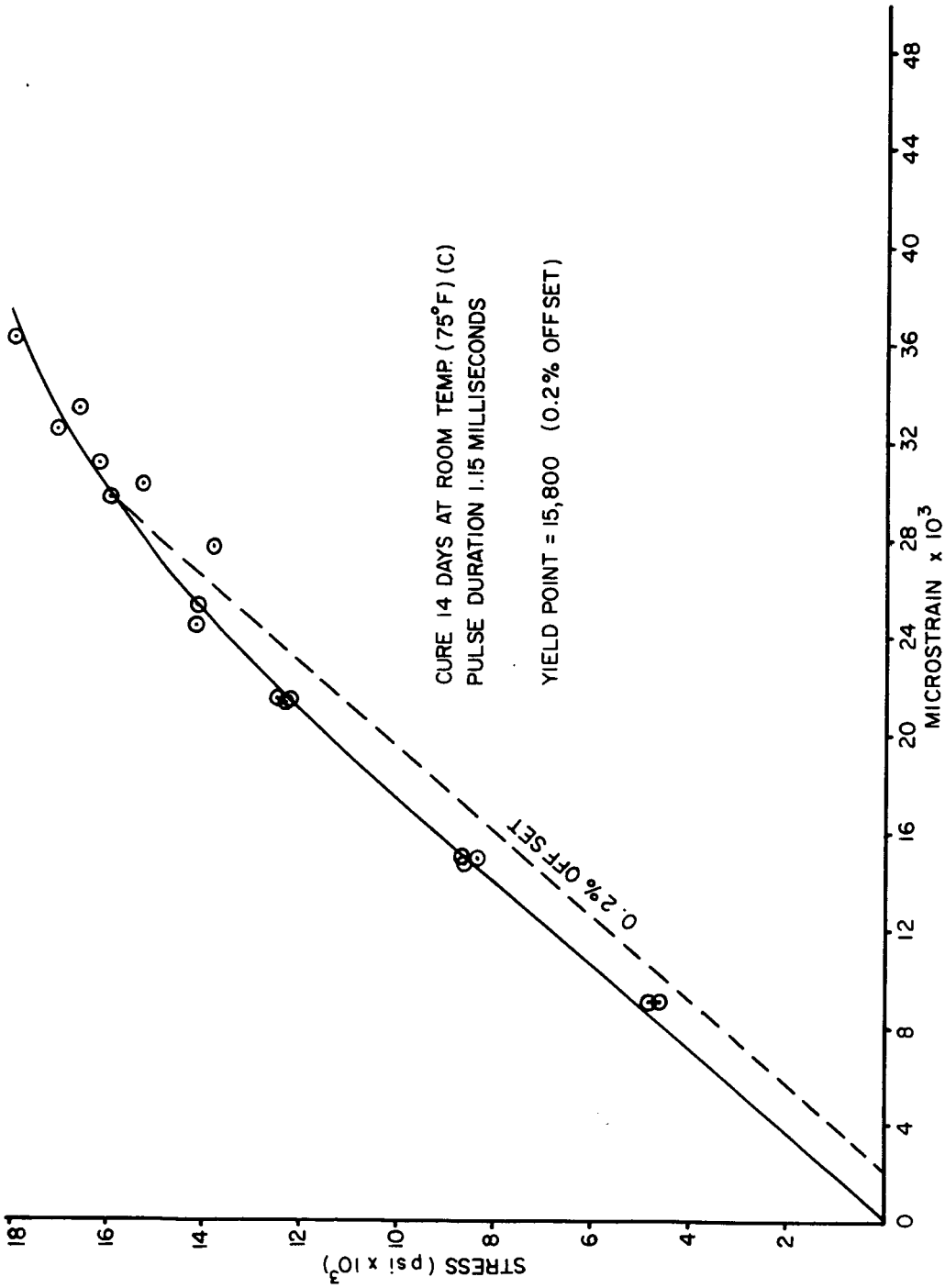

Figure 3-6. Dynamic Properties of RDD5 (Cure 14 days at 75 degrees F)

Figure 3-6.

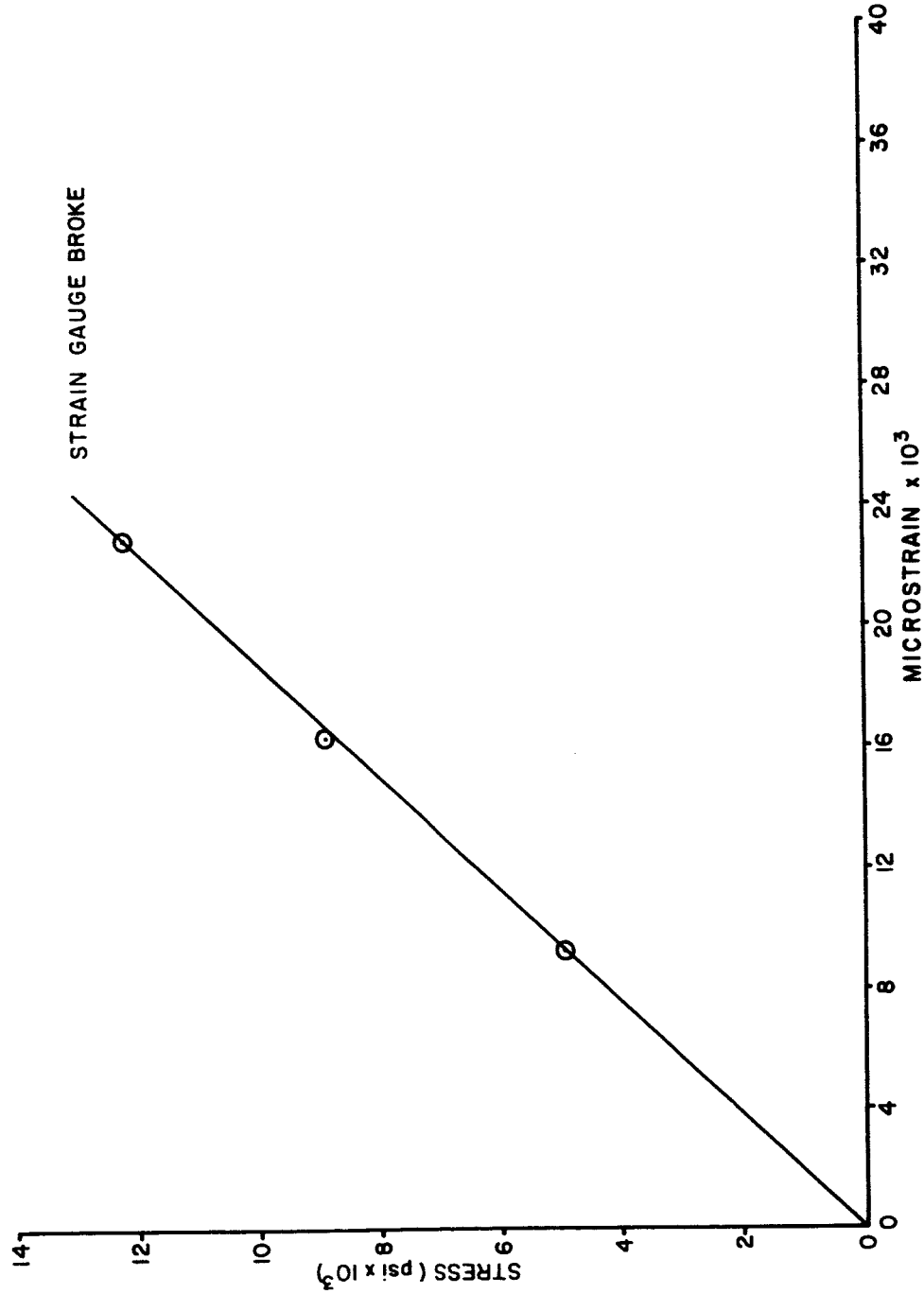

Figure 3-7. Dynamic Properties of RDD5 (Cure 4 months at room temperature)

Figure 3-7.

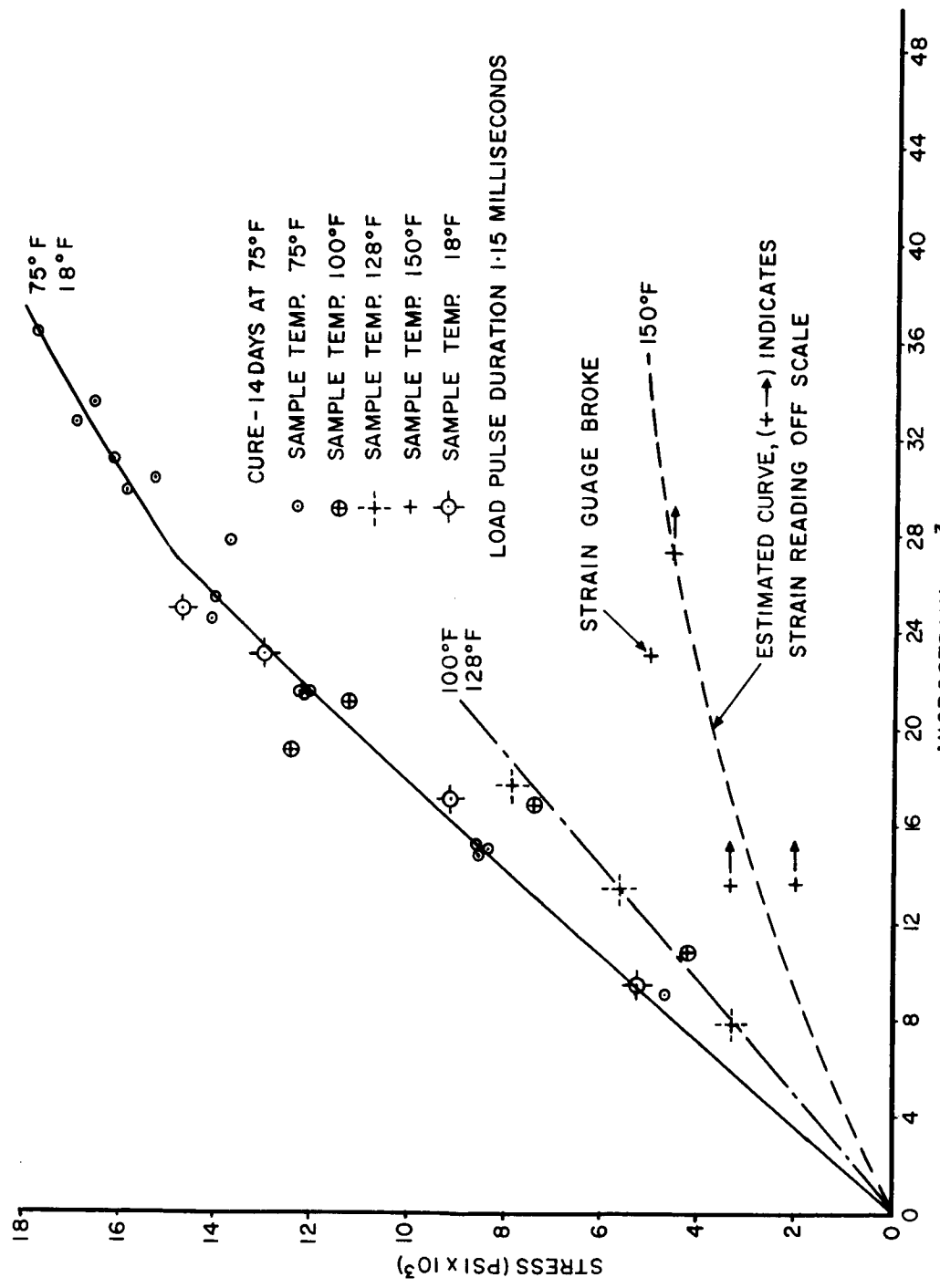

Figure 3-8. Dynamic Properties of RDD5 (Temperature Range 18 degrees F to 150 degrees F)

Figure 3-8.

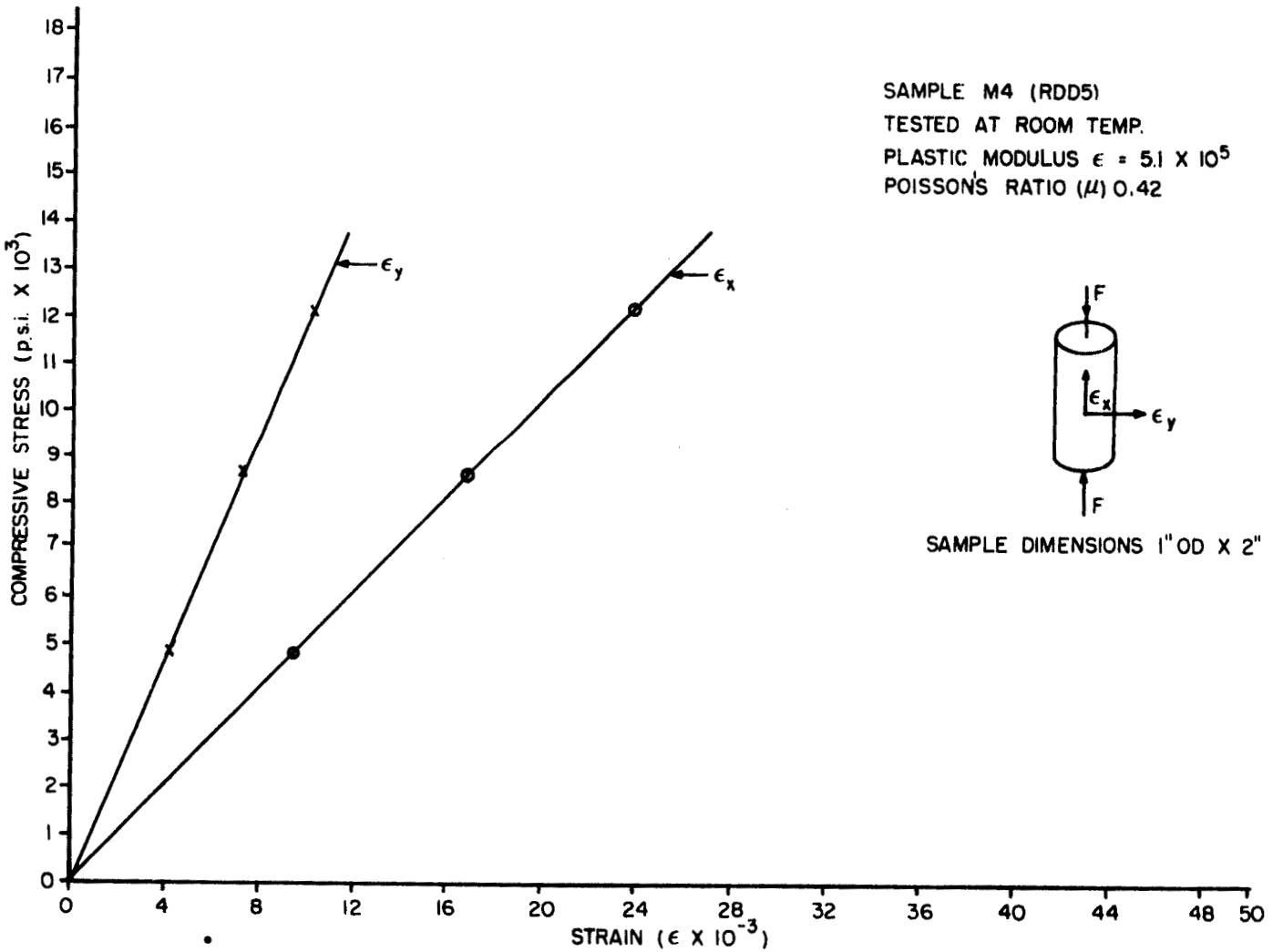

Figure 3-9. Dynamic Poisson's Ratio of RDD5

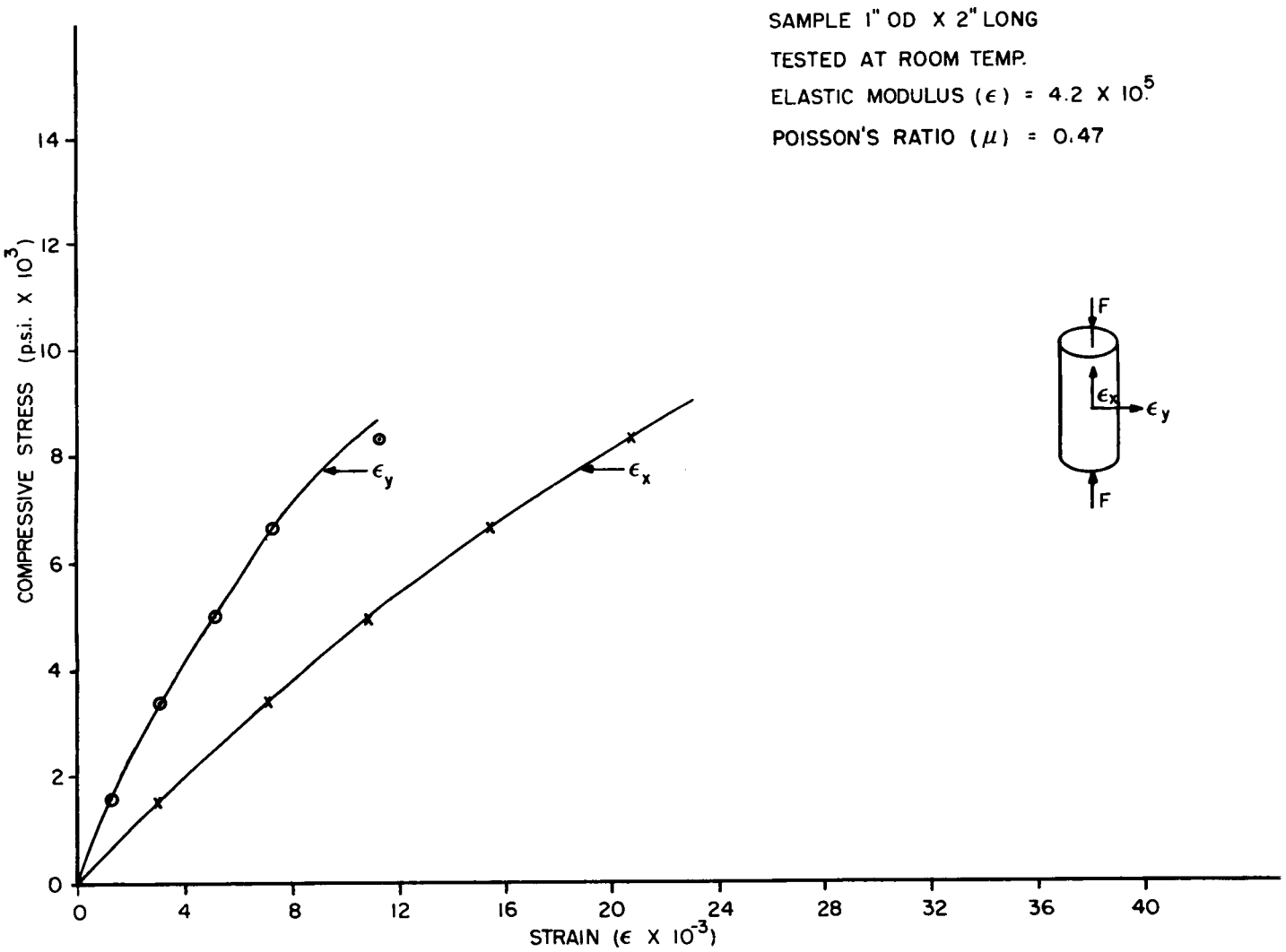

Figure 3-10. Static Properties of RDD5
(Elastic Modulus and Poisson's Ratio)

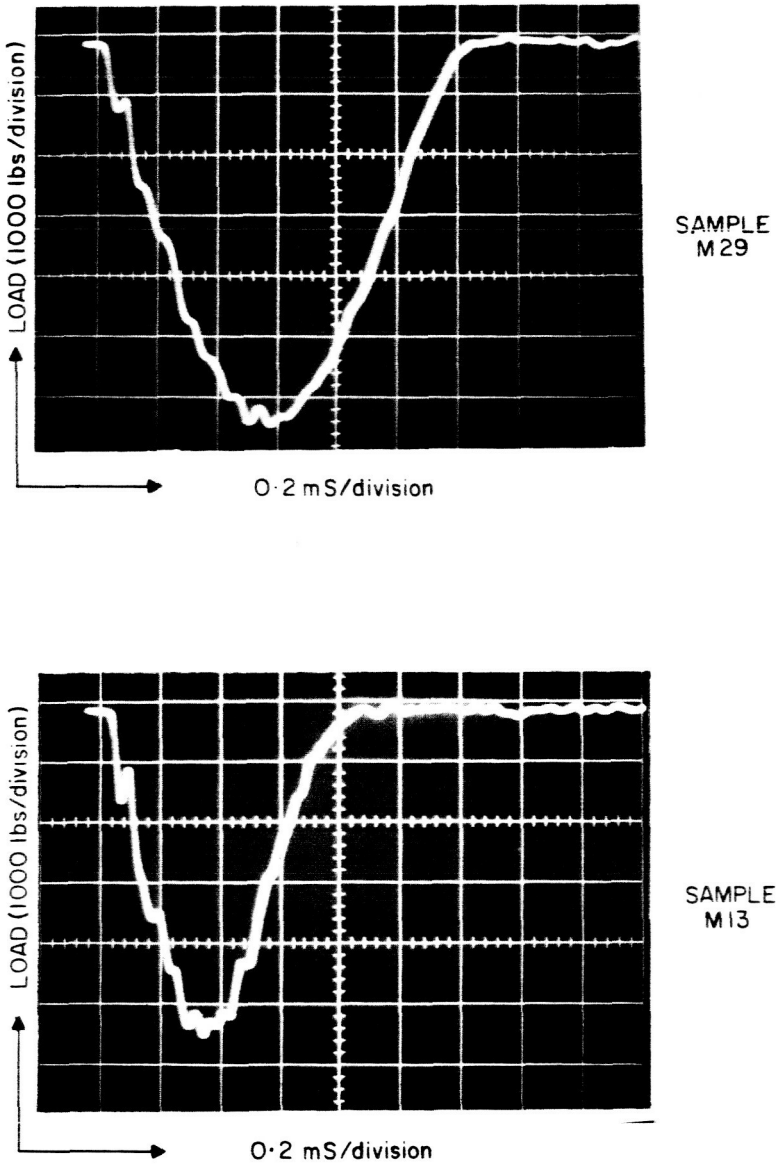

Figure 3-11. Load Pulse Records from Material Survey

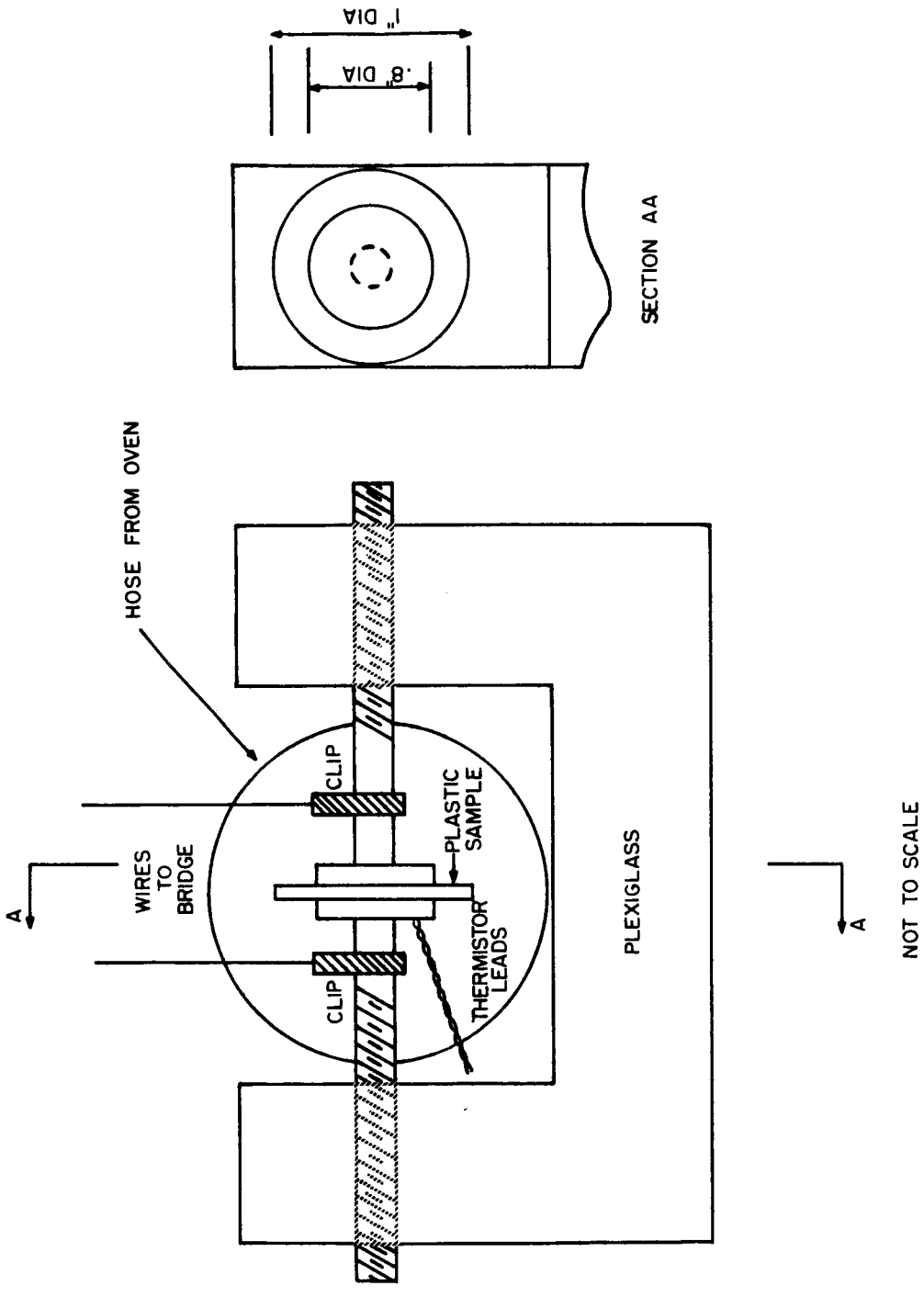

Figure 3-12. Jig for Initial Measurement of Dielectric Properties

Figure 3-12.

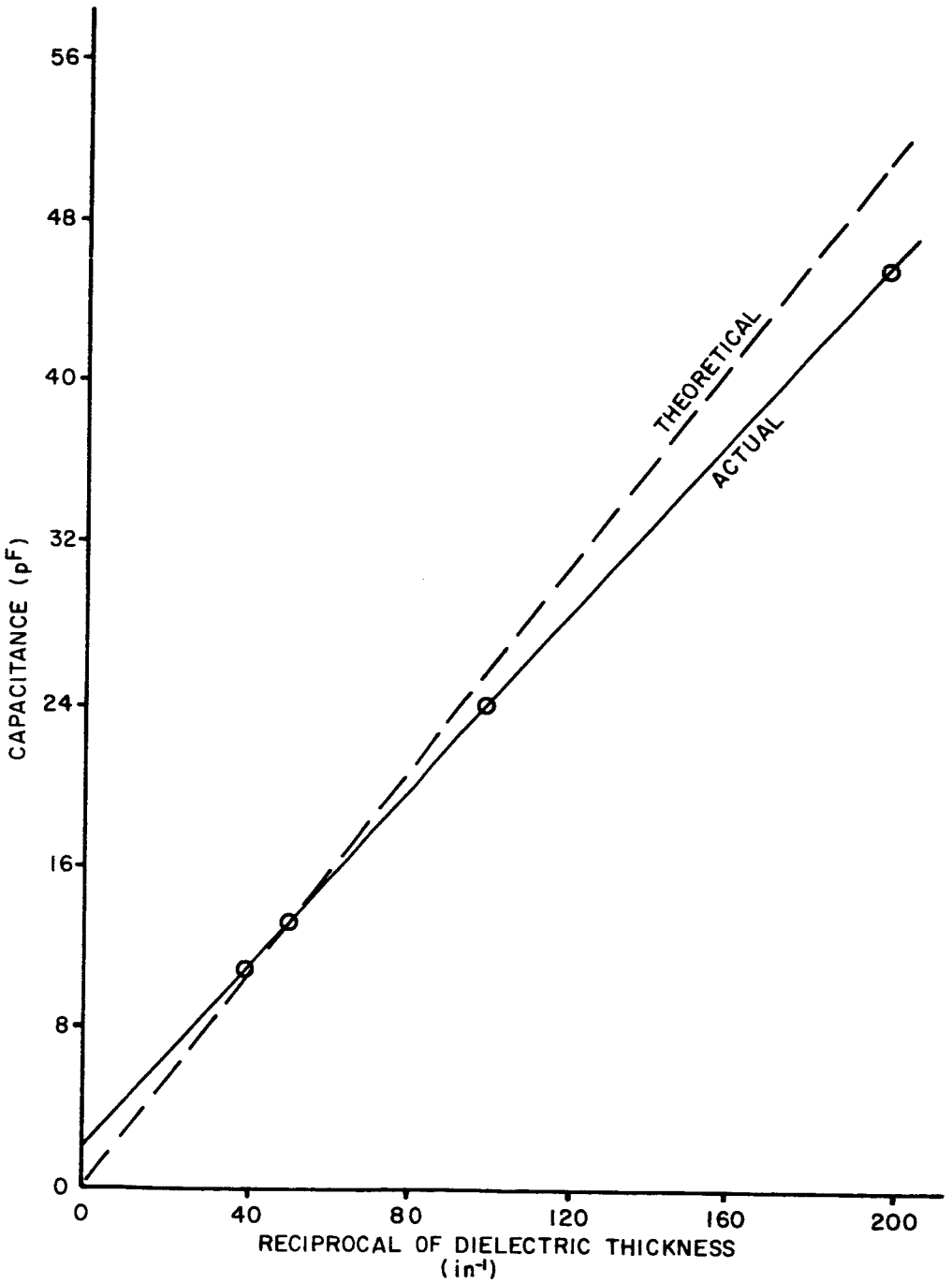

Figure 3-13. Calibration of Dielectric Properties Jig using Polyethylene

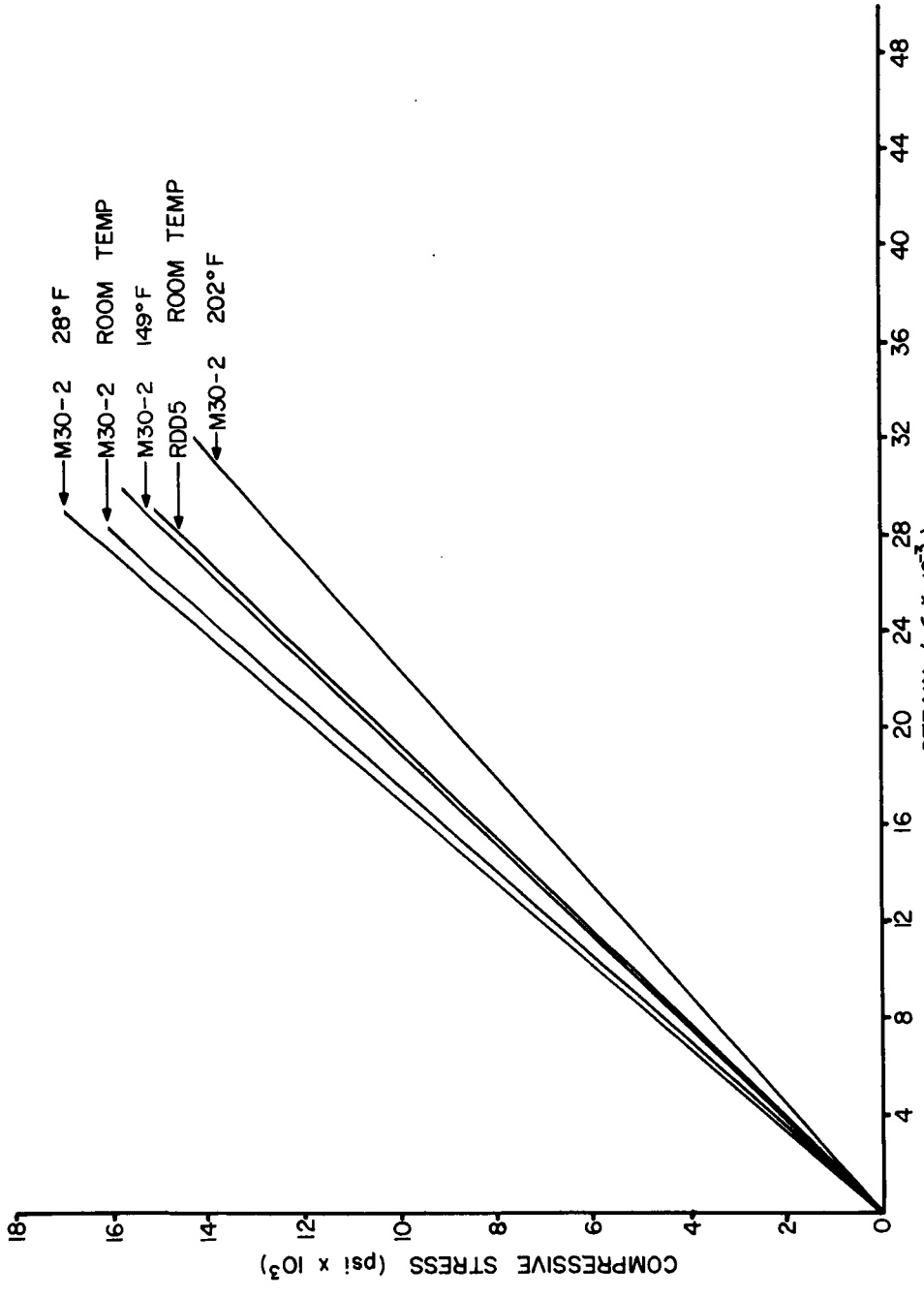

Figure 3-14. Dynamic Properties of M30 over Temperature Range of 28 degrees F to 202 degrees F

Figure 3-14.

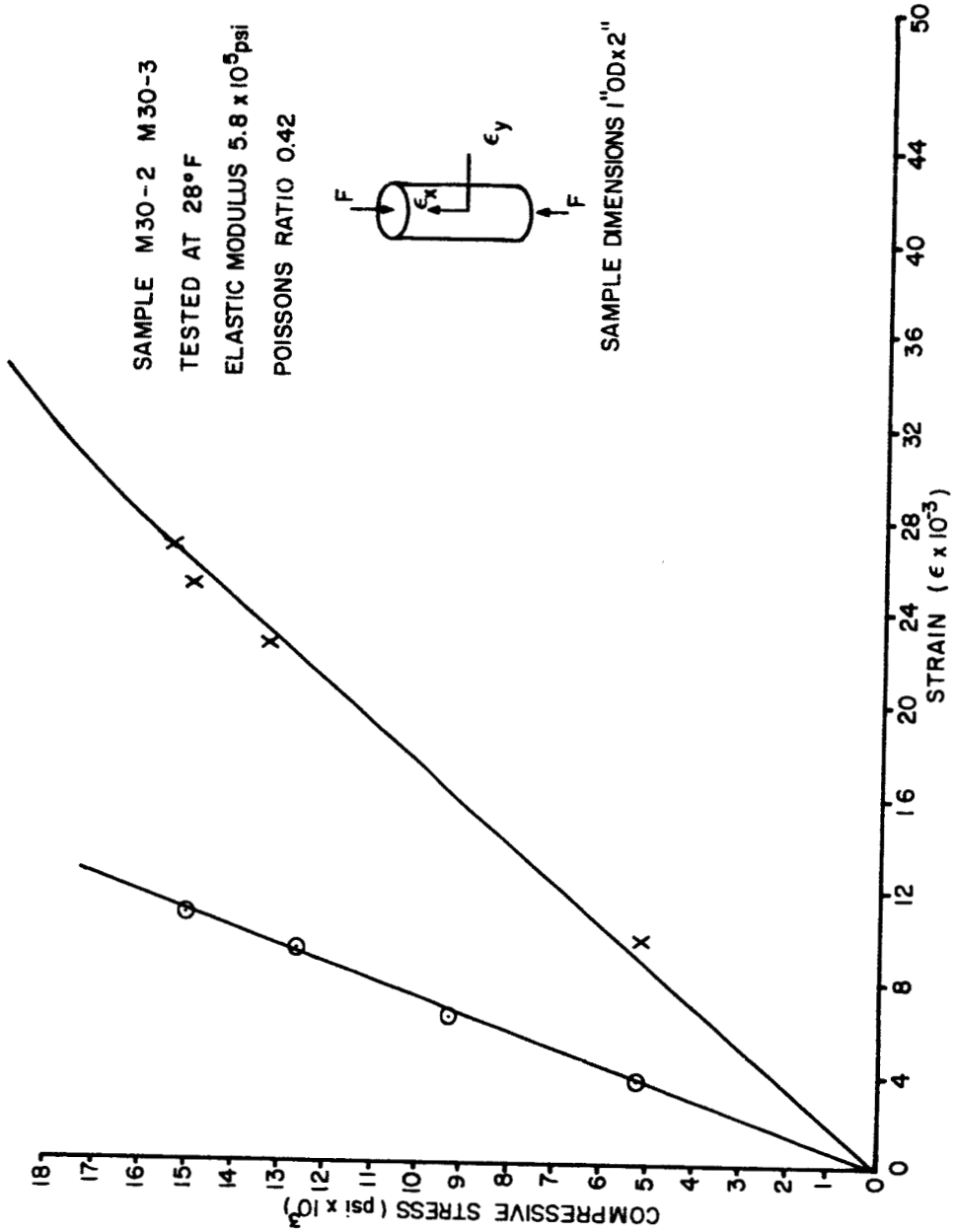

Figure 3-15. Dynamic Properties of M30 (Test Temperature 28 degrees F)

Figure 3-15.

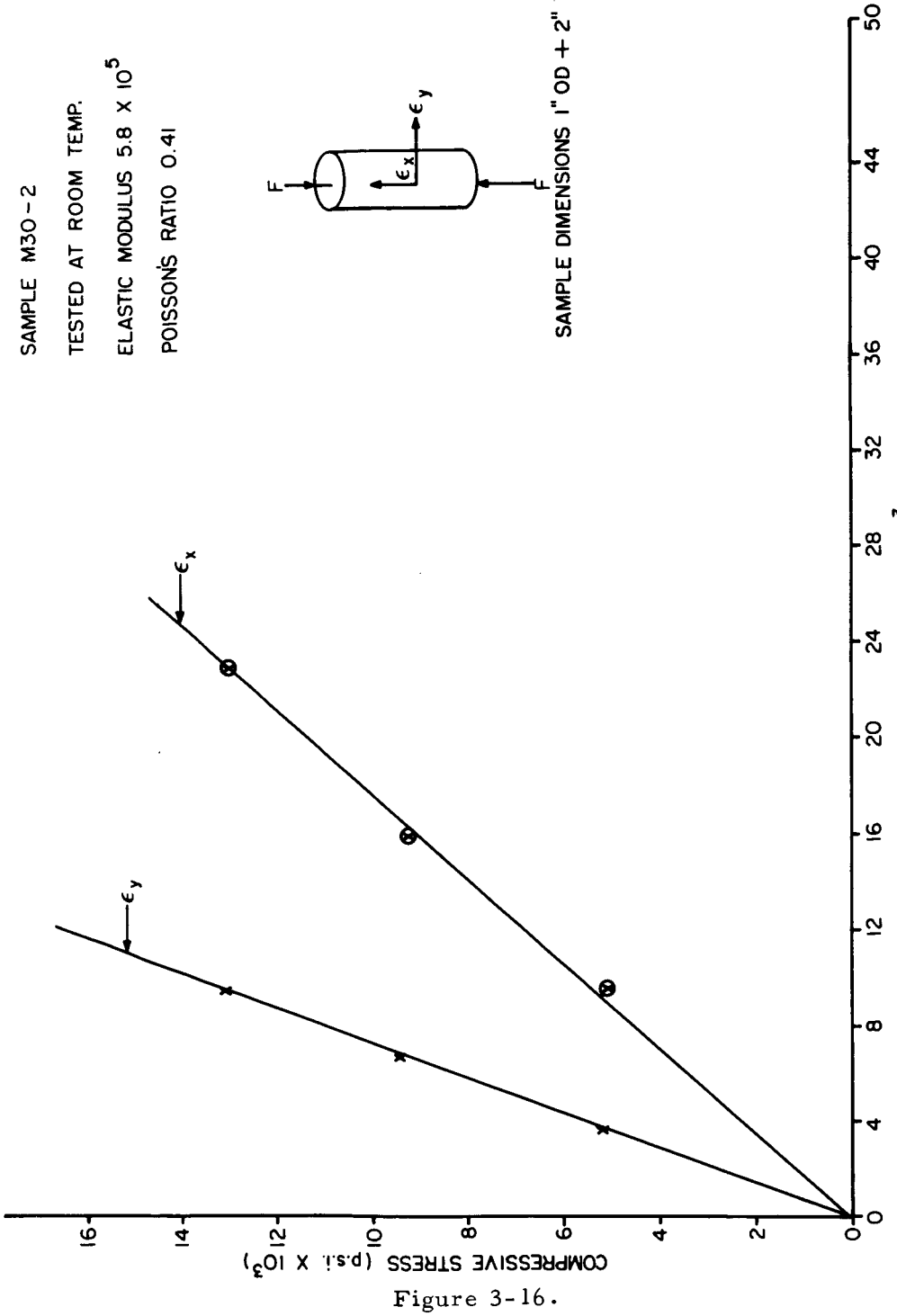

Figure 3-16. Dynamic Properties of M30 (Test at Room Temperature)

Figure 3-16.

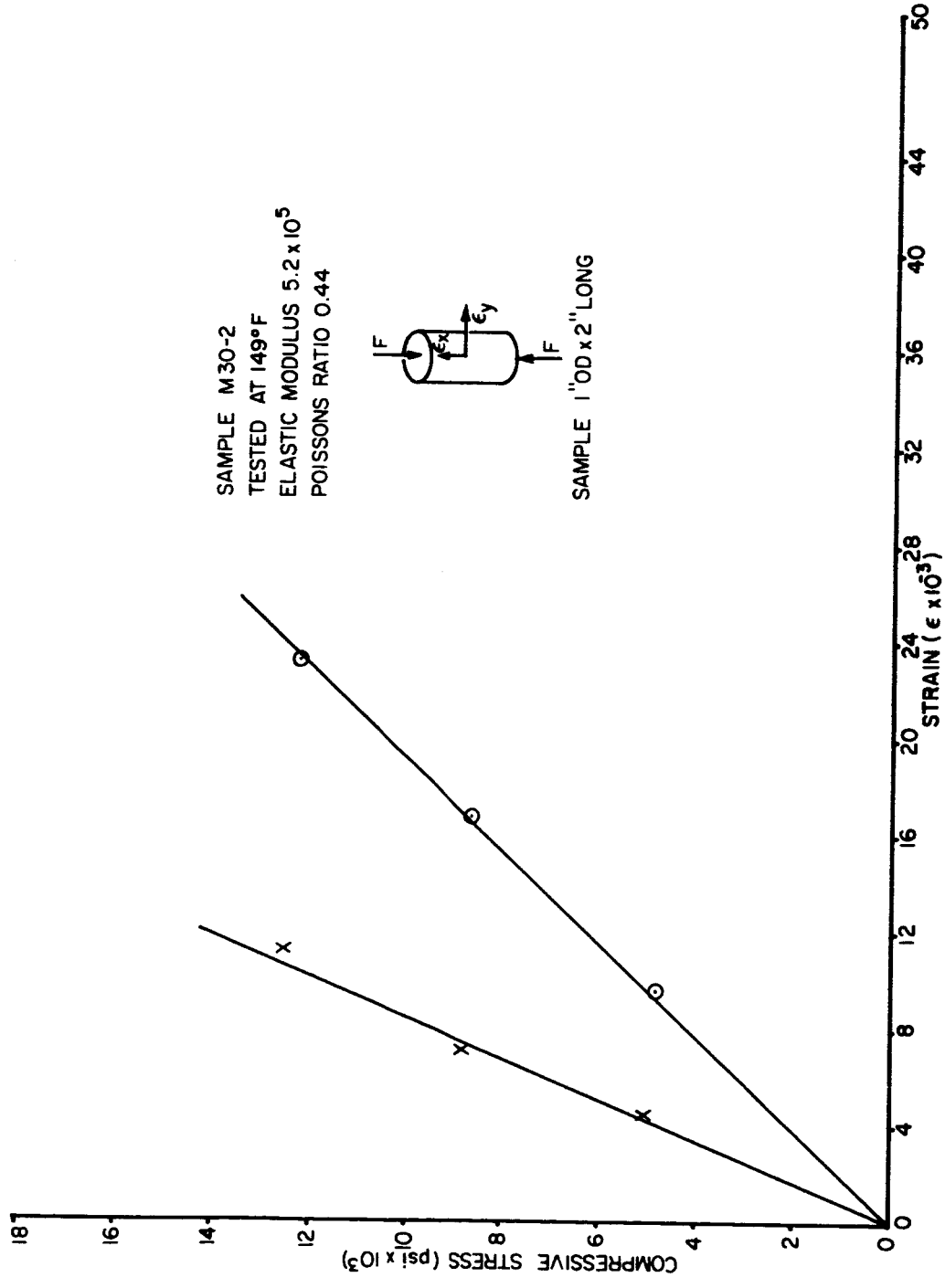

Figure 3-17. Dynamic Properties of M30 (Test Temperature 149 degrees F)

Figure 3-17.

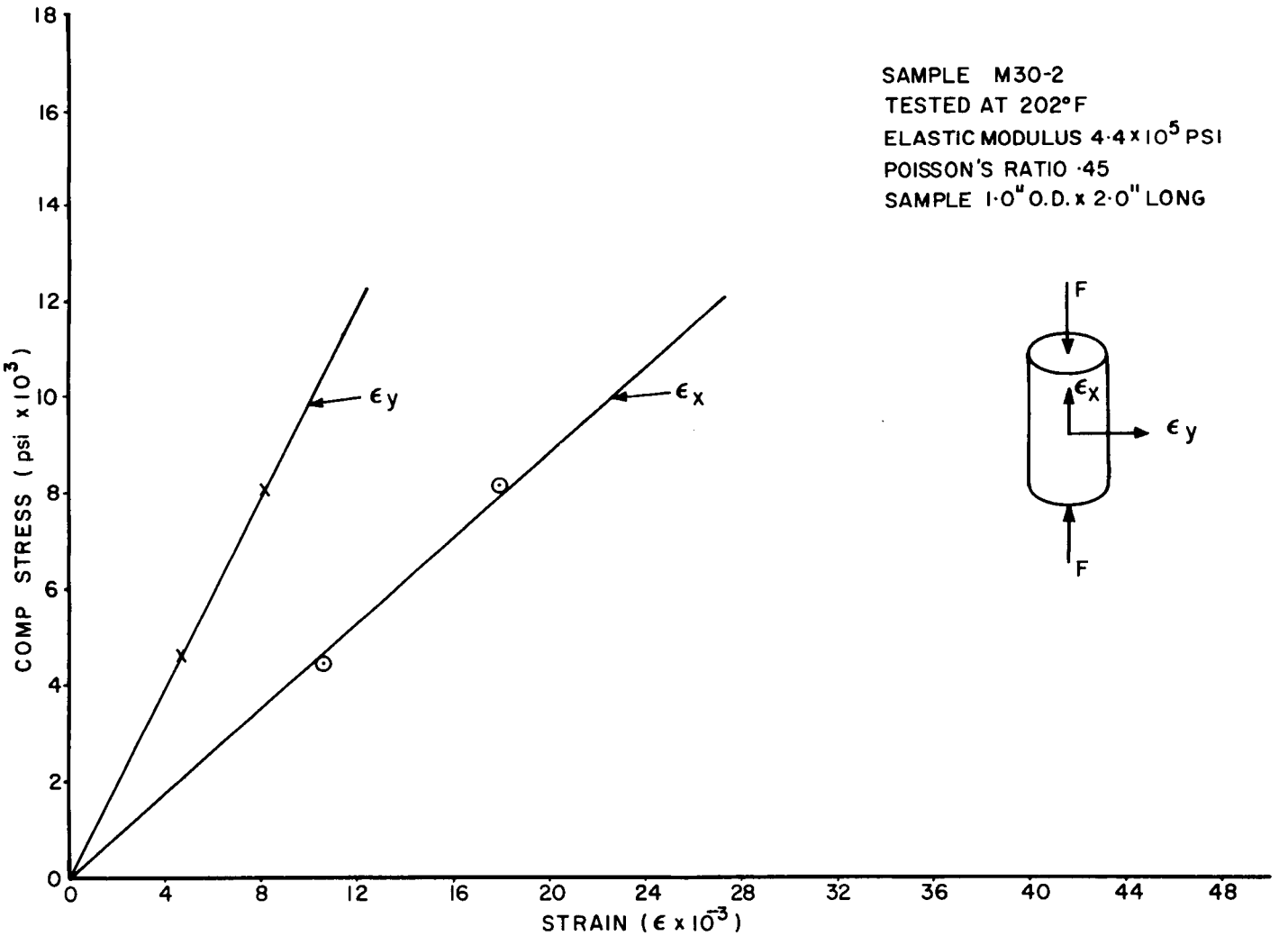

Figure 3-18. Dynamic Properties of M30 (Test Temperature 202 degrees F)

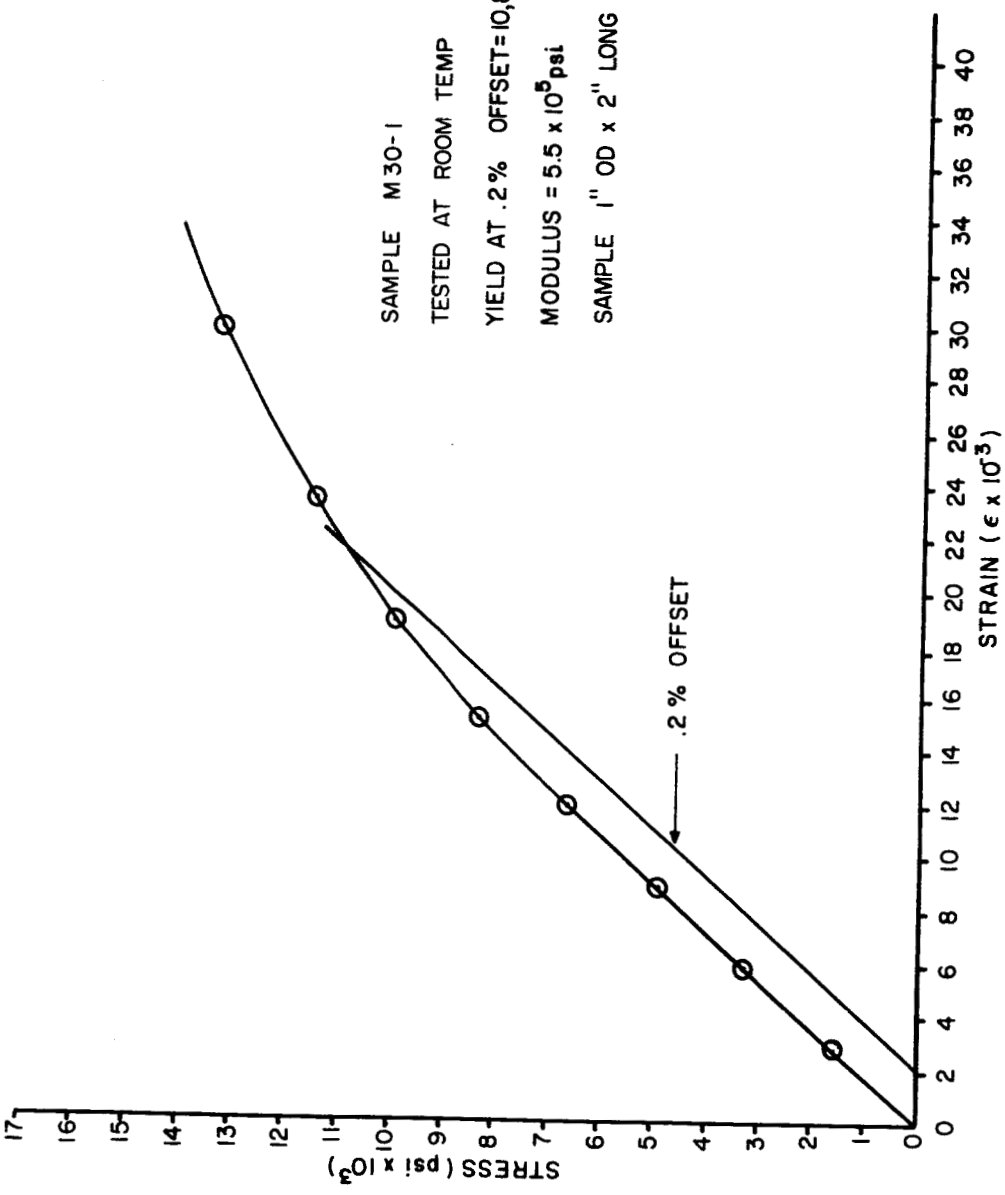

Figure 3-19. Static Properties of M30 (Tested at Room Temperature)

Figure 3-19.

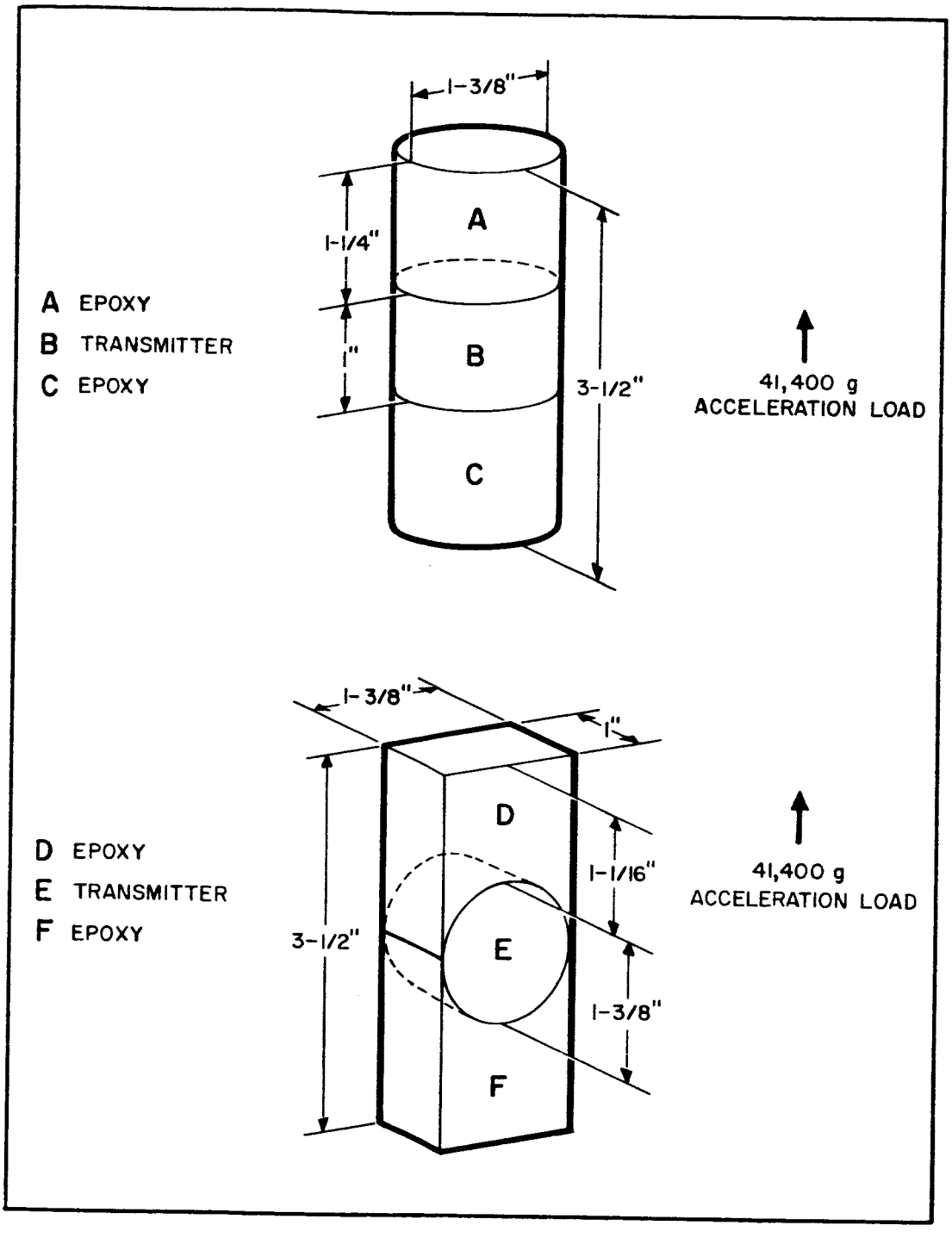

Figure 4-1. Impact Loading of Transmitter in Two Orientations

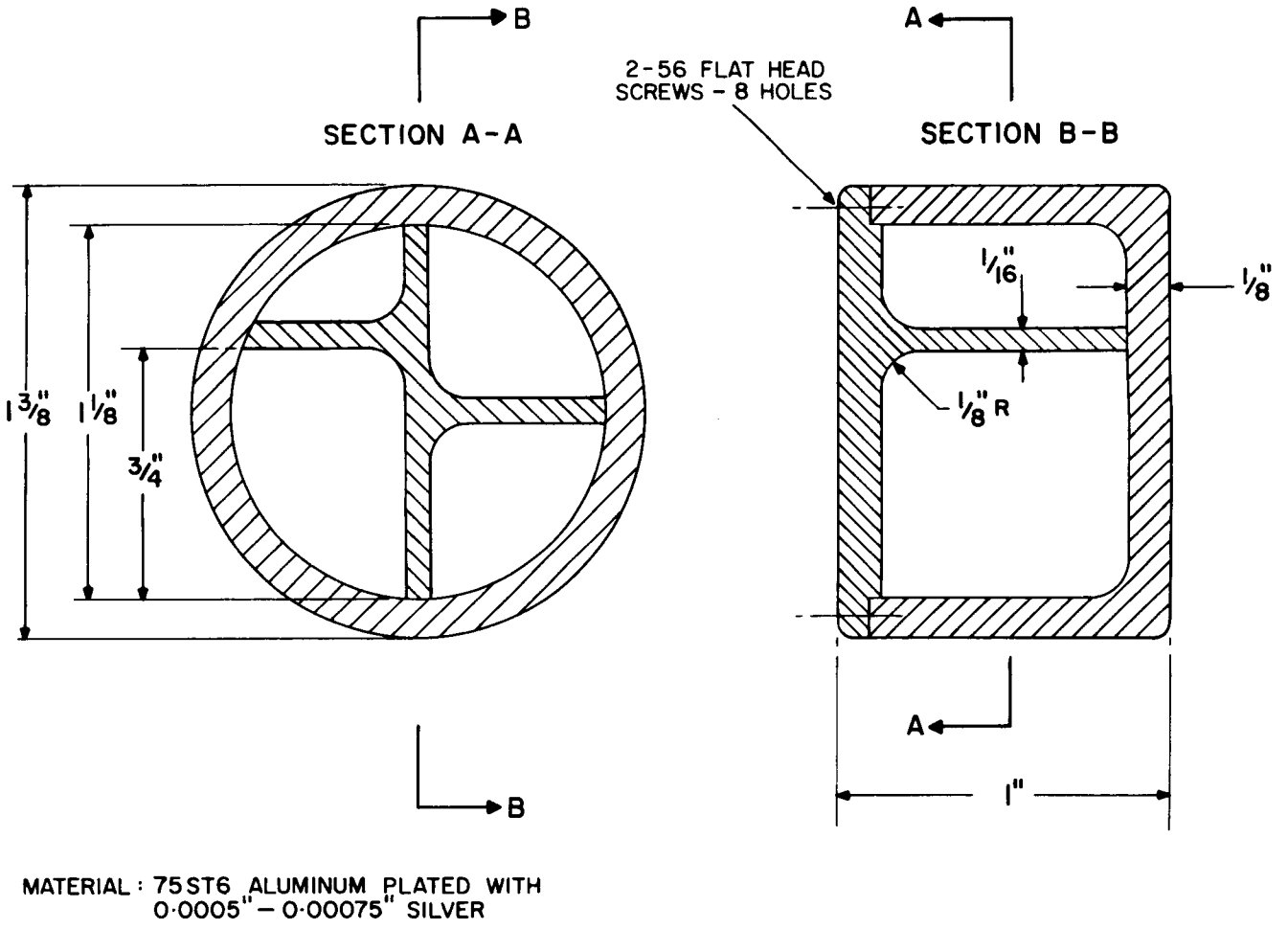

Figure 4-2. Prototype Transmitter Case

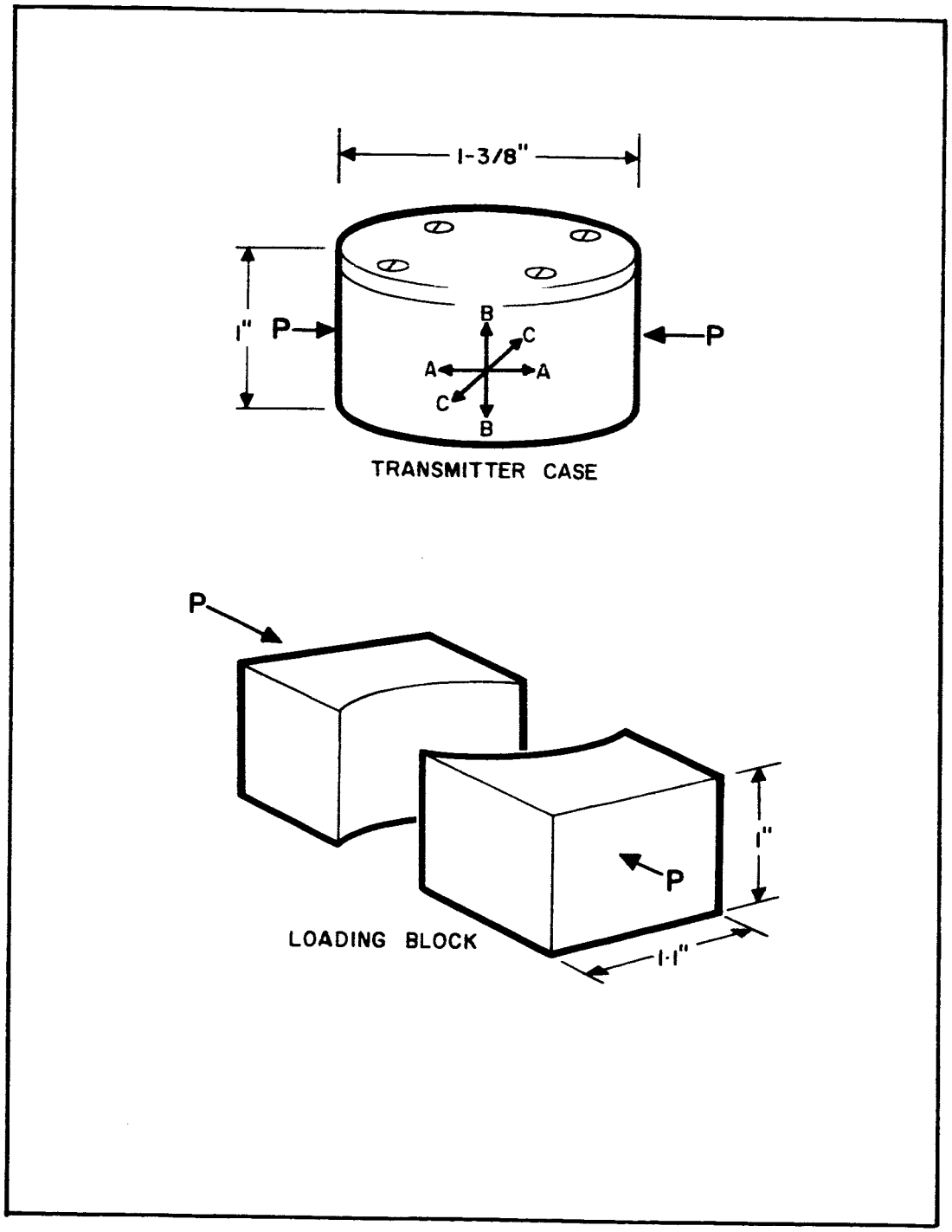

Figure 4-3. Strain Gauge Orientation in Dummy Transmitter Case

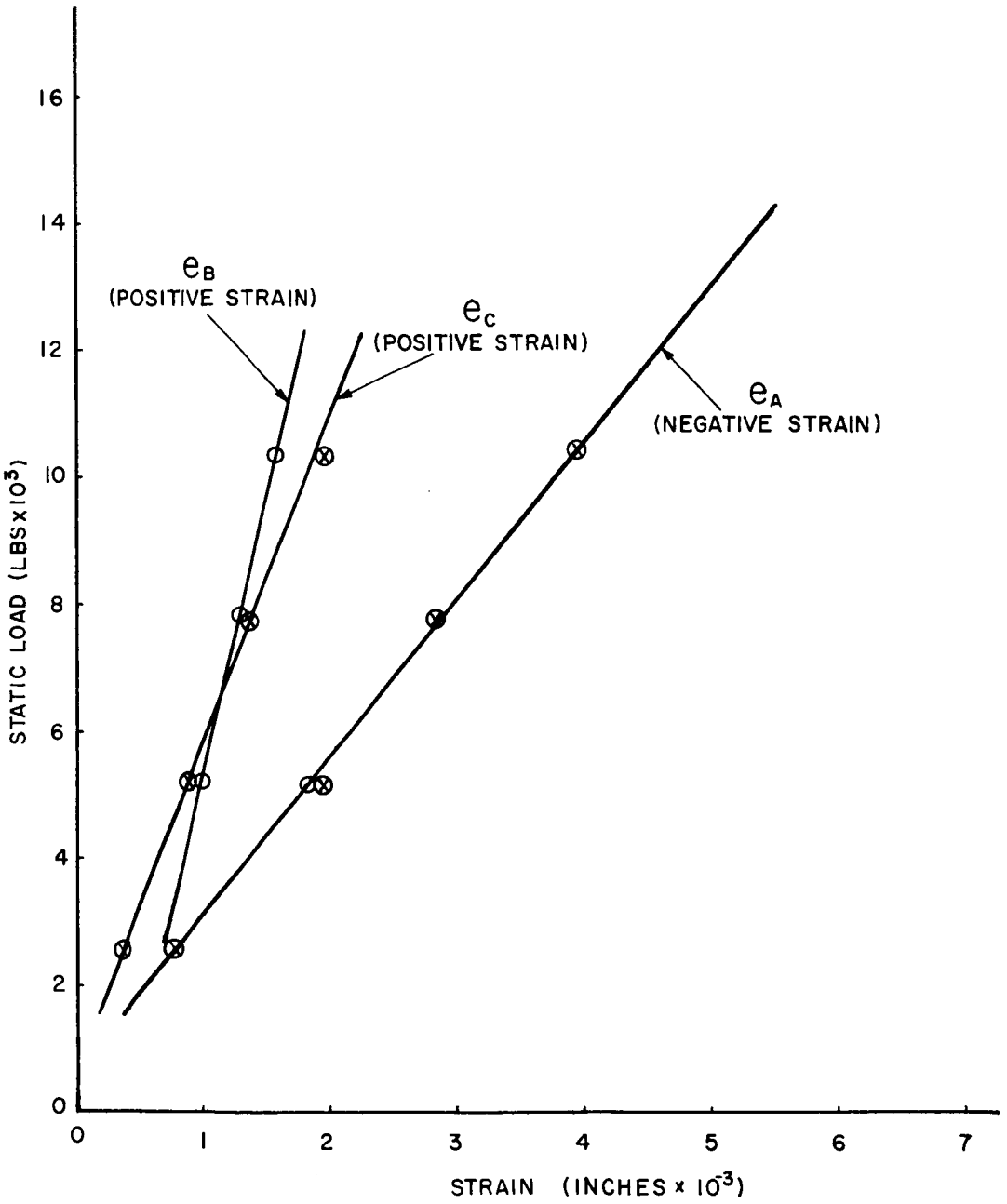

Figure 4-4. Strain Versus Load in Transmitter Case

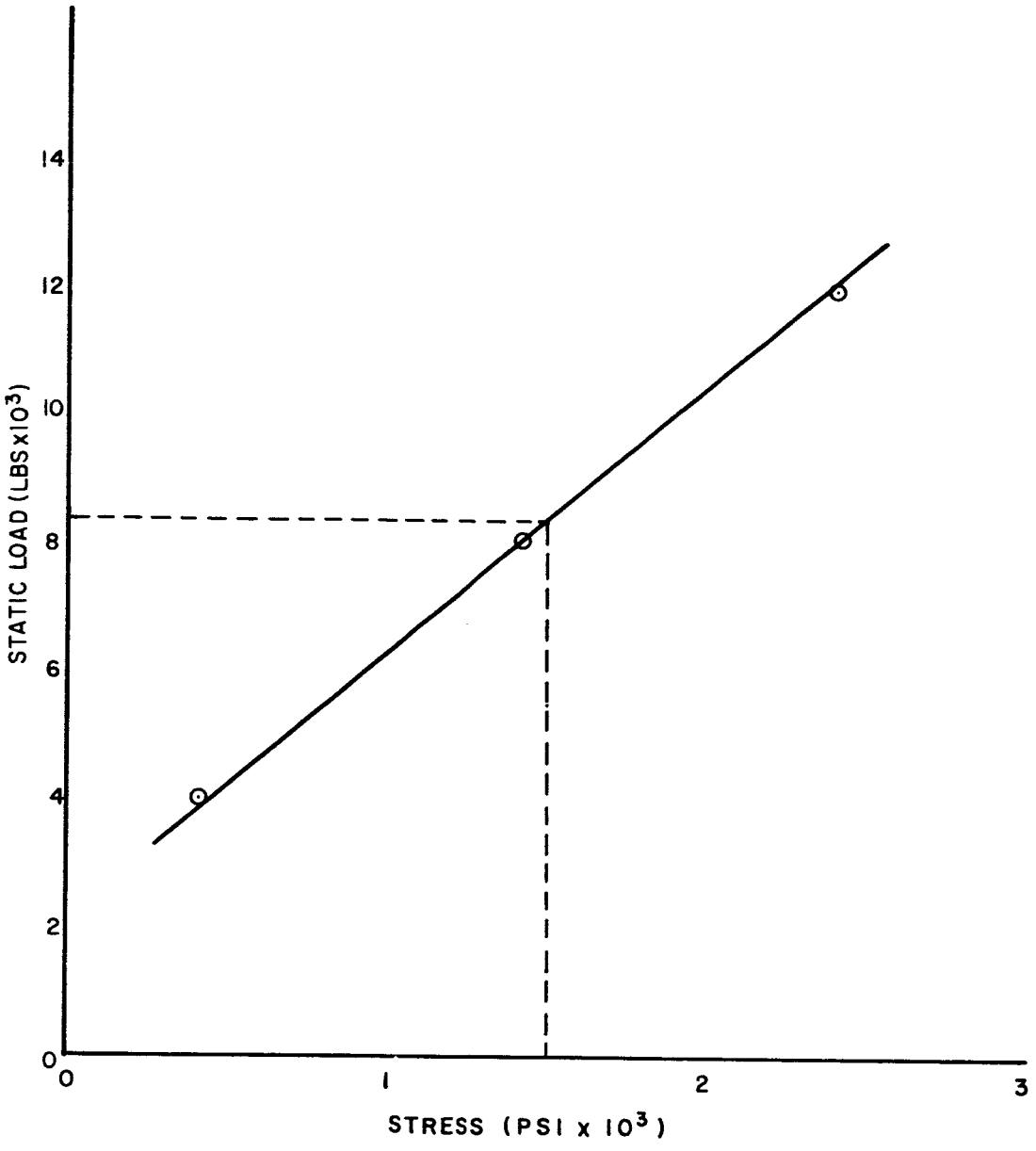

Figure 4-5. Maximum Compressive Stress Versus Load in Transmitter Case

COMPONENTS LIST

FOR FIGURE 5-1

COMPONENT REFERENCE NUMBER	VALUE	TOLERANCE	MANU-FACTURER	PART NUMBER
Resistors				
R1	22K	±10%	ATC	22,000-A-10-L
R2	100K		ATC	100,000-A-10-L
R3	4.7K		ATC	4,700-A-10-L
R4	22K		ATC	22,000-A-10-L
R5	4.7K		ATC	4,700-A-10-L
R6	1.0K		ATC	1,000-A-10-L
R7	470Ω		ATC	470-A-10-L
R8	2.7K		ATC	2,700-A-10-L
R9	330Ω		ATC	330-A-10-L
R10	330Ω		ATC	330-A-10-L
R11	330Ω		ATC	330-A-10-L
R12	470Ω		ATC	470-A-10-L
R13	22K		ATC	22,000-A-10-L
R14	2.2K		ATC	2,200-A-10-L
R15	220Ω		ATC	220-A-10-L
R16	22K		ATC	22,000-A-10-L
R17	50Ω		ATC	50-A-10-L
Capacitors				
C1	8.2pF	±10%	Vitramon	VY04C8R2K
C2	15	±5%	Corning	CY10C150J
C3	2.7	±5%	Vitramon	VY04C2R7J
C4	15	±10%	Vitramon	VY04C150K
C5	1.0	±10%	Vitramon	VY04C1R0K
C6	1.5	±10%	Vitramon	VY04C1R5K
C7	2.2	±10%	Vitramon	VY04C2R2K
C8	22	±5%	Corning	CY10C220J
C9	3.3	±10%	Vitramon	VY04C3R3K
C10	15	±10%	Vitramon	VY04C150K
C11	0.5	±10%	Vitramon	VY04C0R5K
C12	22	±5%	Corning	CY10C220J
C13	6.8	±5%	Corning	CY10C6R8J
C14	6.8	±10%	Vitramon	VY04C6R8K

COMPONENT REFERENCE NUMBER	VALUE	TOLERANCE	MANU-FACTURER	PART NUMBER
Diodes				
D1 to D5		-	TRW	PD101
D6		-	TRW	PD6012
Transistors				
Q1		-	Texas Instruments	2N2907
Q2 and Q3		-	General Electric	2N3663
Q4		-	R.C.A.	2N3866
RF Chokes	1.00 μH	±10%	J.W. Millar Co.	9230
RF Coils				
L1	3 turns	-	Alumina Ceramic Coil form 0.157" dia. × 0.5" long	
L2 and L3	5 turns	-	ESC Stycast 0005 coil form 0.15" dia. × 0.5" long No. 22 Tinned Copper wire	

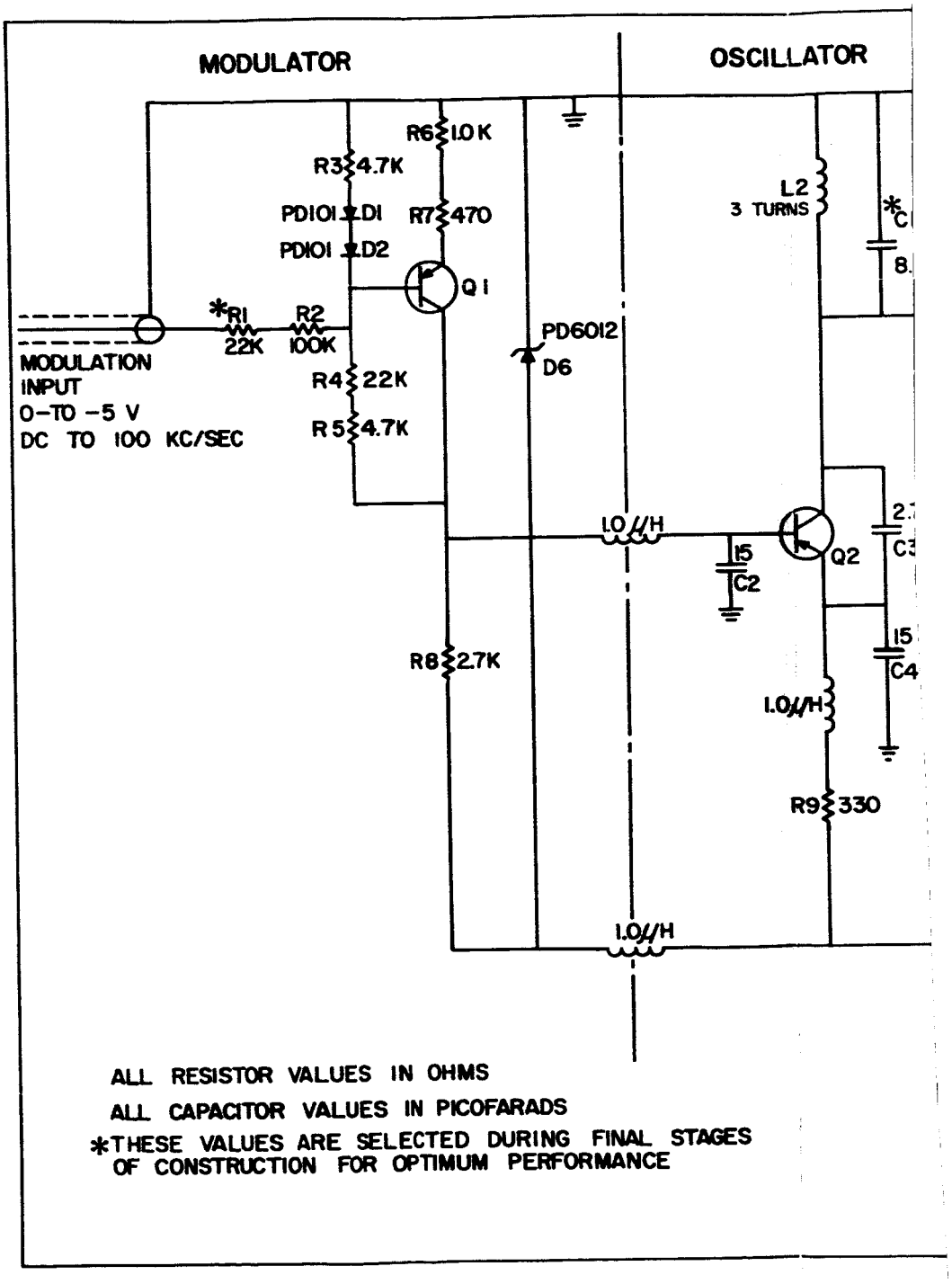
MODULATOR
OSCILLATOR
R6 1.0 K
R3 4.7K
PDIOI D1
R7 470
PDIOI D2
Q1
*R1
22K
R2
100K
MODULATION
INPUT
0-TO -5 V
DC TO 100 KC/SEC
R4 22K
R5 4.7K
PD6012
D6
L2
3 TURNS
1.0 μH
15
C2
Q2
R8 2.7K
1.0μH
R9 330
1.0μH
ALL RESISTOR VALUES IN OHMS
ALL CAPACITOR VALUES IN PICOFARADS
*THESE VALUES ARE SELECTED DURING FINAL STAGES
OF CONSTRUCTION FOR OPTIMUM PERFORMANCE

Figure 5-1.

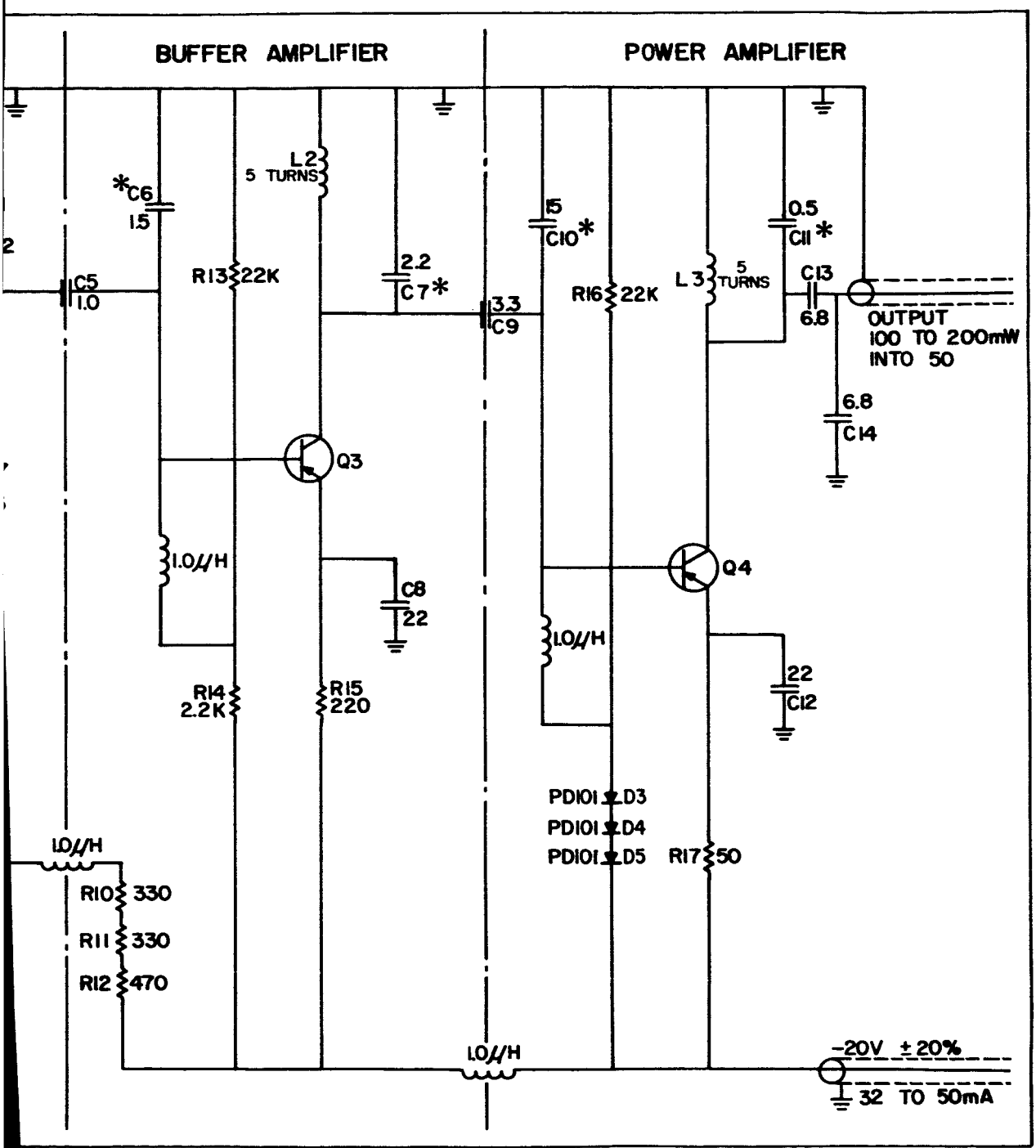

Figure 5-1. Circuit Diagram of Penetrometer 250Mc/s Transmitter

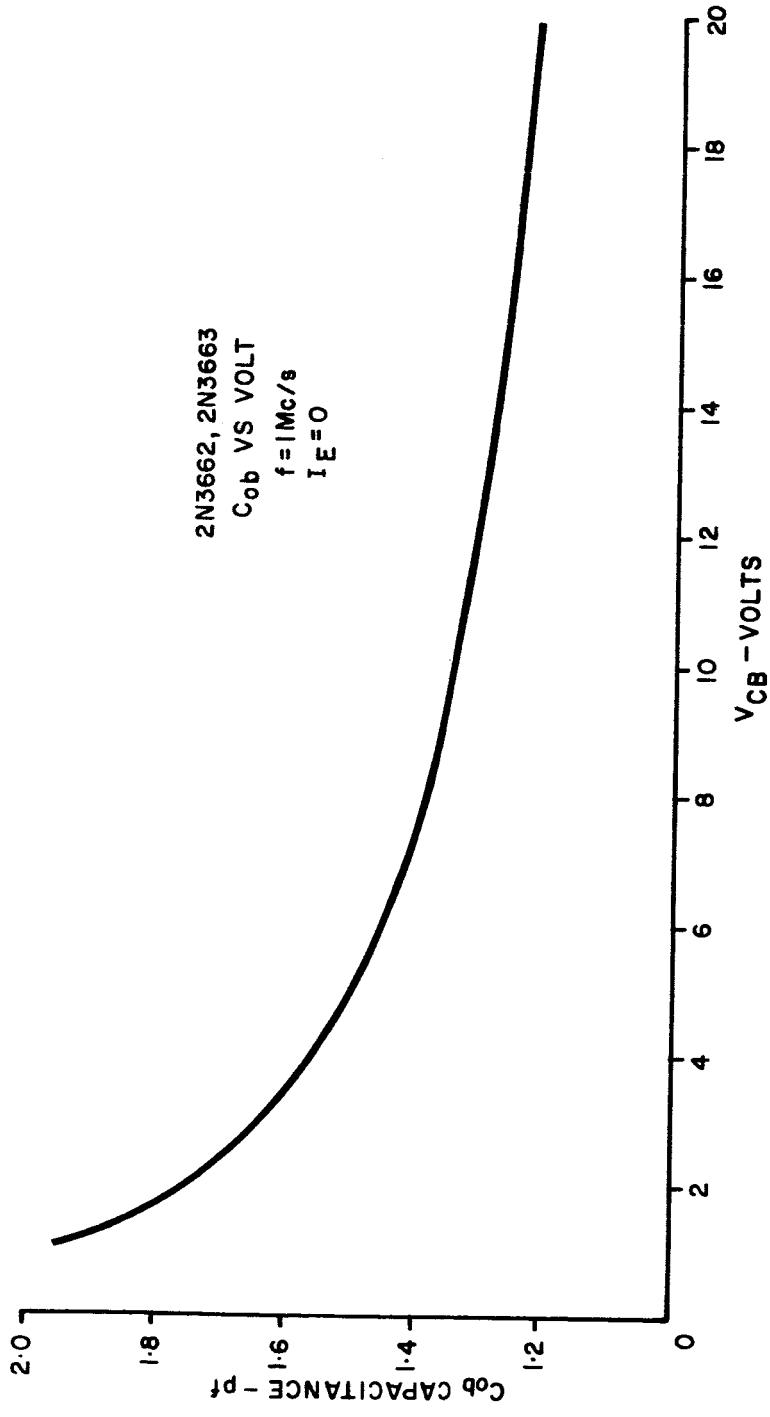

Figure 5-2. 2N3663 Output Capacitance Versus Collector-Base Voltage

Figure 5-2.

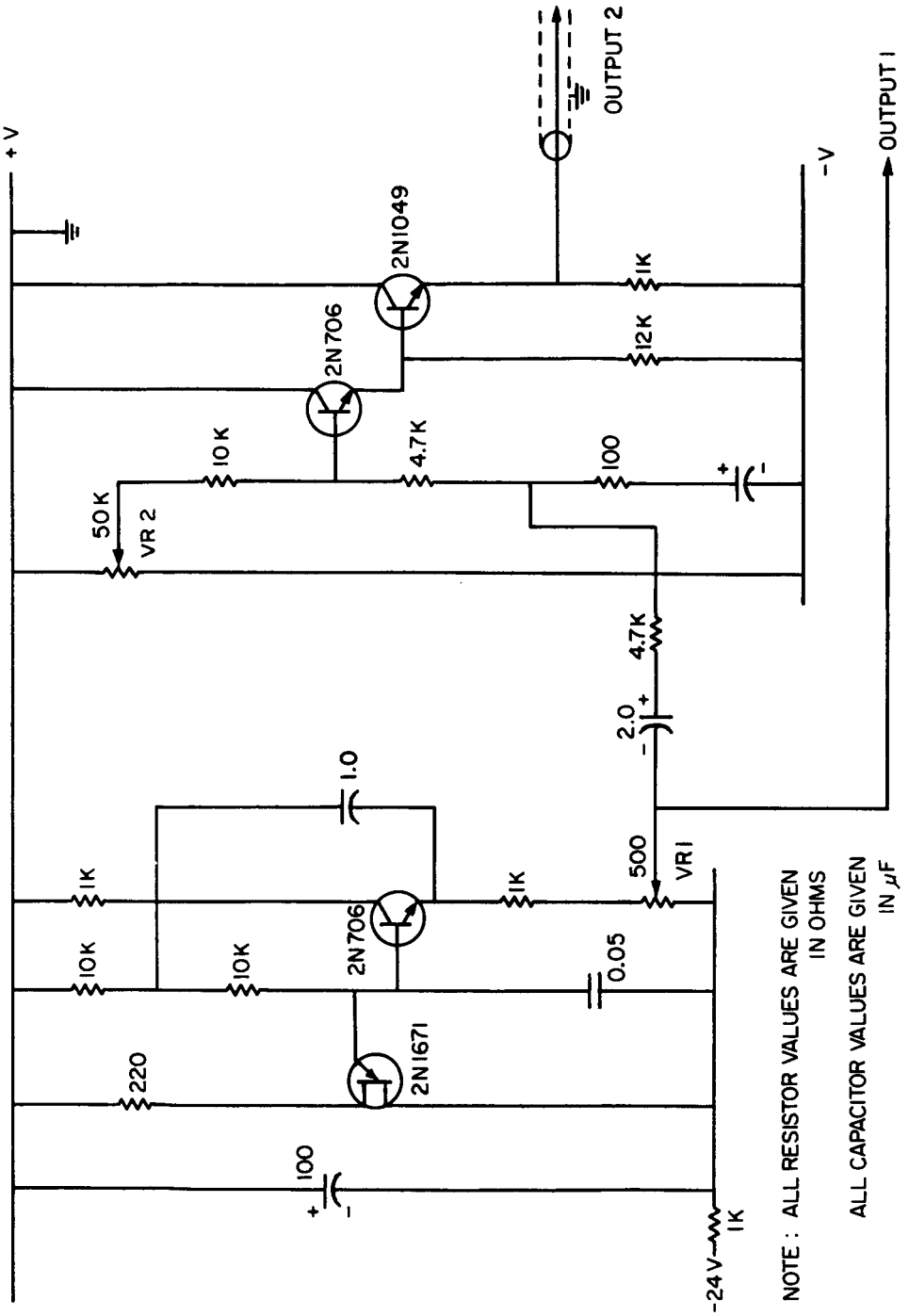

Figure 5-3. Circuit Diagram of Ramp Generator

Figure 5-3.

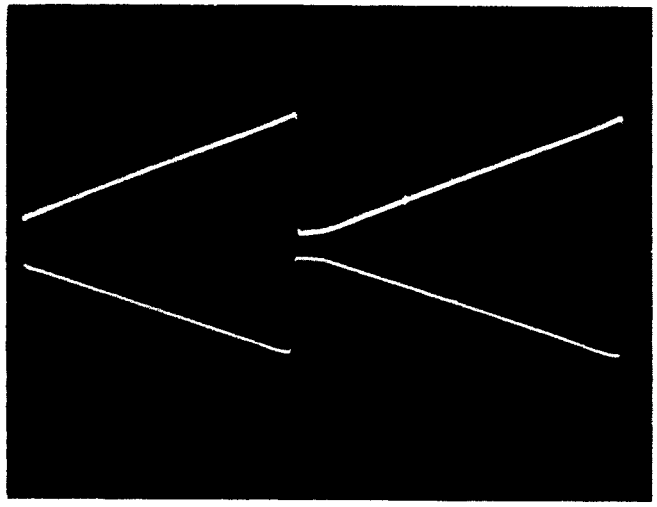

Lower trace:	Ramp generator output 10 mV per cm
Upper trace:	Output from receiver Approximately 100 kc/s deviation per cm
Time base:	0.2 millisecond per cm

Figure 5-4. Ramp Generator and Modulation Waveforms

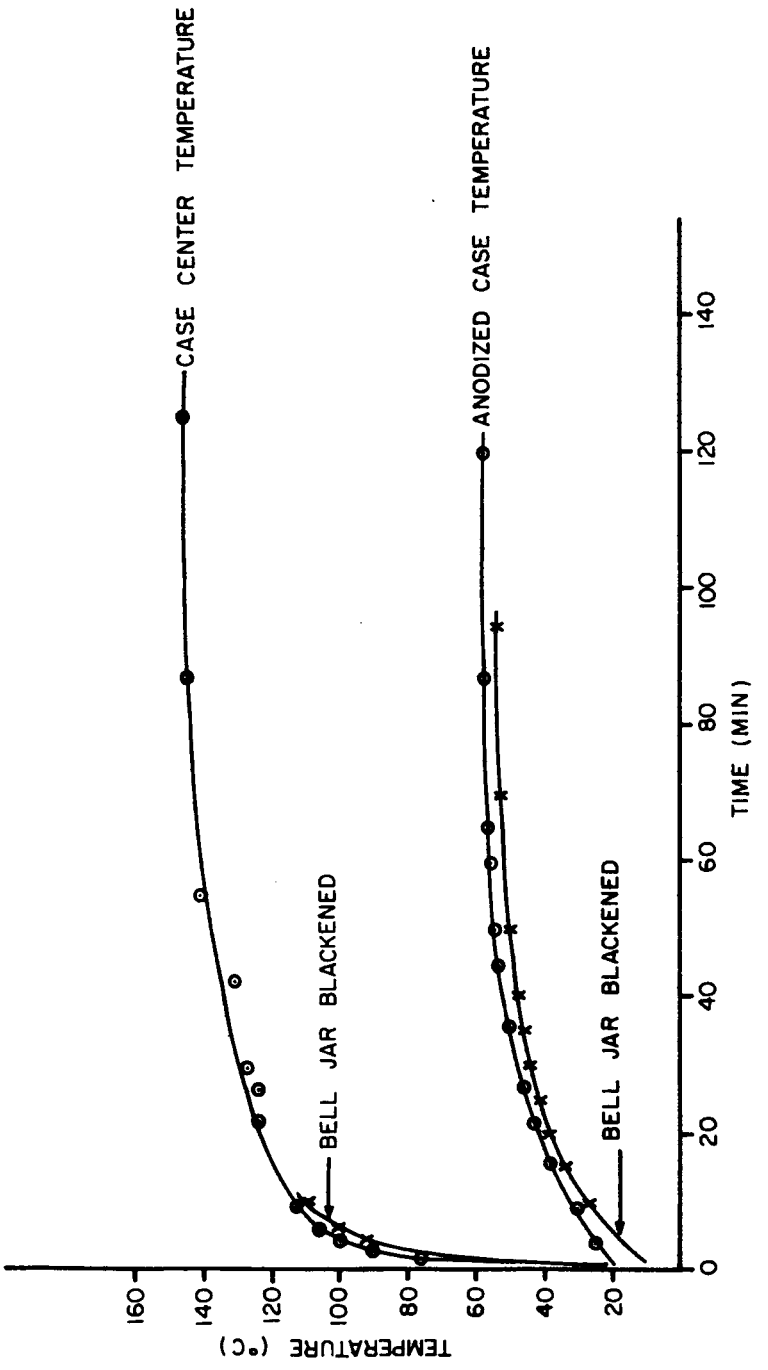

Figure 5-5. Power Dissipation in a Vacuum-Black Anodized Case

Figure 5-5.

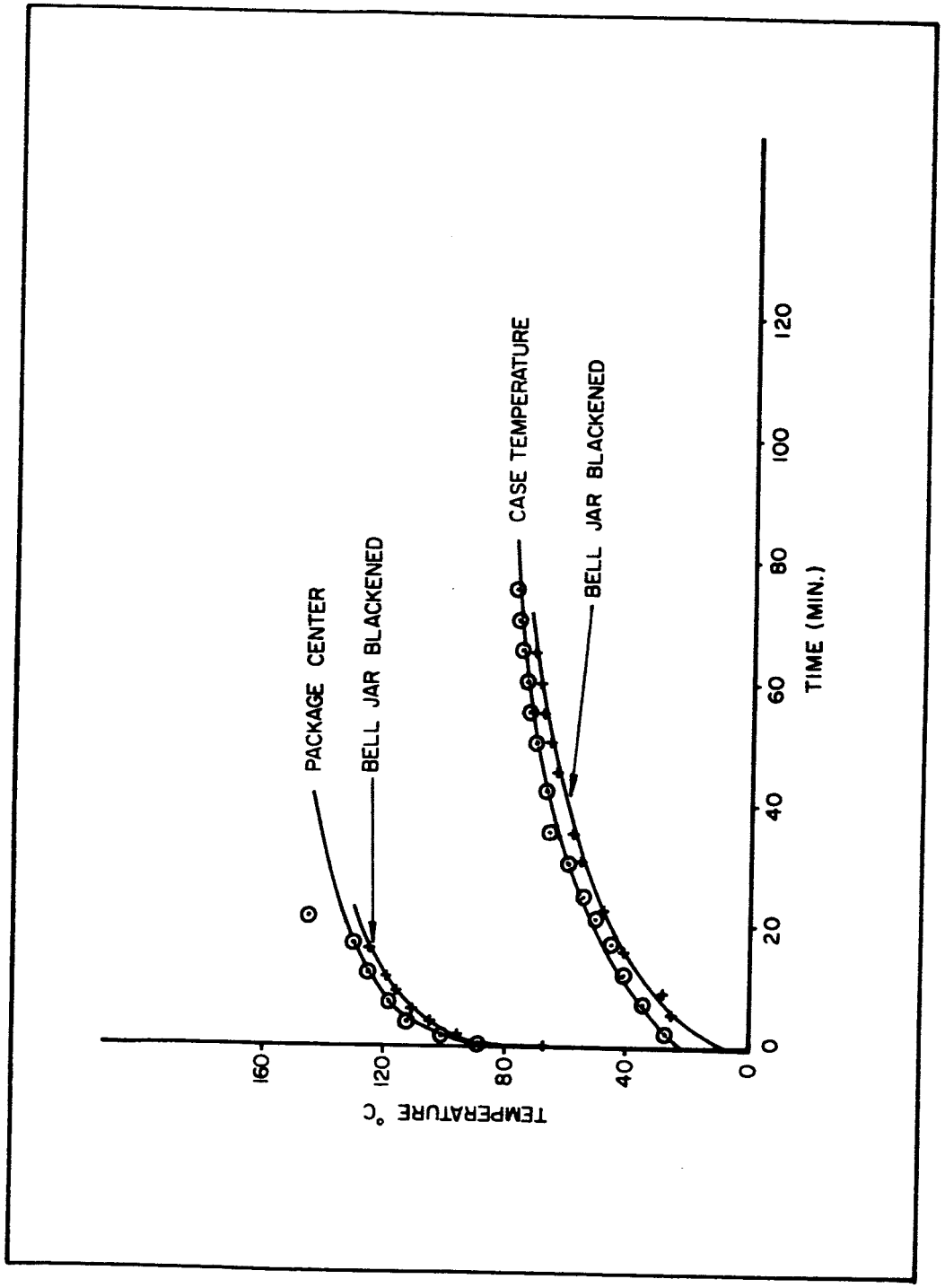

Figure 5-6. Power Dissipation in a Vacuum-Polished Case

Figure 5-6.

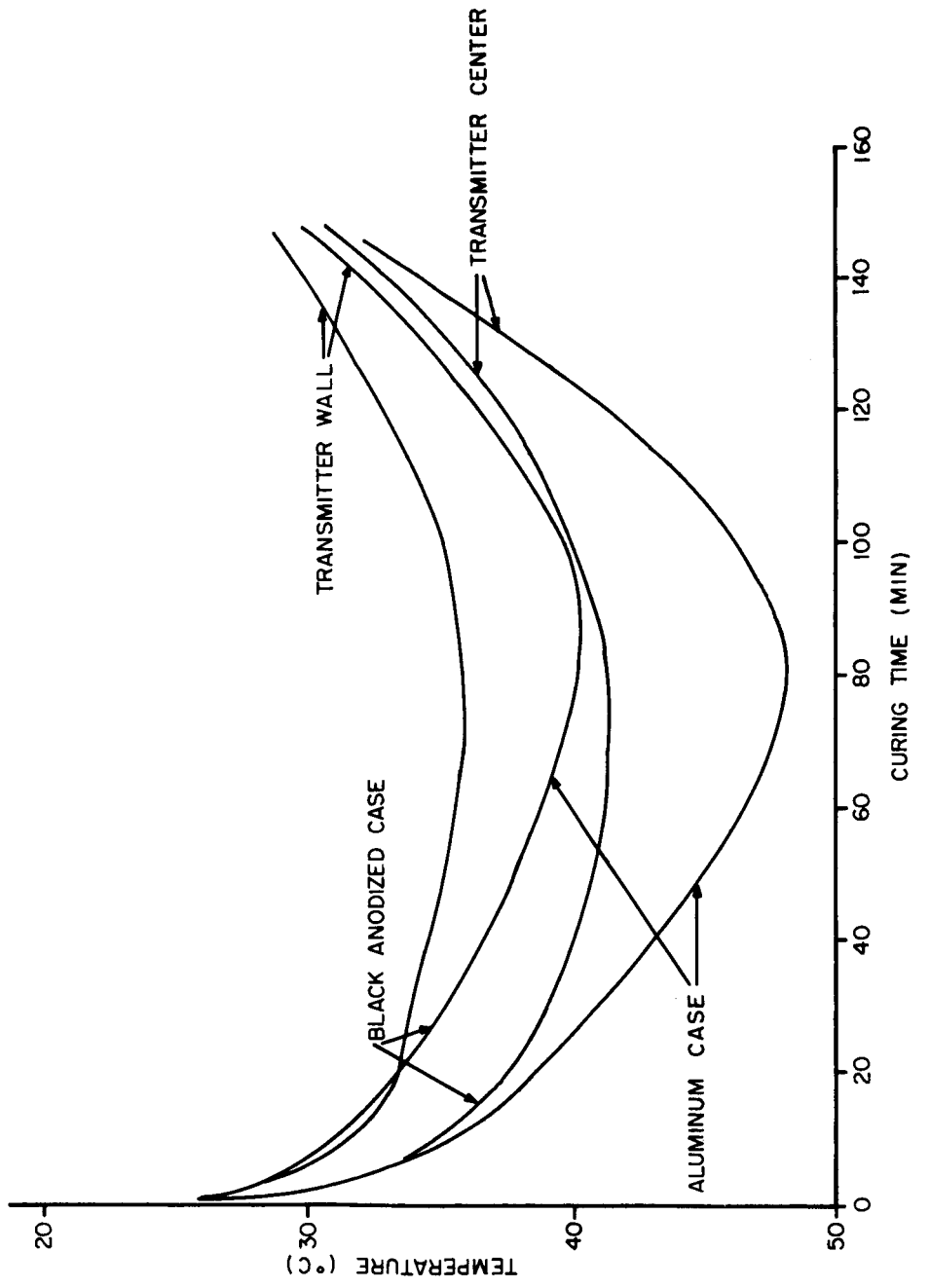

Figure 5-7. Curing Temperature of RDD5 in Transmitter Case

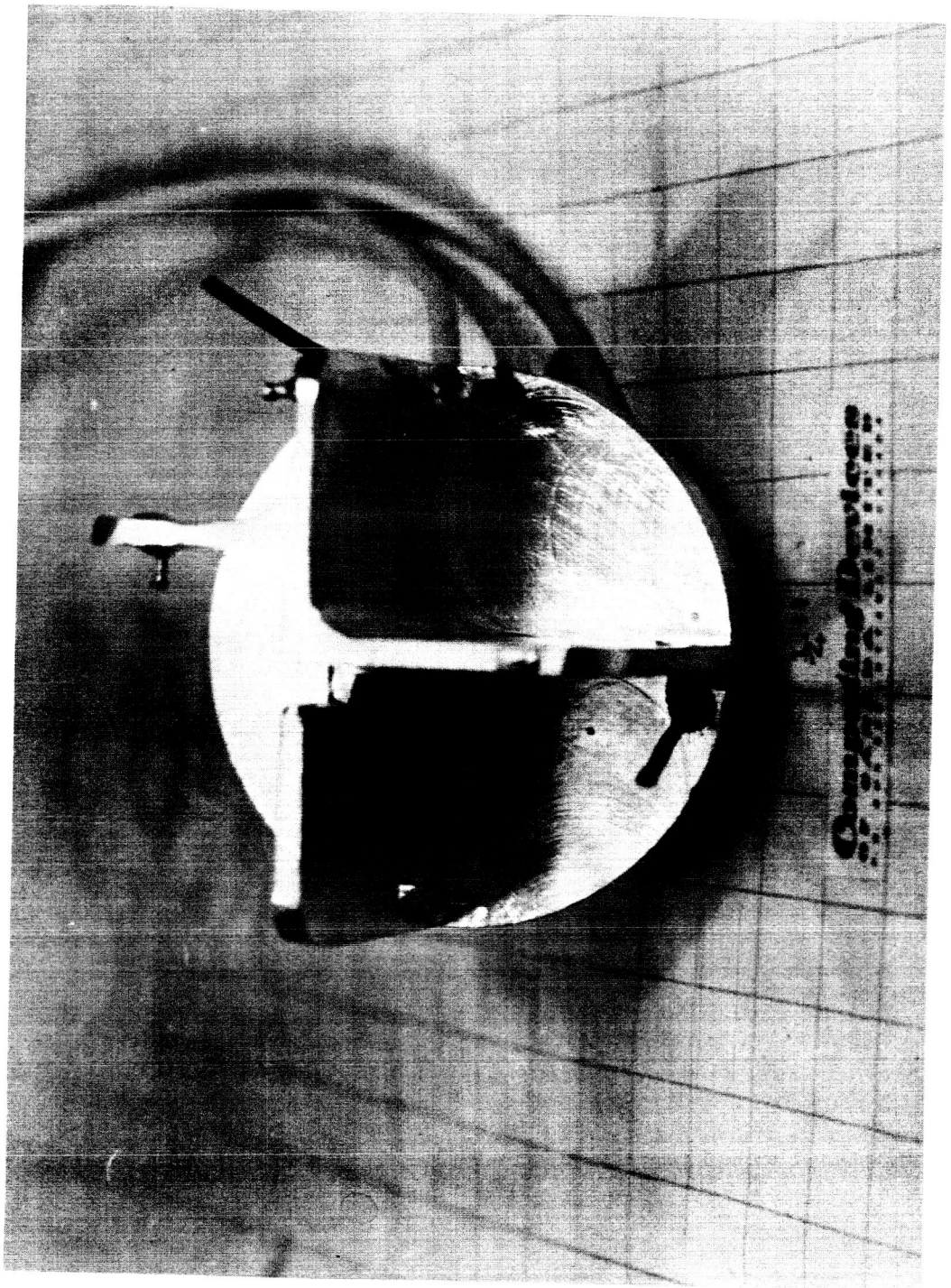

Figure 5-8. Transmitter Base

Figure 5-8.

Figure 5-9. Transmitter Modulator and Oscillator Compartment

Figure 5-9.

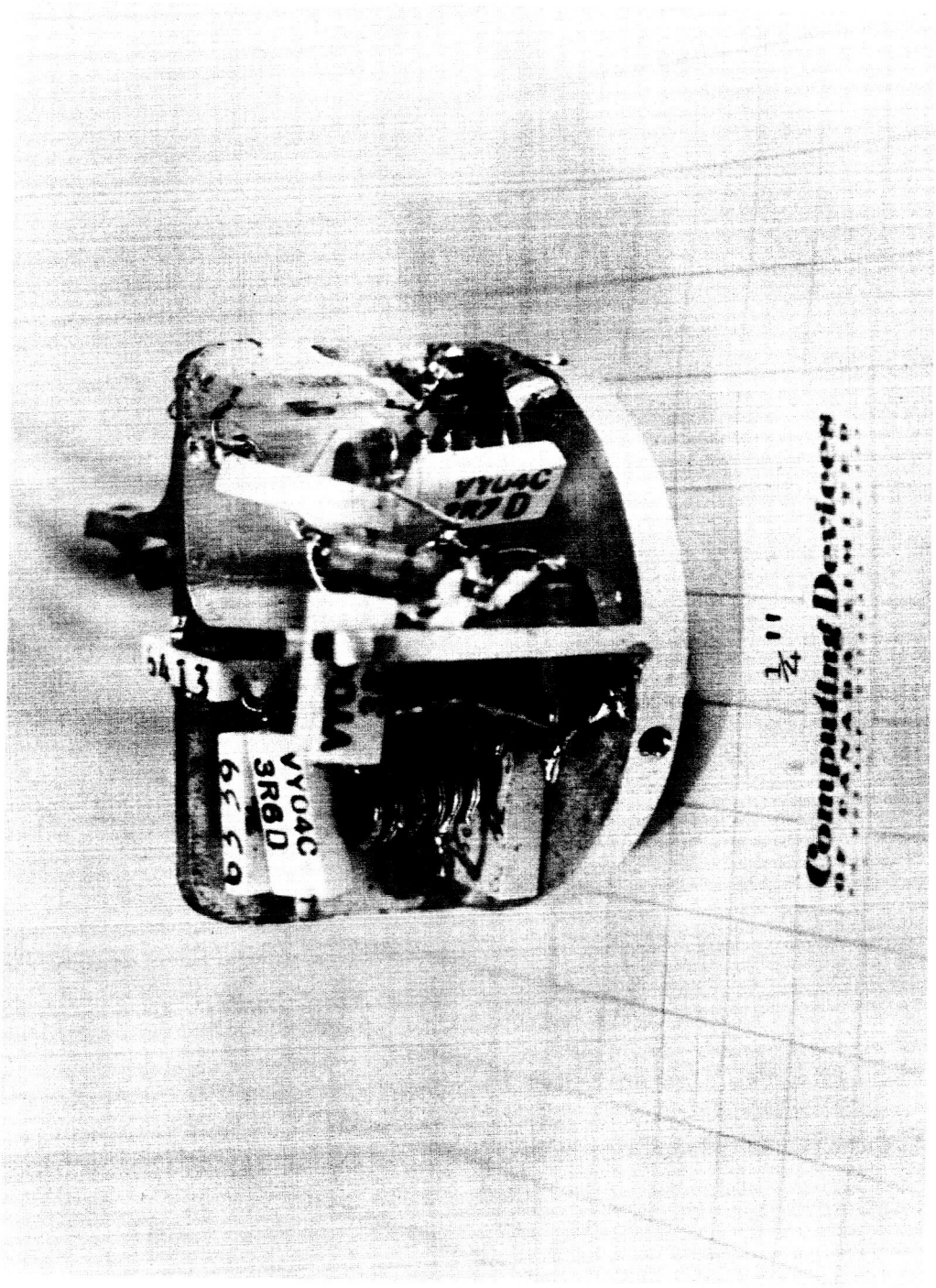

Figure 5-10. Transmitter Buffer Amplifier and Power Amplifier Compartments

Figure 5-10.

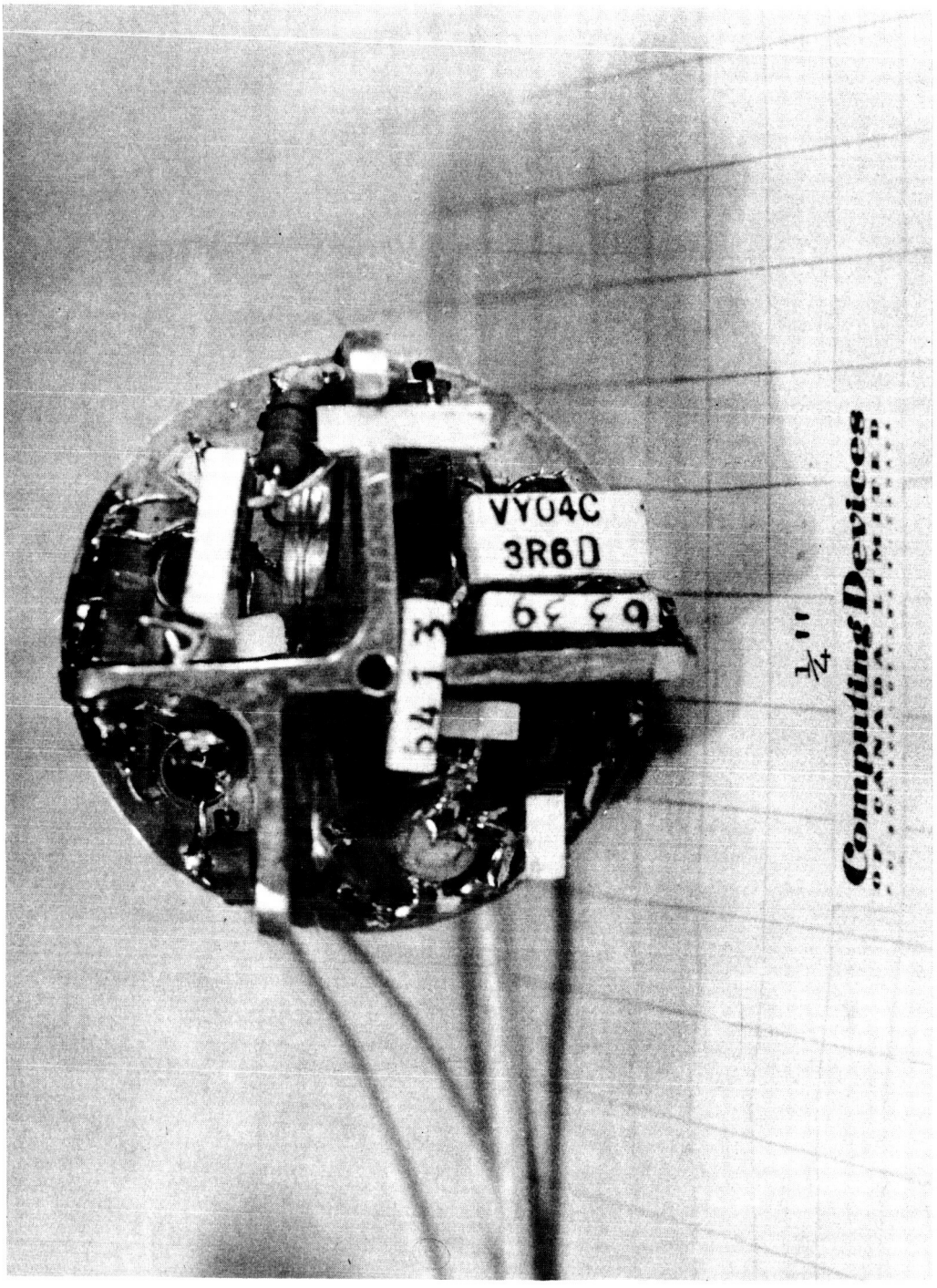

Figure 5-11. Top View of Transmitter

Figure 5-11.

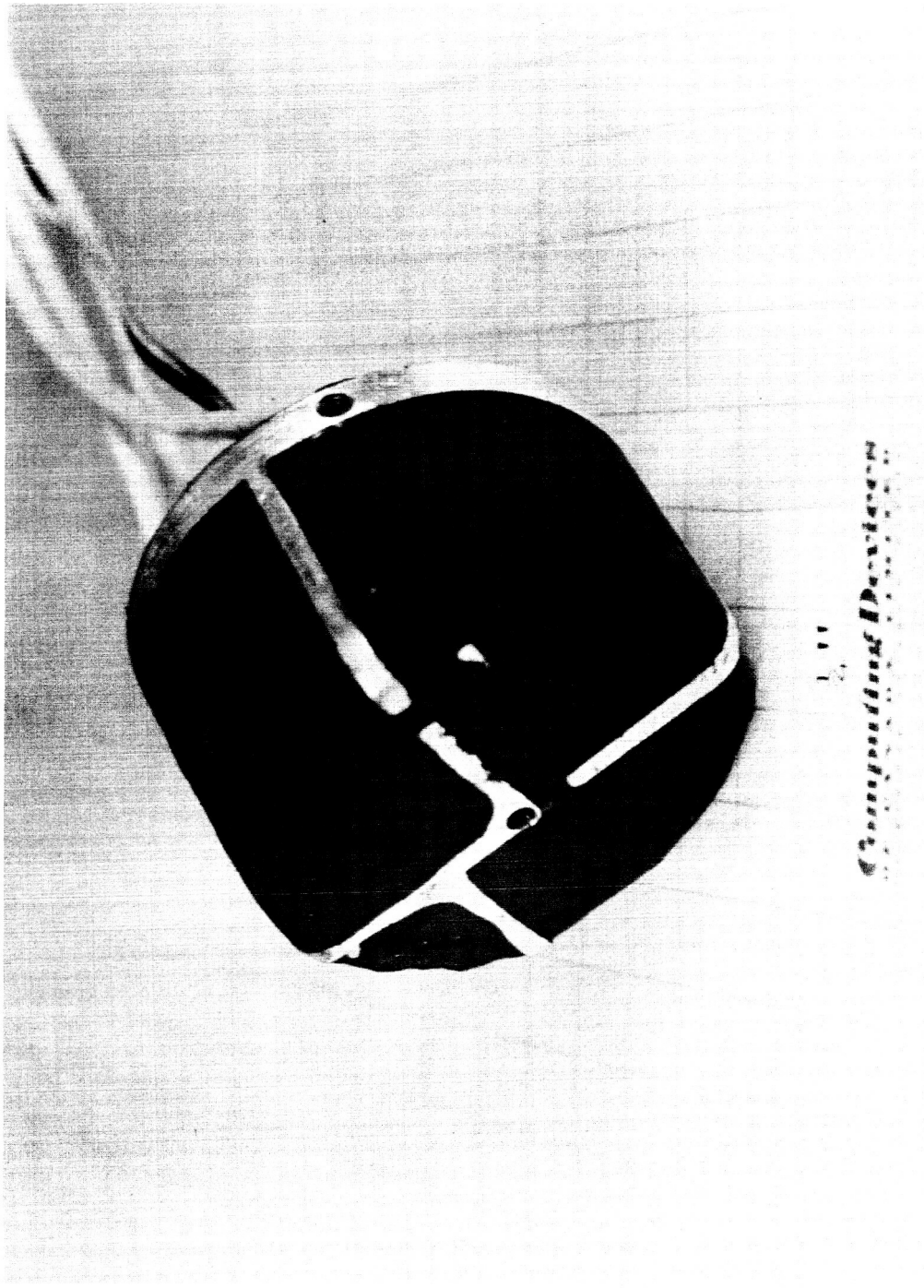

Figure 5-12. Potted Transmitter

Figure 5-12.

Figure 5-13. Complete Transmitter

Figure 5-13.

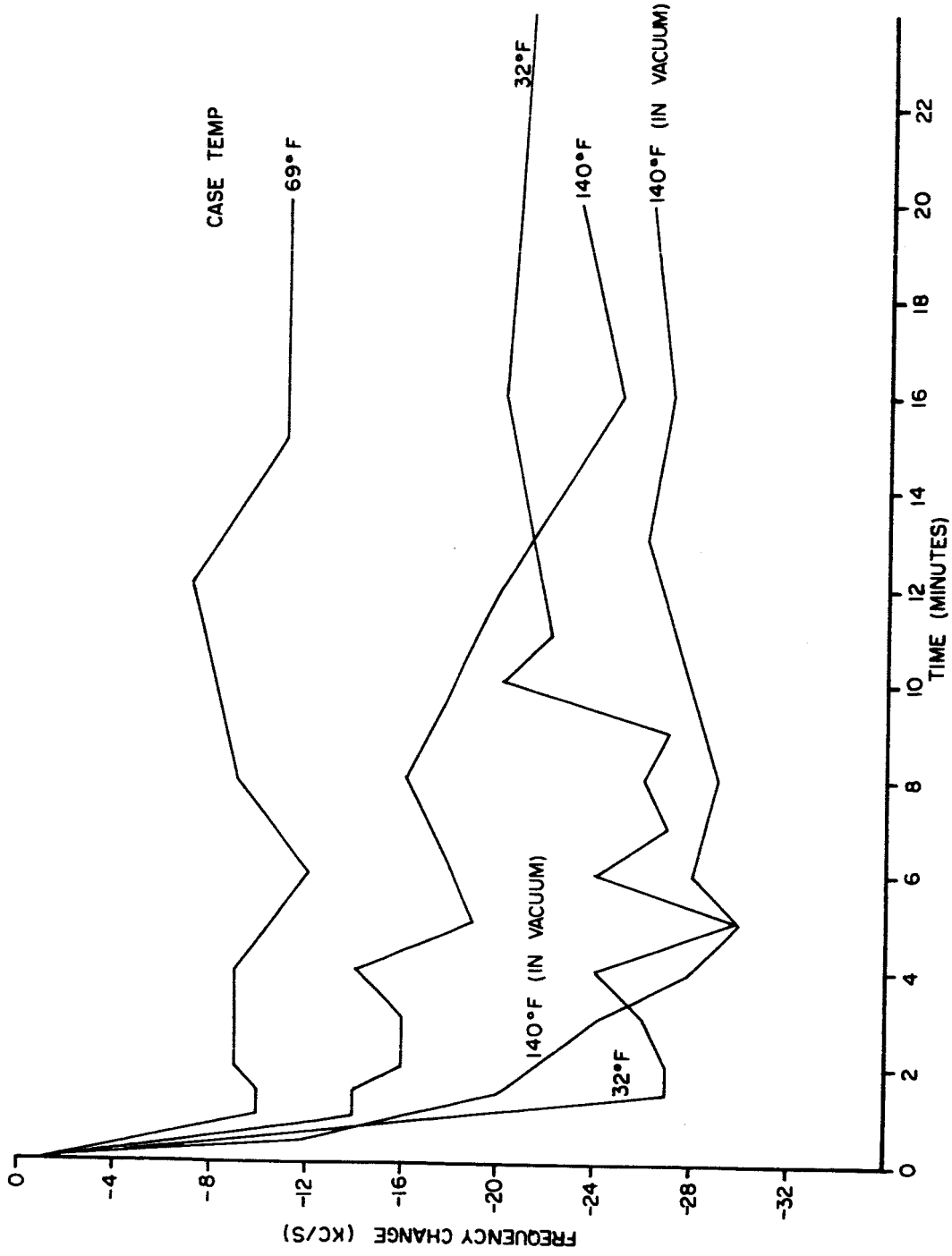

Figure 6-1. Transmitter Warm-up Curves

Figure 6-1.

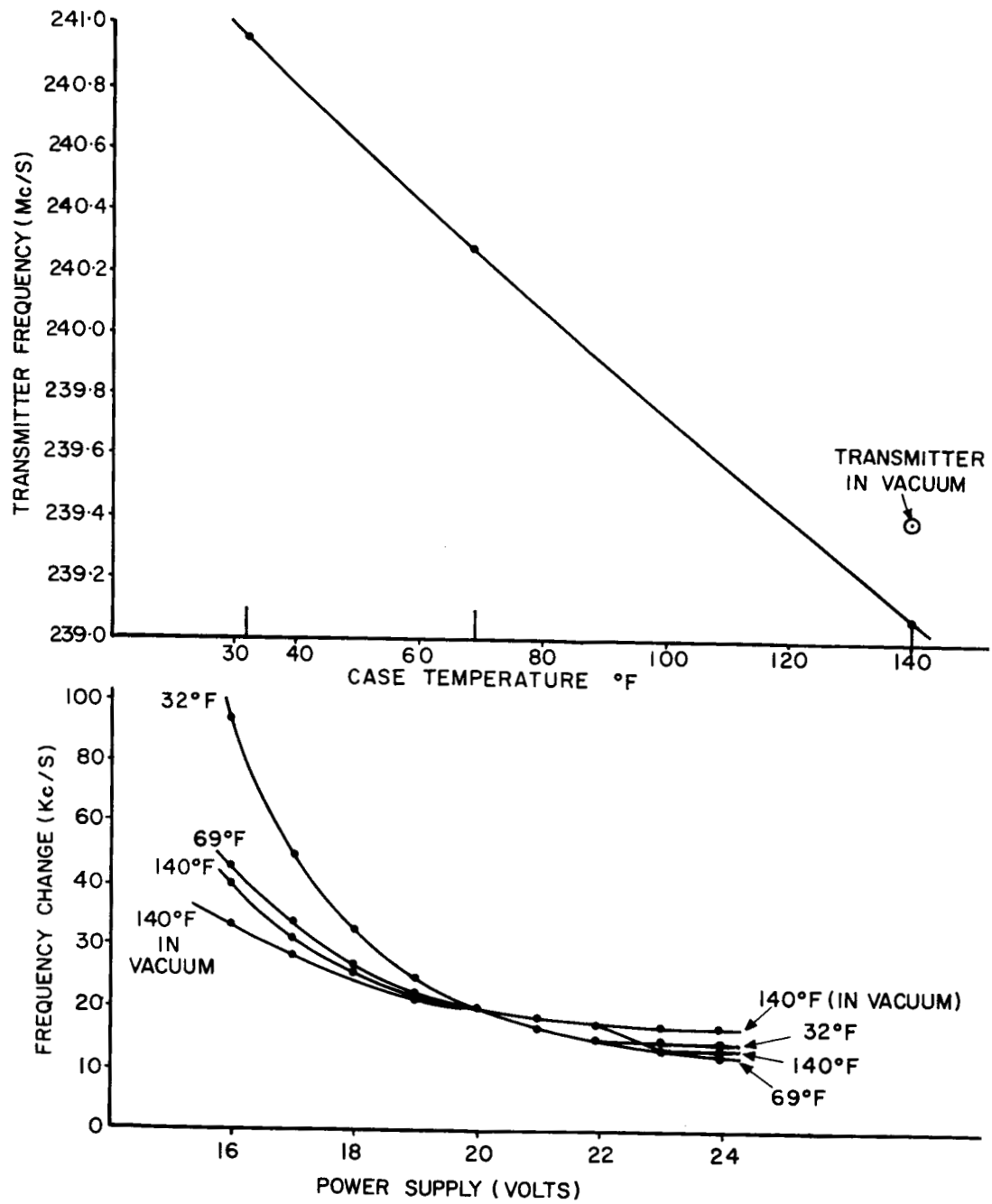

Figure 6-2. Frequency Stability Curves

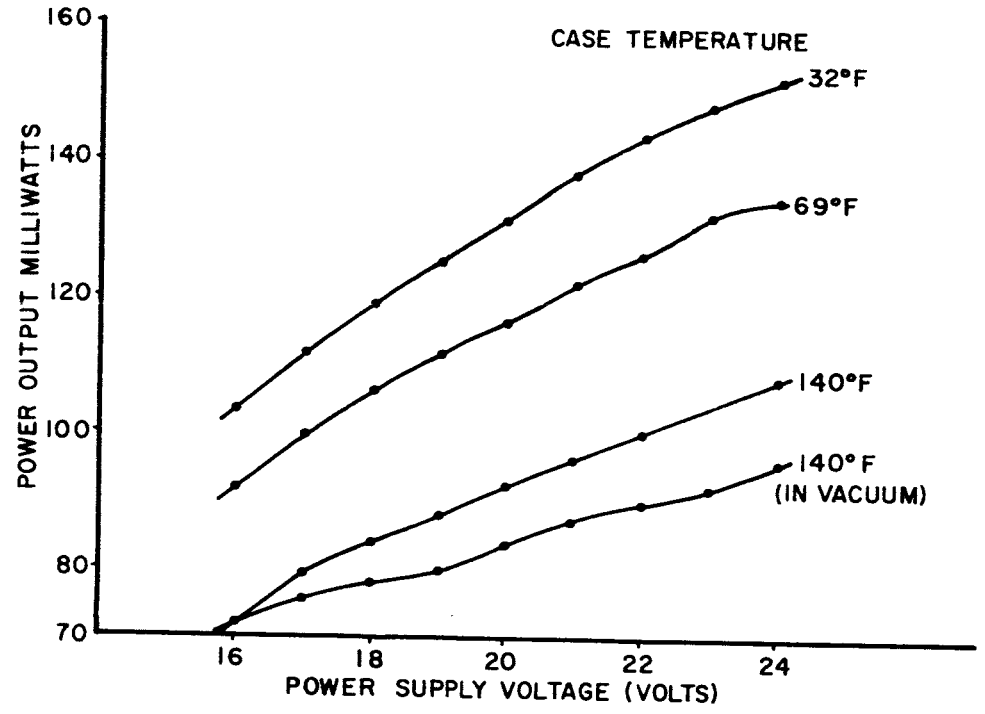

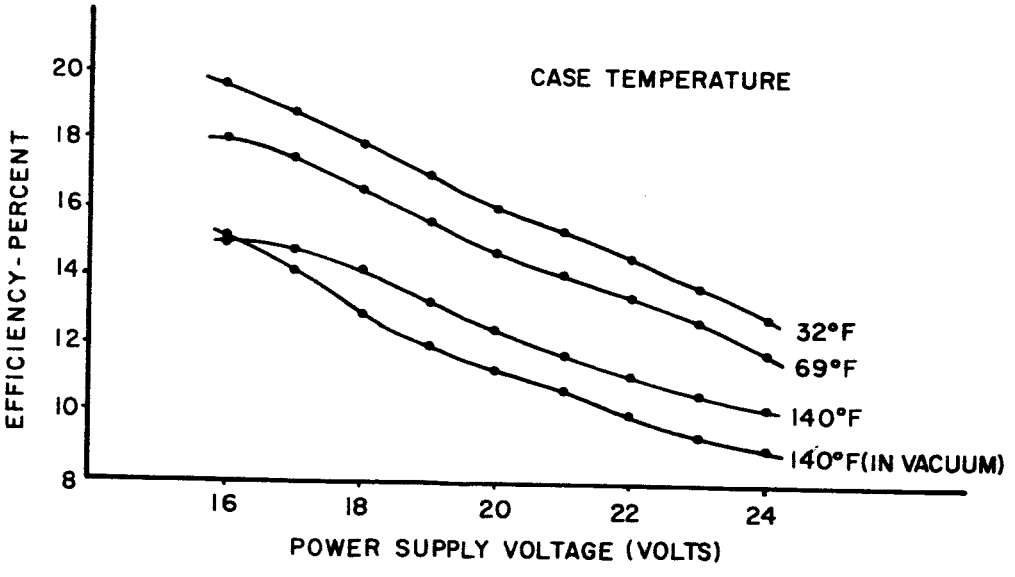

Figure 6-3. Power Output and Efficiency Curves

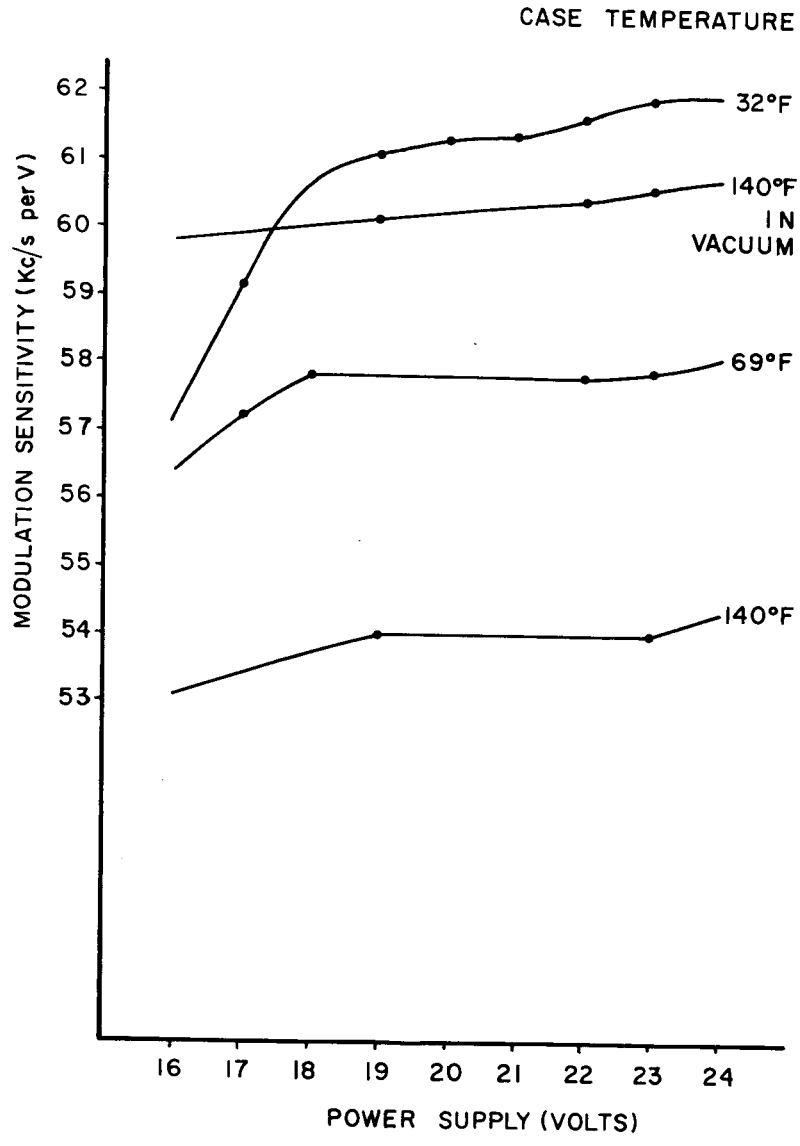

Figure 6-4. Modulation Sensitivity

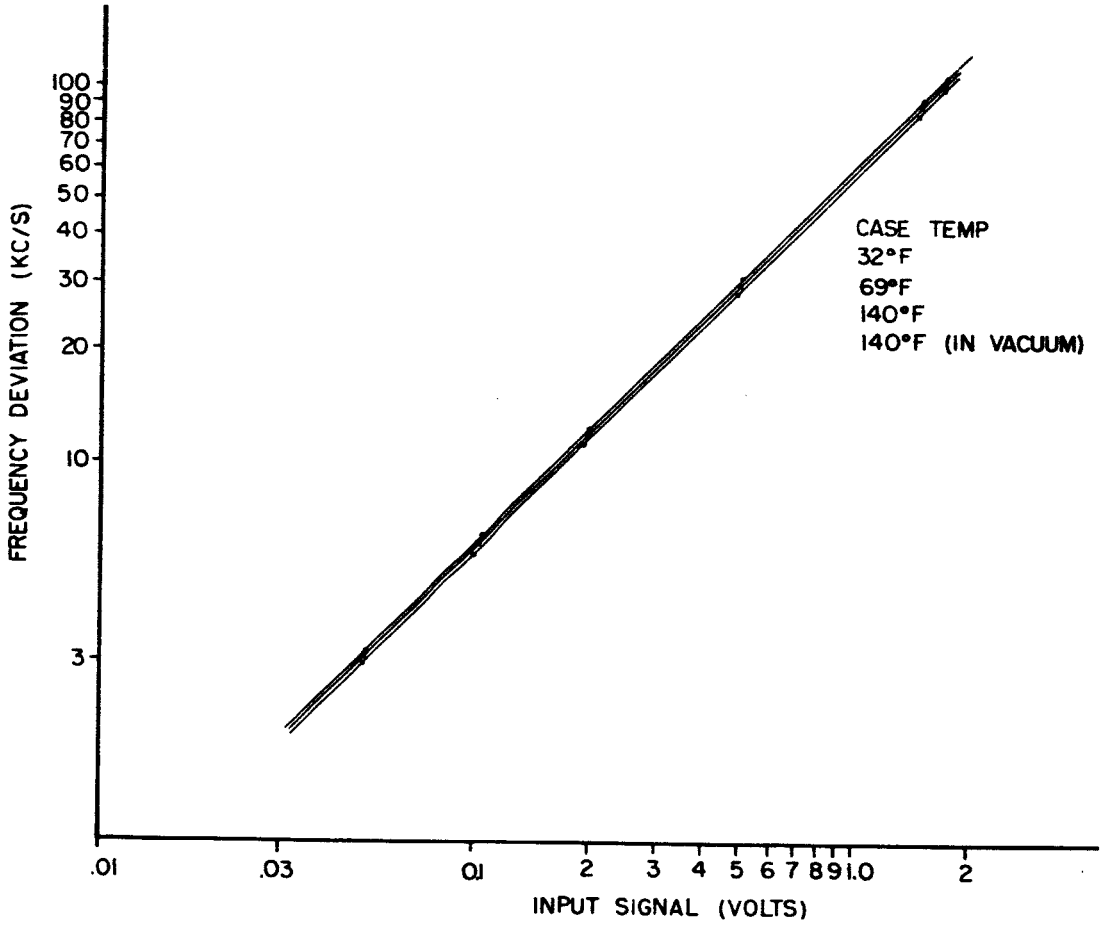

Figure 6-5. Modulation Linearity

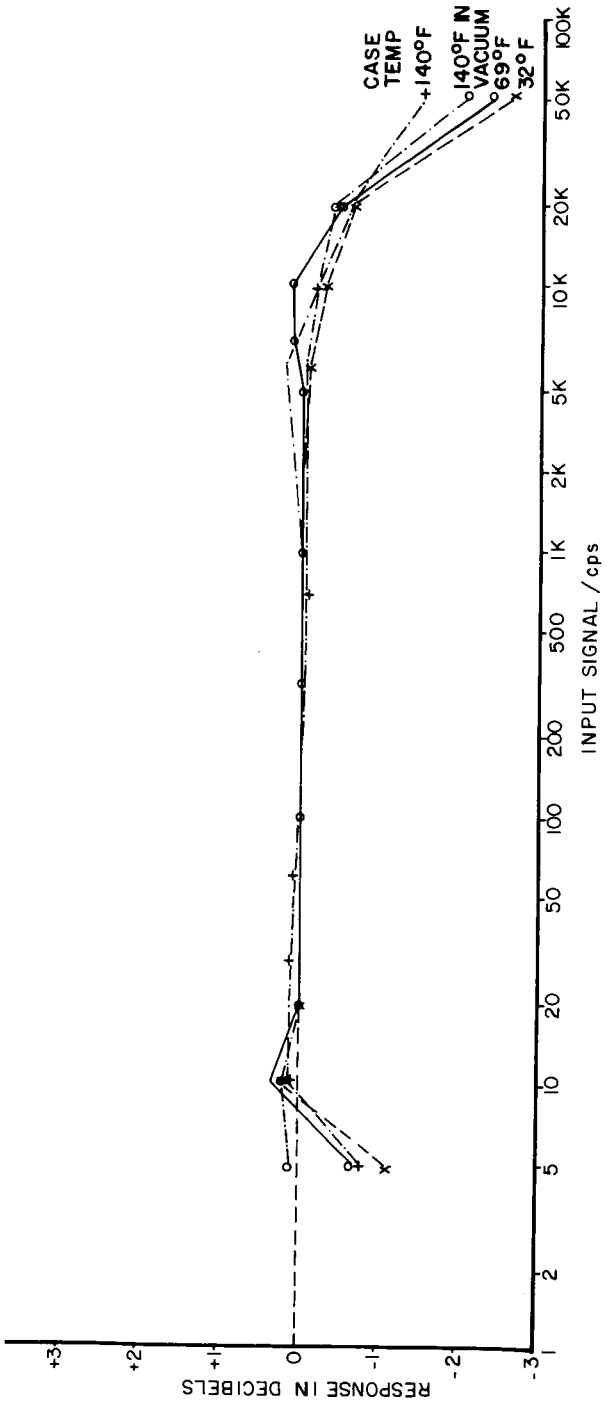

Figure 6-6. Modulation Bandwidth

Figure 6-6.

Printed and published in Canada by
Computing Devices
OF CANADA LIMITED